DEPARTMENT OF THE AIR FORCE
AIR FORCE RESEARCH LABORATORY
WRIGHT-PATTERSON AIR FORCE BASE OHIO 45433

24 May 2001

MEMORANDUM FOR US EPA
NCEA (MD-52)
RTP, NC 27711
ATTN: ANNIE M. JARABEK

FROM: Rebecca Clewell
AFRL/HEST
Operational Toxicology Branch
2856 G St, Bldg 79
Wright-Patterson AFB, OH 45433-7400

SUBJECT: Consultative Letter, AFRL-HE-WP-CL-2001-0007, Physiologically-Based Pharmacokinetic Model for the Kinetics of Perchlorate-Induced Inhibition of Iodide in the Lactating and Neonatal Rat

1. This letter describes a physiologically-based pharmacokinetic (PBPK) model for predicting the distribution and kinetics of iodide and perchlorate and the perchlorate-induced inhibition of iodide uptake in the thyroid of the lactating rat. The current model is a continuation of the preliminary work presented in the Consultative Letter, AFRL-HE-WP-CL-2000-0037, Preliminary Physiological Model for Perchlorate in the Lactating Rat.

2. The improved model is able to describe perchlorate distribution due to drinking water exposure over three orders of magnitude in addition to the acute kinetics of perchlorate from intravenous dosing. It is also able to simulate the kinetic behavior of iodide in the lactating rat and neonate at doses spanning four orders of magnitude. The model was used to predict the inhibition of iodide as a result of acute perchlorate exposure and kinetic iodide data reported in literature.

3. For further information, please contact me by phone: (937) 255-5150 ext. 3141, fax: (937) 255-1474 or e-mail: rebecca.clewell@wpafb.af.mil.

REBECCA A. CLEWELL
Operational Toxicology Branch

Attachments:
1. Physiologically-Based Pharmacokinetic Model for the Kinetics of Perchlorate-Induced Inhibition of Iodide in the Lactating and Neonatal Rat
2. Goodyear, C.: PND10 Drinking Water Consumption Statistical Summary
3. Goodyear, C.: Serum Hormone (TSH, T_3, T_4) Statistical Report (Postnatal Day 5)

1st Ind, AFRL/HEST 24 May 2001

MEMORANDUM FOR US EPA
ATTN: MS. ANNIE JARABEK

This letter report has been coordinated at the branch level and is approved for release.

RICHARD R. STOTTS, DVM, PhD
Branch Chief
Operational Toxicology Branch
Human Effectiveness Directorate

Physiologically-Based Pharmacokinetic Model for the Kinetics of Perchlorate-Induced Inhibition of Iodide in the Lactating and Neonatal Rat

Rebecca A. Clewell[1], Elaine A. Merrill[2], Kyung O. Yu.[3],
Deirdre A. Mahle[4], Teresa R. Sterner[2], Jeffrey W. Fisher[3*], Jeffery M. Gearhart[4]

[1]GEO-CENTERS, Inc.
2856 G St, Bldg 79
Wright-Patterson AFB, OH 45433

[2]Operational Technologies
1370 N. Fairfield Rd., Ste. A
Dayton, OH

[3]AFRL/HEST
2856 G St, Bldg 79
Wright-Patterson AFB, OH 45433

[4]Mantech Environmental Technology, Inc.
PO Box 31009
Dayton, OH 45437-009

*Current Address:
Department of Environmental Health Science
The University of Georgia
206 Environmental Health Science Bldg
Athens, GA

24 May 2001

INTRODUCTION

Ammonium perchlorate is a powerful oxidizer and the primary component of solid rocket fuel mixtures. It is also present in fireworks, ammunition and commercial fertilizers. Most perchlorate salts are highly soluble in water due to the large surface area and the small, dissociated charge of the anion. Perchlorate, the anion formed by the dissociation of the ammonium salt, has been found in the drinking water supplies of more than 11 states (Urbansky, 1998; Urbansky and Shock, 1999). Contamination of surface and groundwater by perchlorate has resulted in concern over the health effects of long-term ingestion of perchlorate (Mattie and Jarabek, 1999).

Use of perchlorate dates to the early 20th century, when its potassium salt was prescribed for the treatment of Grave's disease, an advanced form of hyperthyroidism. This treatment was eventually terminated due to complications and reported side effects (Wolff, 1998). However, perchlorate is often used in the investigation of the endocrine system's regulation of iodide. The ability of perchlorate to interfere with hormone production is a result of its ability to competitively bind to the sodium iodide symporter (NIS) in the thyroid, thereby reducing the amount of iodide available in the thyroid for hormonogenesis. NIS, a protein that resides in the basolateral membrane of thyroid epithelial cells, actively and simultaneously transports both Na^+ and I^- ions from extracellular fluid (plasma) into the thyroid epithelial cell. Energy is provided by the electrochemical gradient of sodium across the cell membrane; the low intracellular concentration of sodium is maintained by sodium-potassium pumps (Ajjan *et al.*, 1998). In addition to the thyroid, active transport via NIS has been shown to occur in several tissues, including the mammary gland, salivary gland, placenta, skin, ovary and gastric mucosa (Brown-Grant, 1961; Spitzweg *et al.,* 1998; Kotani *et al.,* 1998). The presence of NIS and the ability of perchlorate to interfere with iodide uptake suggests a similar mode of action to the thyroid, although only the thyroid is capable of converting inorganic iodide to hormones, such as thyroxine (T_4), triiodothyronine (T_3) and reverse triiodothyronine (rT_3) (Brown-Grant, 1961).

Hormone homeostasis is achieved through a complicated feedback system, wherein diminished hormone levels signal the hypothalamus, which in turn signals the pituitary to increase production of thyroid stimulating hormone (TSH), which stimulates the thyroid to increase iodide symporter activity (Wolff, 1998). Although perchlorate has been shown to perturb the system, interfering with thyroid iodide uptake and serum hormone concentrations, the body's compensatory mechanism is usually able to bring the system back to equilibrium. Drinking water studies with perchlorate have demonstrated this compensation of iodide uptake and hormone levels in the male, pregnant female and lactating female rats (Yu, 2000). Male rat studies suggested a dose-dependent behavior, where the time required to return the system to a state of equilibrium was dependent upon the level of exposure to perchlorate (Yu *et al.,* 2000).

The first two years of human life constitute a critical period in which the thyroid hormones play a major role in physical and mental development (Bakke *et al.*, 1976; Porterfield, 1994). A short-term iodide deficiency during this critical window has been shown to produce lifelong consequences. In humans, iodide deficiency and hypothyroidism during early development have been associated with increased incidence of stillbirths, congenital abnormalities, lowered IQ, mental retardation and impaired hearing resulting from abnormalities in the inner ear (Delange,

2000; Hetzel and Dunn, 1989 and Dobbing, 1974 as cited in Gokmen and Dagu, 1995; Porterfield, 1994; Haddow *et al.*, 1999; Klein *et al.*, 1972). In rats, studies have shown developmental hypothyroidism to result in brain cell disorganization and delayed onset of puberty and estrus (Bakke *et al.*, 1976; Clos *et al.*, 1974).

By the twelfth week of gestation in a human (Porterfield, 1994; Roti *et al.*, 1983), or gestational days 18 to 20 for the rat (Geloso, 1961 as cited in Eguchi *et al.*, 1980), the fetus has a functional thyroid-pituitary axis, is sequestering iodide and is also beginning to synthesize and secrete its own hormones (Geloso, 1961 and Nataf and Sfez, 1961 as cited in Eguchi *et al.*, 1980). Eguchi *et al.* (1980) further contend that a reciprocal relationship (or the thyroid-pituitary feedback) is in place by days 19 through 20 of gestation in the rat. The iodine needed for fetal hormone production is obtained from the mother during gestation. Iodine is thought to pass freely through the human placenta and has been shown to be actively concentrated by the placenta in the rat (Roti *et al.*, 1983; Brown-Grant, 1961).

After parturition, hormone production is the sole responsibility of the neonate. While small amounts of T_3 have been found in milk, very little or no T_4 is present in rat or human milk. What little hormone is transferred in milk is thought to be broken down within the gut of the newborn (Potter *et al.*, 1959; Vigouroux and Rostaqui, 1980; Vigouroux *et al.*, 1980; Sato and Suzuki, 1979; Brown-Grant and Galton, 1958). However, nursing infants are dependent upon maternal milk as their only source of the necessary iodide. Inorganic iodide is actively sequestered in the mammary gland in a process similar to that of the thyroid and is then transferred to the suckling pup via the milk primarily in its inorganic form or as the hormone precursors, monoiodotyrosine (MIT) and diiodotyrosine (DIT) (Iino and Greer; 1961; Vigouroux *et al.*, 1980; Brown-Grant and Galton, 1958; Brown-Grant, 1957).

Perchlorate competitively inhibits the uptake of iodide into the mammary gland in a manner reminiscent of the thyroid, thereby reducing the amount of available iodide to the infant. Studies utilizing radiolabeled iodide in lactating rats have shown perchlorate to be an effective inhibitor of iodide secretion of into breast milk (Potter *et al.*, 1959, Brown-Grant, 1961). An additional risk to the neonate is characterized by the fact that perchlorate not only inhibits the uptake of iodide, but is also taken up itself into the mammary tissue by way of the Na^+/I^- symporter. The perchlorate is then concentrated in the milk and transferred to the litter through suckling. Although early papers suggest that perchlorate is not transferred in milk (Zeghal *et al.*, 1992), newer technology with better analytical sensitivity has detected perchlorate in the milk of rats dosed with as little as 0.01 mg/kg-day perchlorate in drinking water. The perchlorate levels in 5- and 10-day old neonate serum comparable are to those of the mother (Yu *et al.*, 2000), indicating that the pups are in fact exposed to significant levels of perchlorate through the maternal milk. This information highlights the need for more information regarding the effect of perchlorate exposure to the neonate. Yet, it is also vital to develop a method for predicting the dose and the subsequent risk to the infant with the information that is currently available.

In response to the concern about postnatal perchlorate exposure, a physiologically-based pharmacokinetic (PBPK) model was developed to predict the distribution of perchlorate within the lactating and neonatal rat during the first few weeks of life, and to predict the short-term effect of acute perchlorate exposure on iodide kinetics, including iodide uptake in the maternal

thyroid. Mathematical equations are used to describe the uptake, excretion, lactational transfer and inhibition kinetics of perchlorate and iodide within the dam and pup. The purpose of this paper is to report the progress to date on this lactation model. Model development was initially based solely on perchlorate distribution data from drinking water exposure. However, recently acute time course data have been acquired for perchlorate (ClO_4^-) and radiolabeled iodide ($^{125}I^-$). Inhibition data were also available for $^{125}I^-$ after exposure to ClO_4^- in both acute and drinking water scenarios.

METHOD

Supporting Experiments

Drinking Water Study. Perchlorate drinking water experiments used in model development were performed at AFRL/HEST. Pregnant dams of the Sprague-Dawley strain were exposed to drinking water treated with perchlorate from gestational day (GD) 2 through postnatal day (PND) 5 or 10 at perchlorate doses of 0.0, 0.01, 0.1, 1.0 and 10.0 mg/kg-day. GD 0 was determined by the presence of a vaginal plug. Litters were standardized to eight pups (four male and four female, when possible) on PND 2. Dams and their litters were euthanized on either PND 5 or 10; maternal and neonatal serum was analyzed for free and total thyroxine (fT_4 and tT_4), triiodothyronine (T_3) and TSH. Maternal serum, thyroid, skin and gastric contents were analyzed for ClO_4^- at all of the above doses. Neonatal serum, skin and GI contents were also analyzed for ClO_4^- at all of the doses. Milk was available only on PND10 at all doses. Perchlorate analysis was performed only on maternal gastric tract, mammary tissue and neonatal gastric tract samples from the PND 5 study at the 10.0 mg/kg-day dose. Two hours before euthanization, the dams were given intravenous (*iv*) doses of 33 mg/kg radiolabeled $^{125}I^-$ with carrier. Tissue concentrations of iodide were measured in order to determine the inhibition in the various tissues after long-term exposure to ClO_4^-. These studies are described in detail in another report (Yu, 2000).

Cross-fostering Study. The cross-fostering study involved four groups of rats with varied experimental conditions: true control, control, exposed and true exposed. True control rats were never dosed with perchlorate. Neonates remained with the dam after birth. In the control group, dams were never exposed to perchlorate in drinking water. However, at the time of birth, the neonates were replaced with pups (less than 24 hours old) that had been exposed to perchlorate throughout gestation (1.0 mg/kg-day to mother through drinking water). In the exposed group, the dams were dosed with 1.0 mg/kg-day perchlorate in drinking water from GD2 to PND10. At the time of birth, the neonates were replaced with pups (less than 24 hours old) that had never been exposed to perchlorate. The true exposed dams were dosed with 1.0 mg/kg-day perchlorate from GD 2 to PND 10. Neonates remained with mother after birth. All dams and pups were euthanized on PND 10; skin, GI contents and serum from the neonates and dam were analyzed for perchlorate. Results indicated that both true control and control (exposed neonates with control dams) showed no perchlorate present on PND 10. True exposed and exposed (exposed

dams with control litters) showed comparable perchlorate levels on PND 10. This study is described in detail in another consultative letter (Mahle, 2001).

Perchlorate Kinetics Study. In order to evaluate the acute kinetics of perchlorate in the lactating dam and neonate, AFRL/HEST performed a study of the kinetic behavior of perchlorate after the administration of an acute dose. PND 10 Sprague-Dawley dams were given 0.1 mg/kg ClO_4^- by tail vein injection. The dams were left with their neonates until the time of euthanization at 0.5, 1, 2, 4, 8 and 12 hours post-dosing. Maternal serum, thyroid, stomach contents, skin and mammary gland were collected and analyzed for ClO_4^- content at all time points. Neonate serum, stomach contents and skin were also collected for ClO_4^- analysis at all time points. Fat, liver, kidney and bladder tissues were also collected from the dam at the eight hour time point. Perchlorate analysis was performed on the serum of the dam and neonates and the maternal thyroid, mammary gland, GI contents and skin.

Iodide Inhibition Kinetics Study. A study of iodide time course and inhibition kinetics was performed by AFRL/HEST, in which Sprague-Dawley timed-pregnant dams were given 1.0 mg/kg body weight (BW) ClO_4^- via tail vein injection on PND 10. The perchlorate dose was followed at two hours post-dosing with a tail vein injection of carrier free $^{125}I^-$ at an average dose of 2.10 ng/kg BW. Dams (n=6) were euthanized after 0.5, 1, 2, 4, 8 and 24 hours. Maternal and neonatal serum, skin and GI contents and tract, as well as the maternal thyroid and mammary gland tissue, were collected and analyzed for total iodide content at each time point. Neonatal serum was pooled by sex in each litter. Neonatal skin and GI contents and tract were analyzed individually.

Literature Studies

Sztanyik and Turai (1988). Five groups of CFY albino rats (BW = 200 to 250 g) were dosed intraperitoneally with either 370 kBq (0.081 ng) or 740 kBq (1.61 ng) carrier free $^{131}I^-$ on PND 1 (24 hours). Sztanyik and Turai measured the total iodide burden of each litter at 29 hours and PNDs 2, 5, 7, 9 and 14. Since the litters were not standardized, the number of pups in each litter varied.

Potter *et al.* (1959). Four dams of the Long-Evans strain (PND 17-18) were dosed via intraperitoneal injection of carrier free $^{131}I^-$ (500μCi). Potter and coworkers measured iodide uptake in the milk and plasma of the dam at 3, 6 and 24 hours post-dosing and maternal thyroid at 24 hours post-dosing.

Model Structure

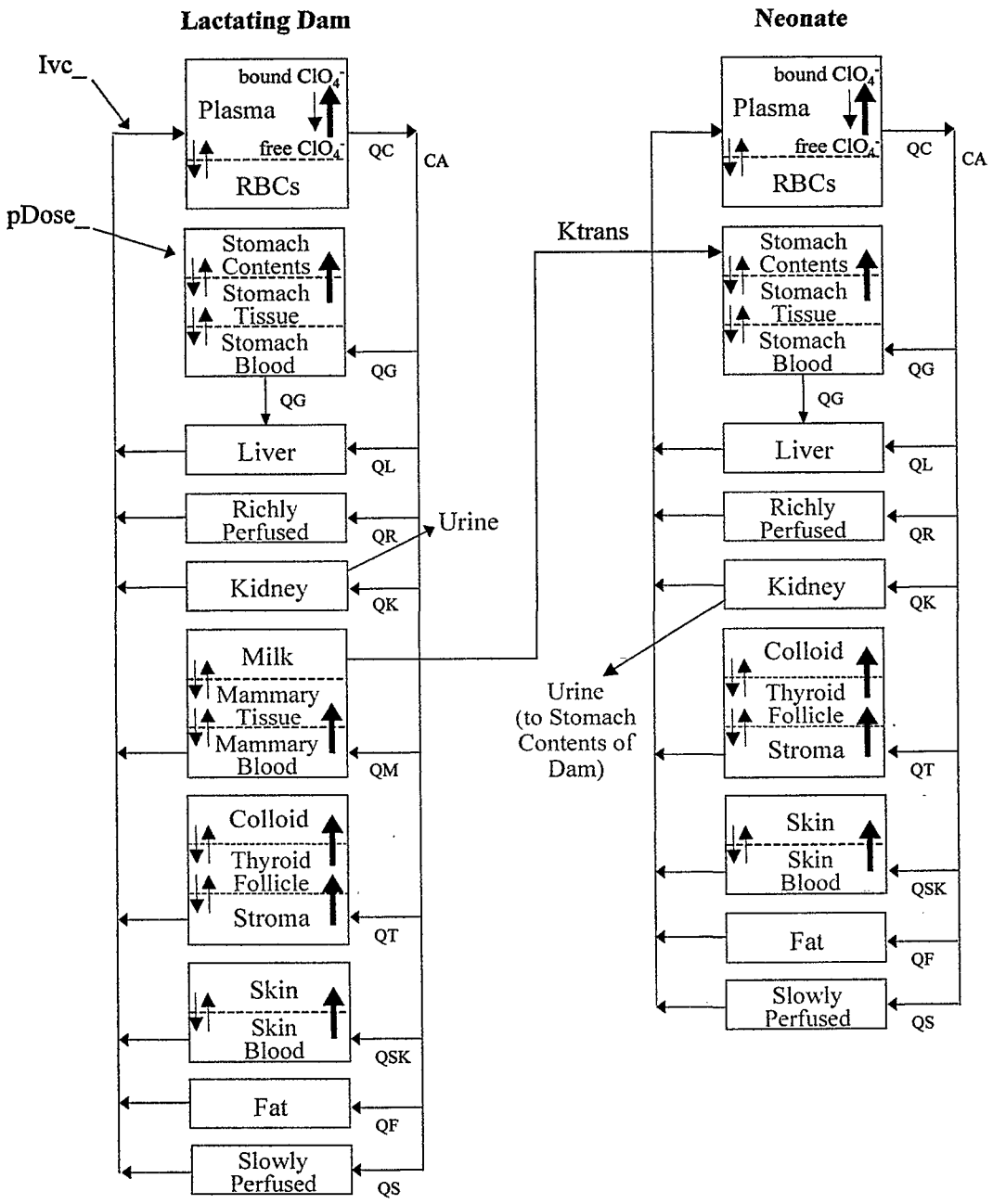

Figure 1. Schematic of PBPK models for lactating dam (left) and neonate (right).

Model Compartments.

Maternal Model Structure. The maternal model consists of two lumped compartments (slowly and richly perfused tissues), a plasma compartment and separate compartments for the thyroid, skin, gut, kidney, liver, fat and mammary gland. The gut and thyroid consist of three sub-compartments representing the stroma, follicle and colloid in the case of the thyroid, and the capillary bed, tract and contents in the gut. The mammary compartment also consists of three sub-compartments, representing the capillary blood, the mammary gland tissue and the milk. The model also includes a skin compartment, consisting of two sub-compartments that represent the capillary bed and tissue. The active uptake into the thyroid colloid, skin, mammary gland tissues and gastro-intestinal (GI) contents were described with Michealis-Menten terms for saturable processes (bold arrows in Figure 1). The sequestration of the anions (ClO_4^- and I^-) into the milk is also described with Michealis-Menten kinetics. Permeability area cross products and partition coefficients were used to describe the first order movement of the anion (ClO_4^-) between the capillary bed, tissue and inner compartments (small arrows), which results from the inherent electrochemical gradients within the tissues. The kidney, liver and fat compartments were described with partitions and blood flows. The binding of perchlorate in the blood was described with a saturable term for the association of the ClO_4^- anions to the binding sites in the plasma and a first order clearance rate for the dissociation. Urinary clearance and transfer of the anions through suckling were represented by first order clearance rates.

Perchlorate and iodide were modeled in a similar manner, based on their shared affinity for NIS. Tissues that have exhibited evidence of NIS and were found to concentrate perchlorate and iodide were given separate compartments in the structure of the model. These tissues include the thyroid, skin, GI contents and mammary gland. Although several other tissues have been known to sequester iodide and perchlorate in the rat and human, such as the salivary gland, ovary and choroid plexus (Brown-Grant, 1961; Honour *et al.*, 1952; Spitzweg *et al.*, 1998; Kotani *et al.*, 1998), the amount of iodide and perchlorate in these tissues was too small to affect plasma concentrations. Therefore, these tissues were lumped with the richly and slowly perfused compartments to simplify the model. Gastric contents and thyroid tissue have been found consistently in experiments to retain higher concentrations of injected perchlorate and iodide than plasma in both the rat and human (Wolff, 1998; Halmi and Stuelke, 1959; Chow *et al.*, 1969; Yu, 2000; Yu *et al.*, 2000). Although symporter in the GI is primarily found in the stomach, data were not available during model development for the stomach compartment alone. Therefore, the whole GI tract with contents was modeled in order to utilize available data.

The behavior of perchlorate and iodide in the skin is not as well studied as the thyroid and GI contents. However, there are a few studies with measured values for either perchlorate or iodide in skin. Yu *et al.* (2000) found $^{36}ClO_4^-$ in male rat skin at higher concentrations than plasma several hours after *iv* administration. A second paper by Yu (2000) reported skin to plasma ratios greater than one in lactating and pregnant dams, GD20 fetuses and PND 5 and 10 neonates after chronic dosing of perchlorate via drinking water. Zeghal *et al.* (1995) examined the effects of perchlorate on the iodide composition of rat skin. Although Zeghal and coauthors did not directly measure skin perchlorate, they reported a significant reduction in skin iodide in young and adult rats after ClO_4^- administration, suggesting competitive inhibition.

Iodide has also been reported at higher concentrations in the skin than plasma after *iv* dosing, but the results have not been as consistent as those seen with perchlorate. Brown-Grant and Pethes (1959) observed skin:serum ratios greater than one in adult male rats and young rats. Skin:serum ratios were not as high in female rats and they did not find the same behavior in the skin of guinea pigs or mice. Yu (2000) reported skin: serum iodide ratios close to one in rats dosed intravenously with radiolabeled iodide. Skin was therefore described utilizing terms for active uptake in both the perchlorate and iodide models of the lactating dam and neonate.

The mammary tissue has been shown to concentrate both perchlorate and iodide during lactation, via the NIS symporter. Additionally, hormones produced during lactation such as prolactin (stimulates milk production), have been shown to regulate the mammary NIS. Suckling of the neonatal rats has also been shown to stimulate mammary NIS activity (Tazebay *et al.*, 2000). An additional symporter has been identified in the experiments of Shennan (2001). *In vitro* studies of iodide transport into the mammary gland and the resulting efflux of sulfate from the cells in the absence of Na^+, indicates that another form of transport exists for iodide in the mammary gland in addition to the NIS. Shennan suggests that this anion transport mechanism is able to transfer perchlorate and iodide into the secretory cells against a concentration gradient. Since the secretory cells are responsible for secreting their contents into the milk, the anion transport mechanism was included in the milk compartment of the model.

The kidney, liver and fat were also separately defined within the general structure of the model. These tissues do not maintain ClO_4^- or iodide concentrations greater than the plasma and therefore do not contain terms for active uptake. The rapid urinary clearance of perchlorate (Yu *et al.*, 2000) called for the inclusion of a kidney compartment in the model. A liver compartment was also utilized, due to its significant impact on iodide homeostasis. The majority of extrathyroidal deiodination takes place within the liver. Although the model does not currently include hormone production or deiodination, the future editions of the model will require the inclusion of a liver compartment. Fat was primarily added as an exclusionary compartment. The changing fat content in the animals could very likely alter the kinetics of perchlorate and iodide, since the polar anions would not be easily absorbed into fatty tissue. Partitioning into the diffusion-limited compartments is based on effective partitioning. This effective partitioning is probably very similar to the thyroid, in which an electrochemical gradient is responsible for moving the ClO_4^- anion between the serum and the tissue (Chow and Woodbury, 1970).

High serum perchlorate concentrations at the low doses (Yu, 2000; Yu *et al.*, 2000) required the use of plasma binding in model simulations. The potential for perchlorate binding to protein is a subject that has not been well studied. However, the inclusion of binding is supported by the consistency between the three rat models and a few studies found in the literature, which explored the possibility of perchlorate binding to plasma proteins.

Shishiba *et al.* (1970) studied the effect of perchlorate on the free thyroxine (fT_4) fraction in human blood. They found that perchlorate interfered with the binding of fT_4 to prealbumin and albumin, but not thyroglobulin (TBG). Yamada (1967) reported an increased fT_4 fraction in rat blood after administration of perchlorate. While Yamada found perchlorate to have a greater effect than thiocyanate (SCN^-) in rats, Shishiba found perchlorate to have less affect in human

blood. These studies suggest a species difference in protein/perchlorate interaction in the blood. Studies performed by Hays and Green (1973) on pertechnetate (an anion with a mechanism similar to that of perchlorate) found that perchlorate blocked the binding of pertechnetate to human serum albumin.

Carr (1952) measured perchlorate binding in bovine albumin. He found that perchlorate bound to nearly the same extent as thiocyanate (SCN^-). Perchlorate binding in human serum was measured by Scatchard and Black (1949). Their studies also revealed that perchlorate binding was very similar to that of SCN^-. It is likely, therefore, that the mode in which perchlorate is able to prohibit albumin binding in human serum is by reversibly binding to the albumin via weak covalent interactions. This binding, although not measured directly in the rat, is evidenced through the displacement of T_4 in rat serum. Given that perchlorate demonstrates a similar or slightly smaller ability to bind to albumin or prealbumin in human serum, it is feasible to assume from Shishiba's studies that perchlorate is bound to a greater extent in rat serum. This is also supported by the fact that thyroxine is primarily transported by albumin in rats as opposed to TBG in humans, which has been shown not to be affected by perchlorate. Thus, is it reasonable to assume that protein binding would have a greater affect on the distribution and clearance of the anion in the rat as opposed to the human.

Neonatal Model Structure. The structure of the neonatal model is similar to that of the pregnant rat, with the exception of the mammary gland compartment. In order to simplify the model, all neonates from a single litter were combined in the structure of the model, essentially viewing the entire litter as one entity, or one large neonate. The dose to the neonate is based on the transfer of perchlorate from the maternal milk to the GI contents of the neonate, rather than through direct exposure to the drinking water. The 60% of urinary excretion of the neonate is then entered back into the GI contents of the dam, in order to account for maternal ingestion of the pup's urine during cleaning, based on the work of Samuel and Caputa (1965).

Growth and Changing Parameters. The lactation model attempts to describe perchlorate and iodide distribution in a highly dynamic system. In addition to total body weight changes in the dam and neonate, maternal mammary tissue and blood flow, cardiac output, fractional body fat and neonatal body weight and fractional body fat are changing with respect to time. In the drinking water studies, daily exposures were also found to change with respect to time. Table functions in ACSL (Advanced Continuous Simulation Language, Aegis Technologies Group, Inc.) were used to account for these changes. All tissue volume and blood flow values were adjusted with respect to the changing parameters.

Dosing Procedures. In order to simulate the daily dosing regimen of the drinking water experiment, the rats were assumed to drink at constant rate for 12 of the 24 hours per day (1800 to 0600 hours). A pulse function in ACSL was used to introduce drinking water to the GI contents of the dam for the first 12 hours of each 24-hour period and then to stop dosing while the rat was presumably sleeping. Intravenous (*iv*) dosing was introduced into the venous blood

compartment of the model. Intraperitoneal injection was introduced into the model in the same manner as the *iv* dosing.

The neonate was assumed to be nursing at a constant rate, 24 hours a day. This assumption is based on the fact that young nursing rats are unable to go for long periods of time without suckling. The loss through suckling was then described with a first order clearance rate from the mother's milk to the gastric juice of the neonate, based on the experiments of Sampson and Jansen (1984). The milk production rate was assumed to be equal to the amount of milk ingested by the litter.

Linking Pregnancy and Lactation Models. Since the experimental data used to develop the lactation model were taken from drinking water studies in which the dosing began on GD 2, it was necessary to include starting ClO_4^- concentrations in the tissues at the time of birth (0 hours). In order to obtain these starting values for tissue load at birth, the pregnancy model had to include all of the compartments contained in the lactation model (Clewell, 2001). The pregnancy model was then allowed to run until the day of birth (GD 22) and the average tissue concentrations of ClO_4^- for the final day of gestation were used as the starting values for the respective tissues in the lactation model.

Model Parameters

Physiological and chemical specific parameters for iodide and perchlorate are listed with the sources from which they were obtained in Tables 1 through 3. Whenever possible, physiological and kinetic parameters were taken from literature or in-house experiments. Allometric scaling was employed to account for the difference in parameters due to variations in body weight of male, female and neonatal rats. The following equations illustrate the method of allometric scaling applied to the maximum velocity (*Vmax*), clearance values (*K*), tissue volumes (*V*) and blood flows (*Q*) in the dam. A value of *c* following the parameter name indicates the value of the parameter before allometric scaling and *X* represents the tissue of interest.

$$V\max\_X = V\max c\_X * BW^{3/4}$$

$$ClX = ClXc * BW^{3/4}$$

$$VX = VXc * BW$$

$$QX = QXc * BW^{3/4}$$

Neonatal values were scaled in the same manner as the maternal parameters. However, since the model actually represents several neonates, it was necessary to scale the values for the individual pup first and then adjust for the total number of pups in the litter. The method for scaling the neonatal parameters allometrically is given below, where *N* indicates that the parameter is a neonate value and *numpups* indicates the number of pups in a litter.

$$V\max\_XN = \left(V\max c\_XN * BW\_N^{3/4}\right) * numpups$$

$$ClX\_N = \left(ClXc\_N * BW\_N^{3/4}\right) * numpups$$

$$VX\_N = \left(VX\_N * VXc * BW\_N\right) * numpups$$

$$\dot{QX}\_N = \left(QXc\_N * BW\_N^{3/4}\right) * numpups$$

Physiological Parameters

Physiological parameters (Table 1) were obtained from various literature sources and were also taken directly from the simulated experiment where available. Values for blood flows and tissue volumes that were not directly affected by the body's response to lactation were scaled allometrically from the available male rat data. Table 1 lists the values for these physiological parameters along with their respective sources.

Maternal Tissues. In the PND 10 drinking water study performed by AFRL/HEST (see Attachment 2), the body weight of the dam showed an average increase of 12% between PND 1 and 10, but did not show a significant difference in weight between dose groups. As a result, the average body weight of the dams was calculated for all dose groups for each day of the study. This changing body weight was then programmed into the model as a TABLE function.

In order to describe the changes in the physiology of the lactating rat, it was not sufficient simply to scale some of the parameters allometrically. As opposed to the typical growth scenario, some of the tissues in the lactating rat cannot be assumed to increase at the same rate in this dynamic system. Rather, a few tissues, such as the mammary gland and fat, are changing at an accelerated rate in comparison to the other organs. These parameters require additional descriptions for their growth beyond the previously described allometric scaling by body weight. The basic approach to modeling these changing parameters is based on the work of Fisher *et al.* (1990) with trichloroethylene. Additionally, the thyroid of the female rat was found by investigators to be significantly larger than that of the male rat (Malendowicz and Bednarek, 1986). Therefore, these parameters were given the values that were relevant to the gender and condition (i.e., lactation) of the animal. Parameters that were not available specifically for the female were described by adjusting the values for the male rat by body weight.

During lactation, the mammary gland grows in response to the increased need for milk production by the growing neonates. Knight *et al.* (1984) measured the mammary gland on several days during lactation. They found the mammary tissue to be 4.4, 5.6, 6.3 and 6.6% of the maternal body weight on days 2, 7, 14 and 21, respectively. The residual milk was assumed to be 0.002 L based on the model of Fisher *et al.* (1990). Naismith *et al.* (1982) examined the change in body fat content of the lactating rat. They reported values for the volume of maternal body fat of 15.2 and 6.9% of the body weight on PND 2 and 16, respectively. The body fat composition of the dam on PND 1 was calculated to be 12.4% from the PBPK model for

perchlorate and iodide kinetics in the pregnant rat. This model, along with the description of the change in body fat during pregnancy is described in another paper (Clewell, 2001).

TABLE 1: PHYSIOLOGICAL PARAMETERS

Physiological Parameters	Lactation		Source
Tissue Volumes *	**Dam**	**Neonate**	
Body Weight *BW* (kg)	0.277 - 0.310	0.0075 - 0.1985	Yu, 2000
Slowly Perfused *VSc* (%BW)	37.07-40.42	53.92-49.31	Brown *et al.*, 1997
Richly Perfused *VRc* (%BW)	5.35	5.36	Brown *et al.*, 1997
Fat *VFc* (%BW)	12.45 - 6.9	0.0 - 4.61	Naismith *et al.*, 1982
Kidney *VKc* (%BW)	1.7	1.7	Brown *et al.*, 1997
Liver *VLc* (%BW)	3.4	3.4	Brown *et al.*, 1997
Stomach Tissue *VGc* (%BW)	0.54	0.54	male rat ClO_4^- kinetics
Gastric Juice *VGJc* (%BW)	1.68	1.68	Yu, 2000
Stomach Blood *VGBc* (%VG)	2.9	2.9	Altman & Dittmer, 1971
Skin Tissue *VSkc* (%BW)	19.0	19.0	Brown *et al.*, 1997
Skin Blood *VSkBc* (%VSkc)	2.0	2.0	Brown *et al.*, 1997
Thyroid Total *VTtotc* (%BW)	0.0105	0.0125	Malendowicz & Bednarek, 1986; Florsheim *et al.*, 1966
Thyroid Follicle *VTc* (%Vttot)	45.89	37.2	Malendowicz & Bednarek, 1986; Conde *et al.*,1991
Thyroid Colloid *VDTc* (%VTtot)	45	13.8	Malendowicz & Bednarek, 1986; Conde *et al.*,1991
Thyroid Blood *VTBc* (%VTtot)	9.1	49.0	Malendowicz & Bednarek, 1986; Conde *et al.*,1991
Plasma *VPlasc* (%BW)	4.7	4.7	Brown *et al.*, 1997, Altman & Dittmer, 1971
Red Blood Cells *VRBCc* (%BW)	2.74	2.74	Brown *et al.*, 1997, Altman & Dittmer, 1971
Mammary Tissue *VMc* (%BW)	4.4 - 6.6	---	Knight *et al.*, 1984
Mammary Blood *VMBc* (%VM)	18.1	---	Assume same % as Thyroid Blood
Milk *VMk* (L)	0.002	---	Fisher *et al.*, 1990
Blood Flows			
Cardiac Output *QCc* (L/hr/kg)	14.0 - 21.0	14.0	Hanwell & Linzell, 1973; Brown *et al.*, 1997
Slowly Perfused *QSc* (%QC)	7.9-1.9	16.9	Brown *et al.*, 1997
Richly Perfused *QRc* (%QC)	40.8	40.8	Brown *et al.*, 1997
Fat *QFc* (%QC)	7.0	7.0	Brown *et al.*, 1997
Kidney *QKc* (%QC)	14.0	14.0	Brown *et al.*, 1997
Liver *QLc* (%QC)	18.0	18.0	Brown *et al.*, 1997
GI *QGc* (%QC)	1.61	1.61	Brown *et al.*, 1997
Skin QSkc (%QC)	0.058	0.058	Brown *et al.*, 1997
Thyroid *QTc* (%QC)	1.6	1.6	Brown *et al.*, 1997
Mammary *QMc* (%QC)	9.0 - 15.0	---	Hanwell & Linzell, 1973

* For calculation of volumes from body weight a density of 1.0 g/mL was assumed.

The physiology of the thyroid in the naive female rat was studied by Malendowicz and Bednarek (1986). They found considerable differences in the thyroid histometry between the male and female rat. Therefore, a value of 1.05% of the maternal body weight was used for the thyroid in the lactation model. From their studies, the volume fractions of the colloid, follicle and stroma were given values of 45, 46 and 9% of the thyroid volume. These are significantly different from the values given for the male rat. The volume of the colloid in particular is much greater in the female than the male rat (46 vs. 24% of the thyroid volume).

Neonatal Tissues. As in the maternal rats, the overall average body weights of the neonates measured on PNDs 3, 5, 7, 9 and 10 were programmed into the model in a TABLE function, in order to estimate growth. Naismith *et al.* (1982) reported the body fat in the pup at PNDs 2 and 16 to be 0.167 and 3.65% of the neonatal body weight, respectively. The amount of body fat in a 41-day old rat was given in Brown *et al.* (1997) as 4.61% of the body weight. These values were then programmed into the model by way of a TABLE function.

The volume of the thyroid was studied by Florsheim *et al.* (1966). They found that the volume of the thyroid increases in a fairly linear relationship with body weight between PND 1 and 22. Florsheim and coauthors reported thyroid volumes of 0.0125, 0.0146, 0.0120, 0.0137, 0.0130, 0.0130 and 0.0131% body weight for neonates on PND 1 through 5, 7 and 11. These values were used in a TABLE function in the model to describe the growth of the neonatal thyroid. The histometry of the thyroid in the neonate was examined by Conde *et al.* (1991). The authors found a significant difference between the volume fractions of the colloid, follicle and stroma in the neonatal rat versus those in the adult. Therefore, their reported values of 18.3, 61.4 and 20.3% thyroid volume were used to describe the colloid, follicle and stroma fractions in the neonatal rat, respectively.

The suckling rate of the neonatal rat has been examined in more than one literature study and has been shown to change over time in response to the growth of the neonatal rats. As the pups grow, they require larger amounts of milk. Sampson and Jansen (1984) measured the amount of milk suckled in rats by removing neonates from the dams for two hours and then allowing the pups to suckle for two hours. This process was repeated throughout the day on several days of lactation. By assuming that the weight gained by the neonates during the suckling period was due to the milk intake and the weight lost while separated from the dam was through excretion, Sampson and Jansen were able to develop an equation that describes the suckling rate of the neonatal rat. Since this equation is dependent on the body weight and growth rate of the neonates, it is able to account for the change over time and the difference between strains and studies. Therefore, this equation was used within the model and is given below, where $yield_{pup}$ is the milk yield in units of mL/pup-day, BW_N is the body weight of the neonate and *gain* is the daily weight gain of the pup. The milk yield of the dam was assumed to be equal to the suckling rate.

$$yield_{pup} = 0.0322 + (0.0667 * BW\_N) + (0.877 * gain)$$

Blood Flows. All maternal and neonatal blood flows that were not directly affected by the changes induced by lactation were scaled by weight from the adult male rat parameters. For those blood flow parameters that change in response to lactation, some additional description was required. Cardiac output has been shown to increase during lactation (Hanwell and Linzell, 1973). Therefore, a TABLE function was used to describe the change in cardiac output over time. The values given by Hanwell and Linzell of 14.0, 18.6, 19.0, 21.0 L/hr-kg BW for days 3, 8, 13 and 23 of lactation were used in the model. Additionally, the blood flow to the mammary tissue was also found to increase during lactation. Hanwell and Linzell reported fractional blood flows to the mammary tissue of 9, 10, 11, 14, 14 and 15% of the cardiac output on PNDs 1, 5, 10, 15, 17 and 21.

Chemical Specific Parameters

Clearance Values. For tissues in which a clearance was described (urinary clearance and dissociation of perchlorate from the binding sites), a clearance value was determined by fitting the model simulation to the appropriate tissue data. Since perchlorate is quickly excreted in urine and binding has little effect on serum levels at high doses, the simulation for the 10 mg/kg-day dose group was primarily dependent on the urinary clearance value (ClUc_p). The urinary clearance value for perchlorate was therefore based on the fit of the model to the serum data at the high dose. The value obtained in this manner was similar to that determined by fitting the male rat PBPK simulation to urinary perchlorate at several doses (Merrill, 2001a). The rate of dissociation of perchlorate from the binding sites was fit to the serum data across doses.

Iodide is incorporated into many of the constituents in plasma. However, it is not bound in the same manner as perchlorate to the plasma proteins (i.e., albumin). Additionally, the iodide model is currently simplified to account for the distribution of total iodine. Therefore, the urinary clearance value was determined primarily by fitting the model simulation to the iodide serum data, as blood levels were more dependent on excretion than on the amount of iodide in other tissues. The following equation illustrates the use of clearance values in the distribution and excretion of perchlorate or iodide, where RAZ_y is the rate of excretion of chemical y by route Z, ClZ_y is clearance value for y by excretion route X and CX_y is the concentration of y in tissue X.

$$RAZ\_y = ClZ\_y * CX\_y$$

Affinity Constants and Maximum Velocities. Kinetic values for the saturable active uptake process (Km_p and Vmax_p) were not available for perchlorate in the literature, nor was it determined experimentally in our laboratory. Only the affinity of iodide for NIS was cited in the literature. Gluzman and Niepomniszcze (1983) derived an average Km of 4.0×10^6 ng/L for iodide from thyroid slices of 5 normal individuals. The thyroid slices were incubated with several medium iodide concentrations. The experimentally determined Km values for iodide are similar across species (Gluzman and Niepomniszcze, 1983) and across different tissues (Wolff,

1998). This average literature value was therefore used for iodide in tissues described with active uptake.

The apical follicular membrane (between the thyroid follicle and colloid) also exhibits a selective iodide uptake mechanism. Golstein *et al.* (1992) measured a Km value of approximately 4.0 x 10^9 ng/L for the transport of iodide between the thyroid follicle and colloid in bovine thyroid. Similar to the mechanism of uptake in the basolateral membrane, this apical channel also appears to be very sensitive to perchlorate inhibition and shares a similar permeability to perchlorate and iodide.

The values for perchlorate affinity were originally assumed to be the same as those for Km of iodide, due to the similar mechanism in which the two anions are transported into the tissues. Thus, the iodide values were adjusted for the difference in mass of the anions to give an estimated value for the affinity of perchlorate. However, these values did not adequately describe the data. Several literature sources suggest that perchlorate may have a significantly higher affinity for NIS than iodide. In his 1963 paper (Wolff and Maurey, 1963) and in his 1998 review, Wolff concludes that perchlorate has a greater affinity than iodide for the NIS. This assumption was based upon his work with iodide, perchlorate and several other anions actively sequestered in the thyroid. Wolff measured the Km of a few of the anions and Ki's (inhibition constants) for several ions, including perchlorate. He found that the relative potency of inhibition by the various anions could be described with the following series: TcO_4^->ClO_4^- >ReO_4^->SCN^->BF_4^->I^->NO_3^->Br^->Cl^-. Wolff reported that the measured Km values for several of these inhibiting anions were not the same as those measured for iodide. In fact, measured values for Km and Ki for several of the inhibiting anions revealed that affinity increased with increased inhibitory potency. Halmi and Stuelke (1959) suggested that perchlorate could have an affinity as much as an order of magnitude higher than that of iodide, based upon the preferential uptake of perchlorate into the GI contents and thyroid in the rat. Their studies showed perchlorate to be ten times as effective as iodide in depressing tissue:blood ratios in both the GI contents and thyroid. Harden *et al.* (1968) showed the same behavior in the human salivary gland. These studies, in addition to the work of Lazarus *et al.* (1974) and Chow *et al.* (1969), support the use of a lower Km for perchlorate uptake in the tissues with sodium iodide symporter. Therefore, the perchlorate Km values used in the models were 2.0 x 10^5 for follicular NIS (Km_Tp) and 1.0 x 10^8 ng/L for colloidal transport (Km_DTp), approximately a factor of 10 lower than those given for iodide.

Whenever possible, chemical specific parameters were kept the same in male, female, neonatal and fetal rats and humans. However, it was necessary to change a few of the parameters, including the maximum velocities (Vmax). The Km values were similar between tissues and between female and male rat and human models. However, the maximum velocity or capacity differs between tissues (Wolff and Maurey, 1961). Since values for the tissue maximum velocities (Vmaxc) for perchlorate were not given in literature, the values were estimated with the model. In order to determine Vmax with the model, the simulation for the tissue of interest was compared to various data sets with several different perchlorate dose levels. The value for Vmax within a given compartment was then determined by the best fit of the simulation to the data.

The following equation demonstrates the use of affinity constants and maximum velocities to describe the active sequestration of a chemical into a compartment. *RupX_y* is the rate of active uptake of chemical *y* into tissue *X*. *Vmax_Xy* and *Km_Xy* are the maximum velocity and affinity of tissue *X* for chemical *y*, respectively. *CZ_y* is the concentration of chemical *y* in tissue *Z*, from which the chemical is being removed in order to sequester the ion in tissue *X*.

$$RupX\_y = \frac{V\max\_Xy * CZ\_y}{Km\_Xy + CZ\_y}$$

Effective Partitioning.

Perchlorate. The highly polar perchlorate anion is not expected to partition into tissues in the classical understanding of the process. Rather, the anion responds to the electrochemical potential present across tissue membranes. Chow and Woodbury (1970) explored the relationship of these electrochemical potentials to perchlorate concentrations in the stroma, follicle and lumen in the male rat thyroid at three different doses of ClO_4^-. Their measured difference in electrical potential between the thyroid stroma and follicle can be used to calculate average partition coefficient as described in Clewell (2001). From Chow and Woodbury (1970), the potential difference for the stroma:follicle interface ranges from –58 to –51 mV, which yields an effective partition coefficient ranging between 0.114 and 0.149. Similarly, for the follicle:lumen interface, $\phi_i - \phi_o$ ranges from +50 to +58 mV, rendering the effective partition coefficient between 6.48 and 8.74.

Though the electrochemical potentials were not measured in the other tissues, tissue:plasma ratios of doses large enough to saturate the active transport process were used as "effective partitions". Effective partition coefficients for ClO_4^- in the skin and GI tract and contents were calculated from the tissue:plasma ratios measured in the 10.0 mg/kg-day drinking water dose of the lactation drinking water study (Yu, 2000). The 10.0 mg/kg-day dose is sufficient to cause saturation of the tissues with NIS and is therefore considered a reasonable dose for estimating the effective partition coefficients. In the drinking water studies, measurements were taken after 18 days of dosing, allowing the assumption that the system was at steady state. The ClO_4^- tissue:plasma ratios measured in the drinking water studies at the 10 mg/kg-day dose group were thus considered to be a realistic estimate of the effective partitioning within these tissues. Effective ClO_4^- partition coefficients for the skin, GI tract and GI contents were calculated to be 1.15, 1.8 and 2.3 in the dam and neonate, respectively. Partitioning in the neonatal skin was given the same value as the dam. The effective partitions for the GI tract and contents were calculated in the same manner as the dam and were calculated to be 3.21 and 5.24, respectively.

The tissues that did not contain NIS were not analyzed for perchlorate in the lactation drinking water studies performed by Yu (2000). Therefore, effective partition coefficients were calculated from data available in literature and from *iv* dosing studies in the male rat (Yu *et al.*, 2000). The effective partitions for the slowly perfused (muscle), richly perfused (liver), kidney and red blood cells were calculated from the tissue:plasma ratios obtained during the clearance stage of perchlorate, after *iv* dosing with 3.3 mg/kg ClO_4^-.

Pena *et al.* (1976) measured tissue:blood ratios in the laying hen after intra-muscular dosing with either a single injection of 10 μCi or 3 sequential doses of 10 μCi radiolabeled $^{36}ClO_4^-$. Although the hen is a very different species, several of other tissues were reported to have values comparable to those found by Yu (2000) and Yu *et al.* (2000) in the male and female rat (0.3 vs. 0.31 in muscle, 0.1 vs. 0.1 in brain, 0.8 vs. 0.99 in the kidney). Therefore, the value of 0.05 reported for the partitioning of perchlorate into the fat of the hen was used to represent the fat in the lactating rat and neonate. The use of this value is supported by the fact that the polarity of the perchlorate anion would severely limit the movement of ClO_4^- into fatty lipophilic tissue. Anbar *et al.* (1959) measured the mammary gland:blood ratios in the rat four hours after an intra-peritoneal injection of radiolabeled $^{36}ClO_4^-$ (100 mg $KClO_4$). They reported an effective partition of 0.66 for the rat mammary gland.

Iodide. Thyroid effective partition coefficients for iodide were assigned within the same range previously calculated for perchlorate, since both perchlorate and iodide are monovalent anions and would be affected similarly by the electrochemical gradient. A partition coefficient for the movement of iodide into fat was not available in literature. Therefore, the values found for perchlorate were utilized in the description of the movement of iodide between fatty tissue and serum. Like perchlorate, the polarity of the iodide anion is expected to severely limit the movement of ClO_4^- into fatty, lipophilic tissue. Since the partition for iodide into the mammary was not available in literature, the mammary gland was assigned the same partition coefficient as that given for ClO_4^- in Anbar *et al.* (1959).

Tissue:blood ratios for iodide in the liver (0.40) and muscle (0.21) given in Halmi *et al.* (1956) were used to estimate the richly and slowly perfused partition coefficients. Halmi measured organ to serum concentration ratios in rats at 1, 4 and 24 hours after administering a tracer dose of radiolabeled iodide by intravenous injection. Similar values were given in Perlman *et al.* (1941) for rabbits, five hours after subcutaneous dosing with a tracer dose of iodide. Perlman also reported a tissue:blood ratio of approximately 0.7 in the skin after *iv* dosing, which remained relatively constant out to 96 hours. Maternal and fetal skin were described using this value as a partition coefficient.

When available, iodide partition coefficients were calculated from the tissue:blood ratios measured during the clearance phase of iodide data in the tissue of interest. For example, GI tract and contents were determined from the clearance portion of the data from the iodide kinetic study in the lactating rat.

Permeability area cross products (PA) are used in the model to limit the movement of the anion between tissues where multiple compartments are described with partition coefficients. Reducing the PA value slows the movement between the compartments; increasing the PA allows the anion to move between compartments more quickly. These values were fit by comparing the model simulation to available data. Effective partitioning into a tissue can be seen in the following equations utilizing both PAs and partition coefficients, where *RAXB_y* is the rate of change of chemical *y* in the blood of compartment *X*, *RAX_y* is the rate of change of chemical *y* in the tissue of compartment *X*, *QX* is the fractional blood flow to the compartment's capillary

bed, *CA_y* is the arterial concentration of *y* and *CVXB_y* is the concentration of *y* in the tissue blood.

$$RAXB\_y = QX * (CA\_y - CVXB\_y) + PAX\_y * \left(\frac{CX\_y}{PX\_y} - CVXB\_i\right)$$

$$RAX\_y = PAX\_y * \left(CVXB\_y - \frac{CX\_y}{PX\_y}\right)$$

Model Equations. The following equations represent the distribution of iodide within the thyroid, in the absence of competitive inhibition. Perchlorate and other tissues of active uptake are described in a similar manner.

$$RATB\_i = QT * (CA\_p - CVTB\_i) + PAT\_i * \left(\frac{CT\_i}{PT\_i} - CVTB\_i\right) - RupT\_i$$

$$RAT\_i = RupT\_i + PAT\_i * \left(CVTB\_i - \frac{CT\_i}{PT\_i}\right) - RupDT\_i + PADT\_i * \left(\frac{CDT\_i}{PDT\_i} - CT\_i\right)$$

$$RADT\_i = RupDT\_i + PADT\_i * \left(CT\_i - \frac{CDT\_i}{PDT\_i}\right)$$

$$RupT\_i = \frac{V\max\_Ti * CVTB\_i}{Km\_Ti + CVTB\_i}$$

$$RupDT\_i = \frac{V\max\_DTi * CT\_i}{Km\_DTi + CT\_i}$$

RATB_i, *RAT_i* and *RADT_i* are the rates of change in perchlorate amount in the thyroid stroma, follicle and colloid, respectively. *PAT_I, PADT_i* and *PT_I, PDT_i* are the PA's and effective partition coefficients for the stroma:follicle and follicle:colloid membranes, respectively. *RupT_i* and *RupDT_i* are the rates of active uptake of perchlorate into the follicle and colloid. *Vmax_Ti*, *VmaxDT_i* and *Km_Ti*, *Km_DTi* are the maximum velocities and affinity constants for the transport of perchlorate into the follicle and colloid, respectively. *QT* represents the fractional blood flow to the thyroid capillary bed. *CA_i*, *CVTB_i*, *CT_i* and *CDT_i* are the perchlorate concentrations in the arterial plasma, thyroid stroma, follicle and colloid, respectively.

The inhibited thyroid is described in the same manner as shown above, with changing only the Michealis-Menten terms for active sequestration. The following equations describe competitive inhibition of iodide uptake by perchlorate. As before, RupDT_i and RupT_i represent the rates of active uptake of iodide into the thyroid colloid and follicle, respectively. These rates are modified by the affinity of transport mechanisms in the follicle and colloid for perchlorate (Km_Tp and Km_DTp, respectively) and the concentration of ClO_4^- in the follicle and colloid (CT_p and CDT_p, respectively), where the Km is equal to the inhibition constant (Ki) for a competitive inhibitor (perchlorate) (Wolff, 1963)

$$RupT\_i = \frac{V\max\_Ti * CVTB\_i}{Km\_Ti * \left(1 + \frac{CVTB\_p}{Km\_Tp}\right) + CVTB\_i}$$

$$RupDT\_i = \frac{V\max\_DTi * CT\_i}{Km\_DTi * \left(1 + \frac{CT\_p}{Km\_DTp}\right) + CT\_i}$$

RESULTS AND DISCUSSION

Model Development

Perchlorate Parameterization. In order to describe the blood perchlorate concentrations at the lower doses (0.01 and 0.1 mg/kg-day), it was necessary to include binding of perchlorate in the serum. Figures 2 and 3 illustrate the importance of binding in the model simulations of maternal serum. Binding does not have a noticeable effect on the plasma concentrations in the highest dose. However, as the perchlorate dose decreases, the effect of binding is more pronounced because a larger percent of the injected dose is bound. As the dose is increased, the binding process is saturated and eventually the amount of bound perchlorate is negligible in contrast to the large amount of free perchlorate in the plasma. In these and subsequent plots, the solid lines indicate the model prediction and cross-bars indicate the mean ± one standard deviation, unless indicated otherwise.

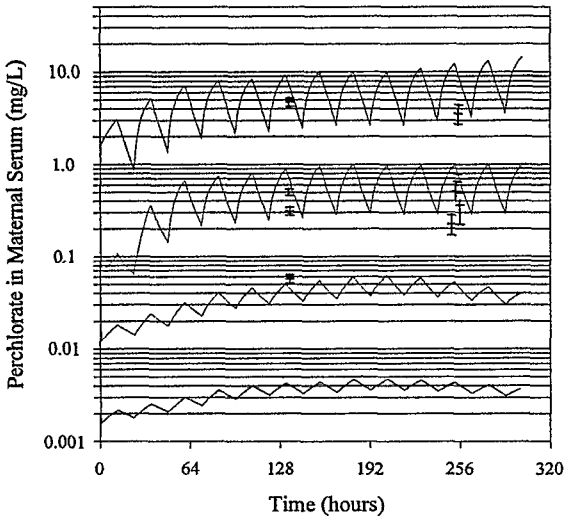

Figure 2. Perchlorate concentration in serum of the dam at the 0.01, 0.1, 1.0 and 10.0 mg/kg-day dose groups on PND 5 and 10, simulated without binding

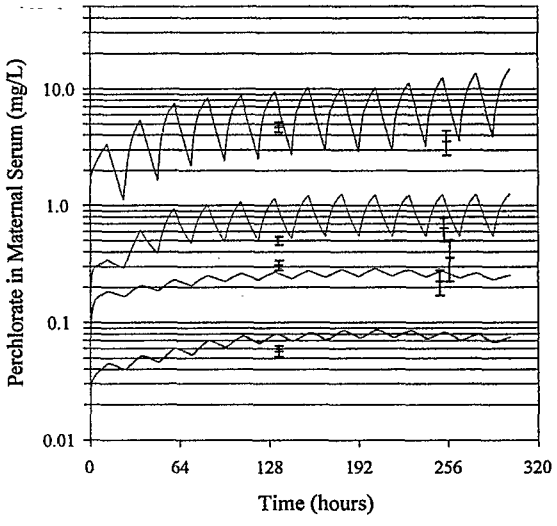

Figure3. Perchlorate concentration in serum of the dam at the 0.01, 0.1, 1.0 and 10.0 mg/kg-day dose groups on PND 5 and 10, simulated with binding

Perchlorate model parameterization for the tissues was performed using data obtained from the PND 5 and 10 drinking water studies. Optimized kinetic parameters (Vmax and PA) were determined by visually fitting the model simulation to the experimental data. Other parameters, such as partition coefficients, were obtained from literature or experiments as described previously. Figures 5 through 8 show the perchlorate tissue concentrations at PND 5 and 10 in the lactating dam at the 0.01, 0.1, 1.0 and 10.0 mg/kg-day doses. It was noticed that during the drinking water studies, the daily dose to the dams varied somewhat due to their changing water intake. Therefore, all of the model simulations of the drinking water studies reflect the actual daily dose to the dam, which was calculated from the daily water consumption and body weight measurements.

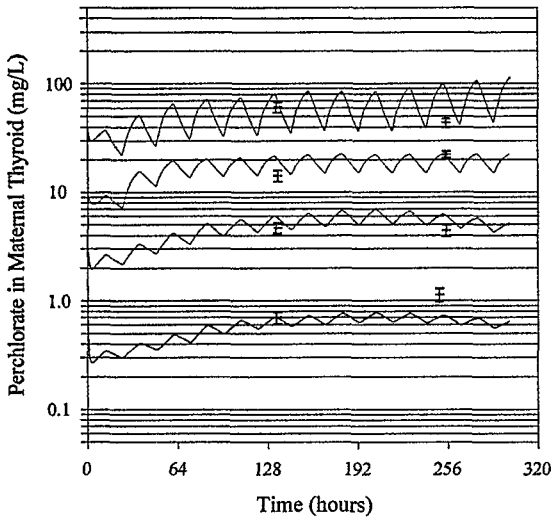

Figure 5. Perchlorate concentration in the thyroid of the dam at the 0.01, 0.1, 1.0 and 10.0 mg/kg-day dose groups on PND 5 and 10

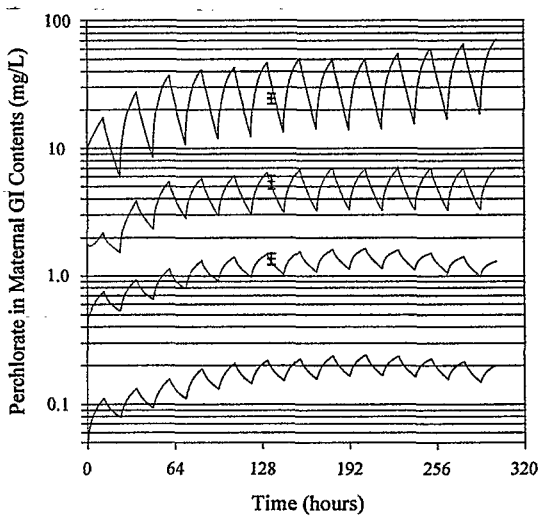

Figure 6. Perchlorate concentration in the GI contents of the dam at the 0.01, 0.1, 1.0 and 10.0 mg/kg-day dose groups on PND 5 and 10. Data from 0.01 mg/kg-day dose were below analytical detection.

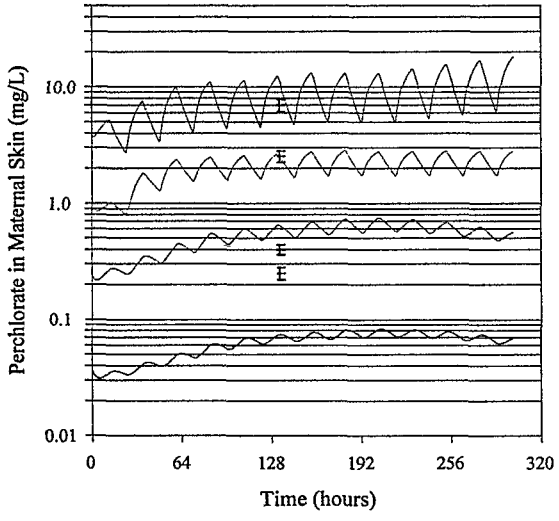

Figure7. Perchlorate concentration in the skin of the dam at the 0.01, 0.1, 1.0 and 10.0 mg/kg-day dose groups on PND 5 and 10

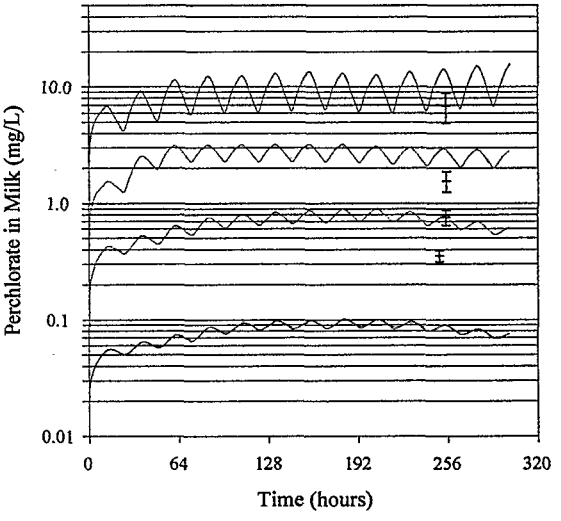

Figure 8. Perchlorate concentration in the milk at the 0.01, 0.1, 1.0 and 10.0 mg/kg-day dose groups on PND 5 and 10

In the tissues with active uptake, perchlorate enters the tissues by two routes, active transport by NIS and diffusion. The behavior of the data suggests that the symporter (NIS) is saturated at a dose between 1.0 and 10.0 mg/kg-day. Therefore, the influence of active uptake in the tissues was primarily in these lower doses and diffusion becomes the dominant route at the 10 mg/kg-day dose. Since the value for Km was estimated from *in vitro* studies in literature as previously described, the Vmax value for the active uptake was used to fit the model simulation of the 0.01

to 1.0 mg/kg-day doses to the available data in the tissues. At the 10 mg/kg-day dose, diffusion was primarily affected by the partition coefficients and PA values. Partition coefficients were assigned as previously described and PA values were obtained by fitting the simulation of the 10 mg/kg-day dose group dose to the available data in the appropriate tissues. The serum, GI contents, milk and thyroid were well described by the model with the described parameters. The simulation of the milk under-predicted the amount of perchlorate transferred in the lowest dose. It is unclear why the model was not able to fit the low dose data. However, the model was able to maintain fits to milk in the three higher doses. Because of the variable nature of the measurements of skin perchlorate, the model was unable to fit the data at all four doses.

Maternal mammary gland perchlorate concentrations were only measured at the 10 mg/kg dose. Therefore, these data were not useful in determining the values for the active uptake parameters. However, the mammary gland data were useful in verifying the applicability of the assigned partition coefficients to the model. Therefore, the Vmax in the mammary gland was fit to the milk and serum data in the drinking water study and the mammary gland values in the perchlorate kinetics study. Figure 9 demonstrates the fit of the simulation to the mammary gland in the 10.0 mg/kg-day dose group.

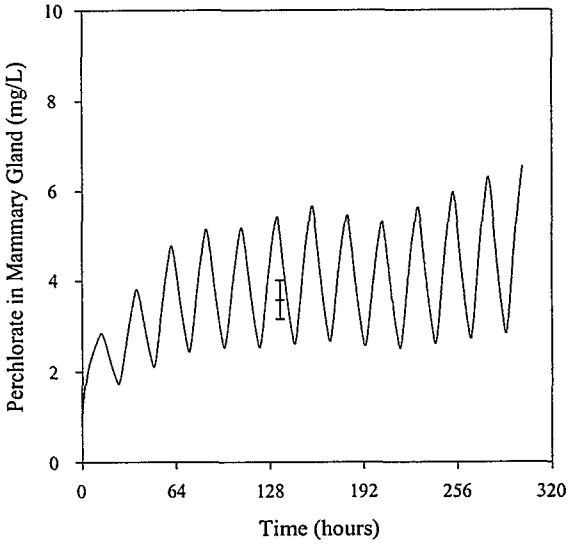

Figure 9. Perchlorate concentration in the maternal mammary gland at the 10.0 mg/kg-day dose group on PND 5

Figures 10 and 11 show the model simulations of the male and female neonate plasma levels compared to the data obtained in the original drinking water study. It was found that plasma concentrations varied significantly between the male and female neonates; this difference appears to be a function of age. At PND 5, the male neonatal plasma concentrations were nearly 4 times higher than those of the female neonates in the 0.1 mg/kg-day dose group. By PND 10, however, no significant sex difference was found in the plasma perchlorate concentrations at the same dose. The dependence of neonatal plasma concentrations on the age and gender of the pups at the 0.1, 1.0 and 10.0 mg/kg-day dose groups is shown in the Figures 10 and 11.

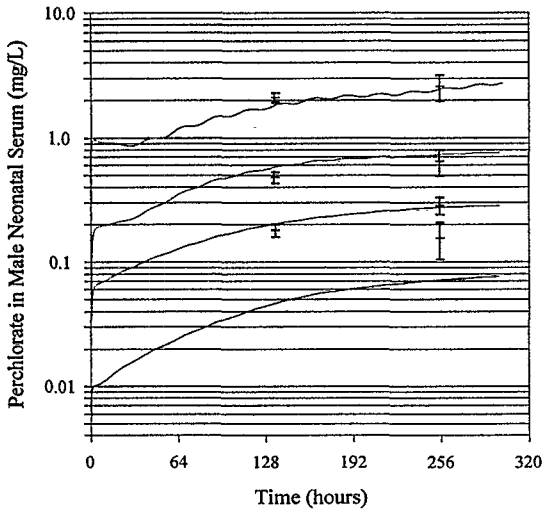

Figure 10. Perchlorate concentration in the plasma of male neonates in the 0.01, 0.1, 1.0 and 10.0 mg/kg-day dose groups on PND 5 and 10

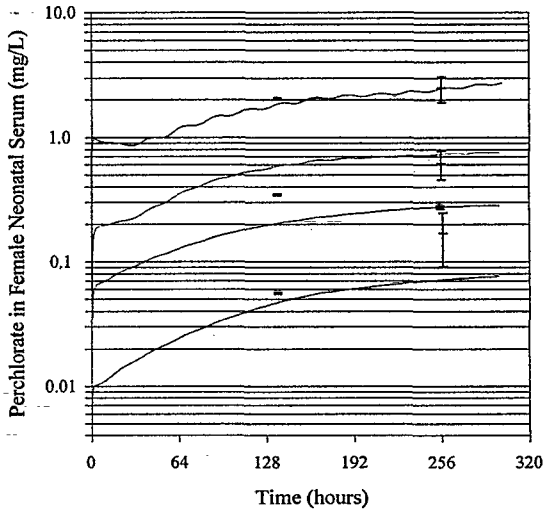

Figure 11. Perchlorate concentration in the plasma of female neonates in the 0.01, 0.1, 1.0 and 10.0 mg/kg-day dose groups on PND 5 and 10

Neonatal serum was fit to the male neonatal data, since the male pups showed higher perchlorate concentrations in the serum than the female pups (Yu, 2000). The neonatal serum was under-predicted by the model in the 0.01 mg/kg-day dose group. This is undoubtedly due to the fact that the milk concentration is also under-predicted in that same dose group. However, the three higher doses are well described in the male neonate. The female pups also show acceptable fits at PND 10. However, since the PND 5 data are much lower in the female than male neonates, the model over-predicts the PND 5 time-points in the 0.1 and 1.0 mg/kg-day doses. As in the maternal model, the clearance value for urinary excretion was determined by the fit of the model to the serum from the 10 mg/kg-day dose, while the lower doses were used to determine the kinetic parameters for the binding in the neonate. Both binding and urinary clearance were considerably lower in the pup than in the dam (see Table 2).

Perchlorate analysis of the neonatal skin in the drinking water study was only available for the 10.0 mg/kg-day dose group on PND 5. However, the cross-fostering data provided neonatal skin data at 1.0 mg/kg-day on PND 10. The cross fostering group that was dosed throughout both gestation and lactation followed a protocol identical to that of the drinking water study. Therefore, these two data sets were used together to determine the parameters for the neonatal skin. Neonatal skin diffusion parameters were determined with the values from the 10.0 mg/kg-day pups and the 1.0 mg/kg-day true-exposed cross-fostering pups were used to determine the parameters for active uptake. Figure 12 shows the prediction of the neonatal skin at maternal drinking water doses of 1.0 and 10.0 mg/kg-day.

TABLE 2: PERCHLORATE SPECIFIC PARAMETERS

Perchlorate Parameters	Lactation Values		Source
Partition Coefficients (unitless)	**Dam**	**Neonate**	
Slowly Perfused / Plasma PS_	0.31	0.31	Yu *et al.*, 2000
Rapidly Perfused / Plasma PR_	0.56	0.56	Yu *et al.*, 2000
Fat/ Plasma PF_	0.05	0.05	Pena *et al.*, 1976
Kidney/ Plasma PK_	0.99	0.99	Yu *et al.*, 2000
Liver/Plasma PL_	0.56	0.56	Yu *et al.*, 2000
Gastric Tissue/Gastric Blood PG_	1.80	3.21	Yu, 2000; Yu *et al.*, 2000
Gastric Juice/Gastric Tissue PGJ_	2.30	5.64	Yu, 2000; Yu *et al.*, 2000
Skin Tissue/Skin Blood PSk_	1.15	1.15	Yu *et al.*, 2000
Thyroid Tissue/Thyroid Blood PT_	0.13/2.0	0.13/2.0	Chow and Woodbury, 1970; Yu, 2000[∞]
Thyroid Lumen/Thyroid Tissue PDT_	7.0	7.0	Chow and Woodbury, 1970; Yu, 2000
Red Blood Cells/Plasma PRBC_	0.73	0.73	Yu *et al.*, 2000
Mammary Tissue/ Mammary Blood PM_	0.66	---	Anbar *et al.*, 1959
Milk/Mammary Tissue PMk_	2.39	---	Yu, 2000
Max Capacity, Vmaxc (ng/hr/kg BW)			
Thyroid Follicle Vmaxc_T	1.50E+03	1.50E+03	fitted*
Thyroid Colloid Vmaxc_DT	1.00E+04	1.00E+04	fitted*
Skin Vmaxc_S	8.00E+05	8.00E+05	fitted
Gut Vmaxc_G	1.00E+06	1.00+06	fitted
Mammary Tissue Vmaxc_M	2.0E+5/2.0E+4	---	fitted[∞]
Milk Vmaxc_Mk	2.00E+04	---	fitted
Plasma Binding Vmaxc_B	9.00E+03	1.00E+03	fitted
Affinity Constants, Km (ng/L)			
Thyroid Follicle Km_T	1.00E+05	1.00E+05	Gluzman & Niepomniszcze, 1983; Wolff, 1998
Thyroid Colloid Km_DT	1.0E+09	1.0E+09	Golstein *et al.*, 1992; Wolff, 1998
Skin Km_S	1.00E+05	1.00E+05	Gluzman & Niepomniszcze, 1983; Wolff, 1998
Gut Km_G	1.00E+05	1.00E+05	Gluzman & Niepomniszcze, 1983; Wolff, 1998
Mammary Km_M	1.0E+05	---	Gluzman & Niepomniszcze, 1983; Wolff, 1998
Milk Km_Mk	1.00E+06	---	fitted
Plasma Binding Km_B	1.00E+04	1.00E+04	fitted
Permeability Area Cross Products, (L/hr-kg)			
Gastric Blood to Tissue PAGc_	1.00	1.00	fitted
Gastric Tissue to Juice PAGJc_	1.00	1.00	fitted
Thyroid Blood to Tissue PATc_	4.0E-05/6.0E-04	4.0E-05/6.0E-05	fitted*[∞]
Thyroid Tissue to Colloid PADTc_	0.01	0.01	fitted
Skin Blood to Tissue PASkc_	0.50	1.00	fitted
Mammary Blood to Tissue PAMc_	0.01	---	fitted
Mammary Tissue to Milk PAMkc_	0.001/1.0		fitted
Plasma to Red Blood Cells PRBCc_	1.00	1.00	fitted
Clearance Values, (L/hr-kg)			
Urinary excretion CLUc_	0.07	0.005	fitted
Dissociation from Binding Sites Clunbc_	0.034	0.034	fitted
Transfer from Milk to Pup Ktransc	6.4E-04 - 1.04E-03		Sampson & Jansen, 1984

* Neonate was given maternal values for Vmax (scaled by body weight) in the absence of data.

[∞] Parameters with two values indicate acute and drinking water parameters, respectively.

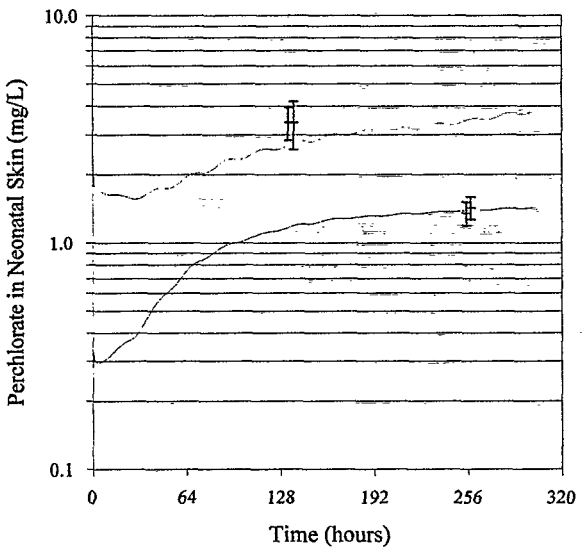

Figure 12 Perchlorate concentration in the skin of the neonate at the 1.0 mg/kg-day dose on PND 10 and the 10.0 mg/kg-day dose on PND 5. Data points are shown for male (left) and female (right) neonates.

As with the neonatal skin, the neonatal GI content data were obtained from the drinking water study at the 10.0 mg/kg-day dose group on PND 5 and the cross-fostering data at the 1.0 mg/kg-day dose on PND 10. Neonatal gastric content diffusion parameters were determined with the values from the 10.0 mg/kg-day pups and the 1.0 mg/kg-day true-exposed cross-fostering pups were used to determine the Vmaxc. Figure 13 depicts the model prediction of neonatal gastric content at maternal drinking water doses of 1.0 and 10.0 mg/kg-day.

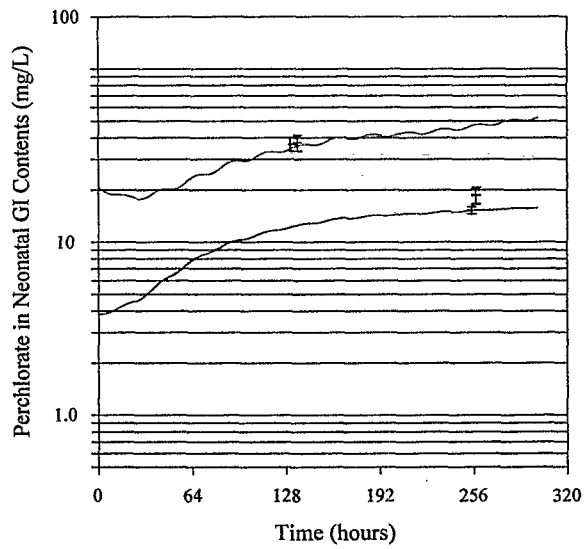

Figure 13. Perchlorate concentration in the GI contents of the neonate at the 1.0 mg/kg-day dose on PND 10 and the 10.0 mg/kg-day dose on PND 5. Data points are shown for male(left) and female (right) neonates.

Iodide Parameterization. Development of the iodide model was performed by visually fitting the model to measured tissue concentrations in the dam and neonate from the control group of the inhibition kinetic study. Partitions and Km values were available from literature and in-house male rat iodide kinetic data, as described previously. Therefore, only the values for Vmax and PA needed to be fit with the model. The model simulations of the *iv* injection of 2.10 ng/kg $^{125}I^-$ on PND 10 versus the experimental data in the lactating dam are shown in Figures 14 through 19.

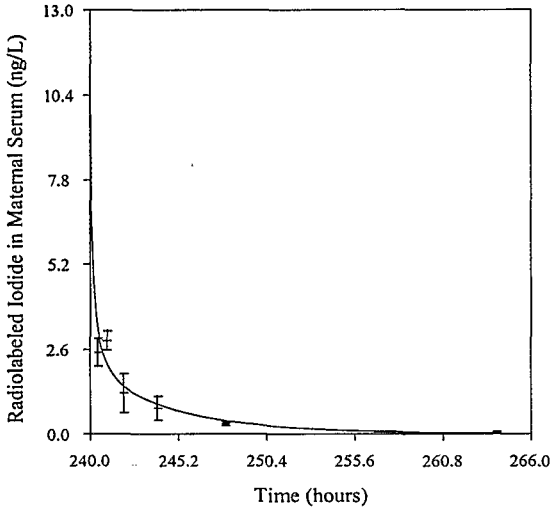

Figure 14. Iodide concentration in maternal serum after *iv* dose of 2.10 ng/kg $^{125}I^-$ on PND 10

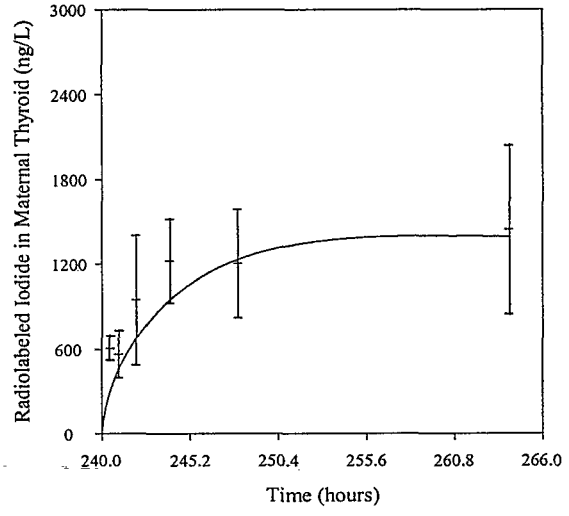

Figure 15. Iodide concentration in maternal thyroid after *iv* dose of 2.10 ng/kg $^{125}I^-$ on PND 10

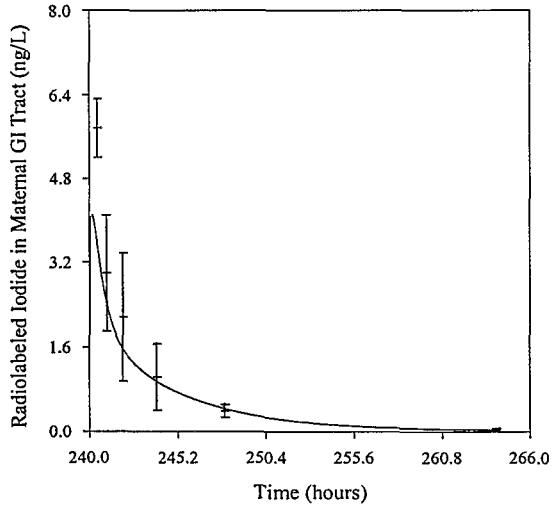

Figure 16. Iodide concentration in maternal GI tract after *iv* dose of 2.10 ng/kg $^{125}I^-$ on PND 10

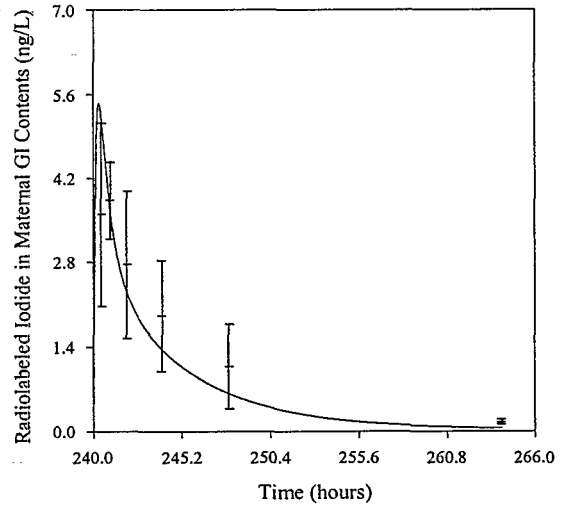

Figure 17. Iodide concentration in maternal GI contents after *iv* dose of 2.10 ng/kg $^{125}I^-$ on PND 10

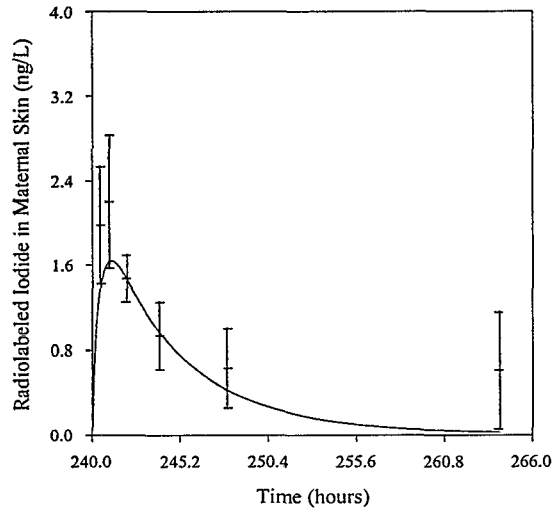

Figure 18. Iodide concentration in maternal skin after *iv* dose of 2.10 ng/kg $^{125}I^-$ on PND 10

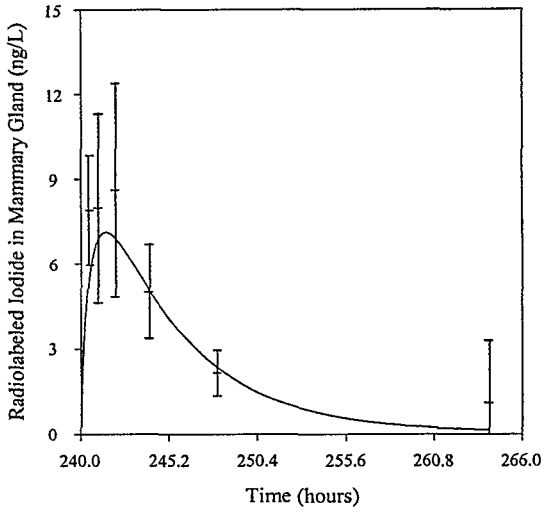

Figure 19. Iodide concentration in mammary gland after *iv* dose of 2.10 ng/kg $^{125}I^-$ on PND 10

The model simulations describe the data well, using the literature and experimental parameters described in the Methods section. The clearance value for urinary excretion was determined by fitting the maternal serum prediction to the above data, while keeping good fits in the other tissues, such as maternal skin, GI and mammary gland. PA values were adjusted to describe the behavior of the iodide data; varying the PA values toward 1.0 L/hr-kg generally increased the rate at which uptake and clearance in a particular tissue occurred; decreasing PA slowed the uptake and clearance. Figures 20 through 24 show the model simulations versus the neonate control data in the inhibition time course study.

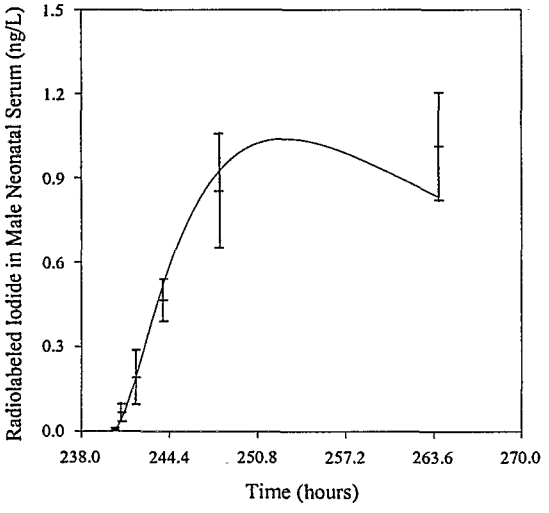

Figure 20. Iodide concentration in serum of male neonate after *iv* dose of 2.10 ng/kg $^{125}I^-$ to the dam on PND 10

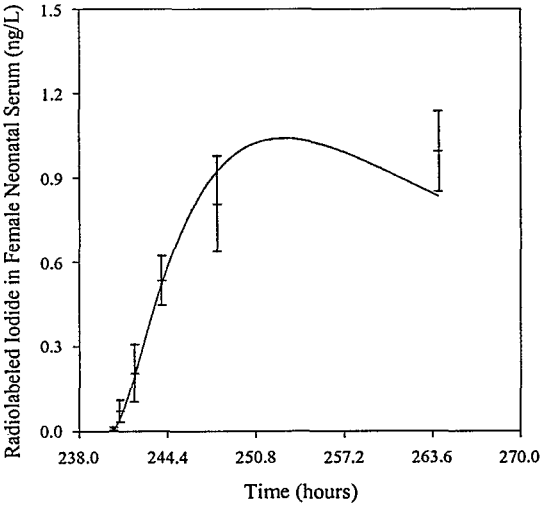

Figure 21. Iodide concentration in serum of female neonate after *iv* dose of 2.10 ng/kg $^{125}I^-$ to the dam on PND 10

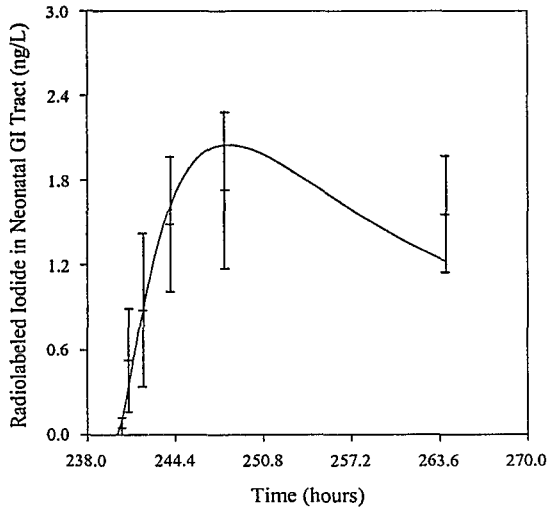

Figure 22. Iodide concentration in neonatal GI tract after *iv* dose of 2.10 ng/kg $^{125}I^-$ to the dam on PND 10

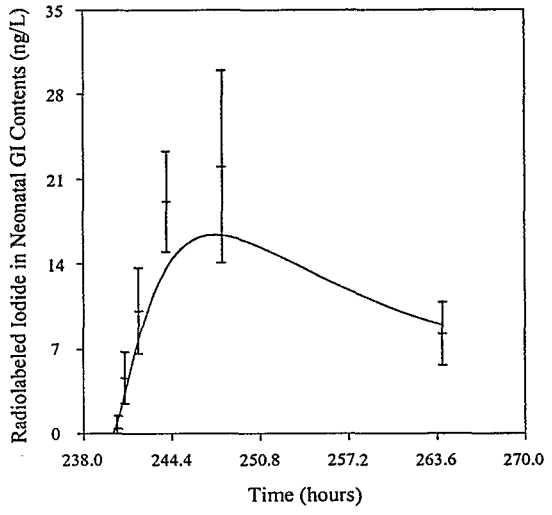

Figure 23. Iodide concentration in neonatal GI contents after *iv* dose of 2.10 ng/kg $^{125}I^-$ to the dam on PND 10

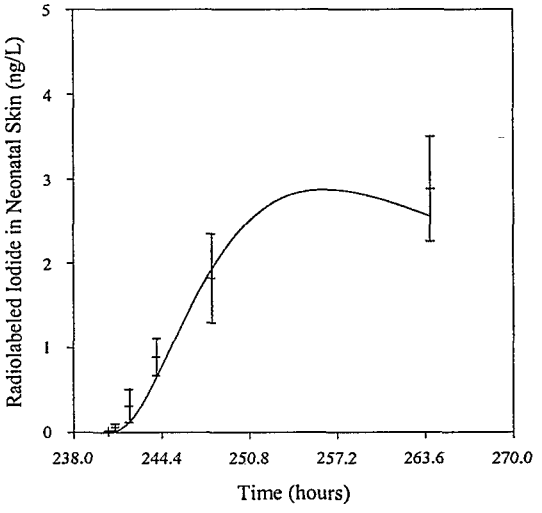

Figure 24. Iodide concentration in neonatal skin after *iv* dose of 2.10 ng/kg $^{125}I^-$ to the dam on PND 10

The behavior of the iodide in the neonatal skin and GI tract and contents appeared to be different from the dam. The iodide tended to stay in the tissue of the neonate longer, requiring a slower clearance in the fetal tissues than was used in the corresponding maternal tissue. As a result, PA values used for the GI and skin in the neonate were lower than those used in the dam (Table 3). For example, the PA value in the skin was determined to be 0.5 L/hr-kg in the dam, but was decreased to 0.02 L/hr-kg in the neonate. However, these values correspond well to the values used for the fetus in the pregnancy model (Clewell, 2001). The neonatal urinary clearance value was determined to be 0.02 L/hr-kg BW of the neonate, which is very similar to the maternal

value (0.03 L/hr-kg BW of the dam). This came as a surprise, since the neonate was expected to have a much lower rate of excretion than the more mature dam. However, this trend is supported in literature. Capek and Jelinek (1956) measured the amount excreted by pups at various ages. They found that the neonates required external stimulation by the mother in order to release the urine from their bladders. However, when that stimulation was supplied, the neonates were able to excrete urine at the same rate as an adult rat. Therefore, it is reasonable that the urinary excretion rate is similar between the pup and adult. The amount of iodide lost to urine is then dependent on both the urinary clearance value and the concentration of the ion in the kidney.

TABLE 3: IODIDE SPECIFIC PARAMETERS

Iodide Parameters	Lactation Values		Source
Partition Coefficients (unitless)	**Dam**	**Neonate**	
Slowly Perfused / Plasma PS_	0.21	0.21	Halmi *et al.*, 1956
Rapidly Perfused / Plasma PR_	0.40	0.40	Halmi *et al.*, 1956
Fat/ Plasma PF_	0.05	0.05	Pena *et al.*, 1976
Kidney/ Plasma PK_	1.09	1.09	Perlman *et al.*, 1941
Liver/Plasma PL_	0.44	0.44	Perlman *et al.*, 1941
Gastric Tissue/Gastric Blood PG_	1.00	1.00	Unpublished Lactation Inhibition Study
Gastric Juice/Gastric Tissue PGJ_	1.00	3.50	Unpublished Lactation Inhibition Study
Skin Tissue/Skin Blood PSk_	0.70	0.70	Perlman *et al.*, 1941
Thyroid Tissue/Thyroid Blood PT_	0.15	0.15	Chow and Woodbury, 1970
Thyroid Lumen/Thyroid Tissue PDT_	7.00	7.00	Chow and Woodbury, 1970
Red Blood Cells/Plasma	1.00	1.00	Rall *et al.*, 1950
Mammary Tissue/ Mammary Blood PM_	0.66	---	Anbar *et al.*, 1959
Milk/Mammary Tissue PMk_	4.00	---	Yu, 2000
Max Capacity, Vmaxc (ng/hr/kg BW)			
Thyroid Follicle Vmaxc_T	4.00E+04	4.00E+04	fitted*
Thyroid Colloid Vmaxc_DT	6.00E+07	6.00E+07	fitted*
Skin Vmaxc_S	6.00E+04	2.50E+05	fitted
Gut Vmaxc_G	1.00E+06	2.00E+05	fitted
Mammary Tissue Vmaxc_M	8.00E+05	---	fitted
Milk Vmaxc_Mk	5.00E+06	---	fitted
Affinity Constants, Km (ng/L)			
Thyroid Follicle Km_T	4.00E+06	4.00E+06	Gluzman and Niepomniszcze, 1983
Thyroid Colloid Km_DT	1.00E+09	1.00E+09	Golstein *et al.*, 1992
Skin_Km_S	4.00E+06	4.00E+06	Gluzman and Niepomniszcze, 1983
Gut_Km_G	4.00E+06	4.00E+06	Gluzman and Niepomniszcze, 1983
Mammary Km_M	4.00E+06	---	Gluzman and Niepomniszcze, 1983
Milk Km_Mk	1.00E+06	---	fitted
Permeability Area Cross Products, (L/hr-kg)			
Gastric Blood to Gastric Tissue PAGc_	0.80	0.05	fitted
Gastric Tissue to Gastric Juice PAGJc_	0.60	0.06	fitted
Thyroid Blood to Thyroid Tissue PATc_	1.00E-04	1.00E-04	fitted*
Thyroid Tissue to Thyroid Colloid PADTc_	1.00E-04	1.00E-04	fitted*
Skin Blood to Skin Tissue PASkc_	0.50	0.02	fitted
Mammary Blood to Tissue PAMc_	0.02	---	fitted
Mammary Tissue to Milk PAMkc_	1.00	---	fitted
Plasma to Red Blood Cells PRBCc_	1.00	1.00	fitted
Clearance Values, (L/hr-kg)			
Urinary excretion CLUc_	0.03	0.02	fitted
Transfer from Milk to Pup Ktransc	6.4E-04 - 1.04E-03		Sampson & Jansen, 1984

* Neonate was given maternal values for Vmax (scaled by body weight) in the absence of data.

Model Validation

Perchlorate Kinetic Study. The ability of the model to simulate the kinetics of perchlorate in the lactating dam and neonate was tested against the perchlorate time course data collected *in vivo* by AFRL/HEST. Since the study was performed with an acute perchlorate dose, it was necessary to make minor changes in the thyroid perchlorate parameters. The long-term exposure to perchlorate in the drinking water studies, which were used to determine the perchlorate parameters, is sufficient to induce up-regulation in the thyroid (Yu, 2000). Therefore, the thyroid parameters in the dam at this point would be different from those seen in an acute situation. The model fits to the acute data were achieved by altering the partition coefficient (from 2.25 in the drinking water to 0.13 in the acute exposure) and PA value (from 6.0E-4 to 4.0E-5) into the thyroid at the basolateral membrane (thyroid follicle). The value for the partitioning into the follicle in a naïve thyroid was calculated as described previously from Chow and Woodbury (1970). The PA value in the naïve thyroid follicle was determined by fitting the model prediction to the thyroid data, while keeping good fits in the serum and other tissues. Figures 25 through 30 depict the prediction of the model versus the data collected in the acute perchlorate kinetics study.

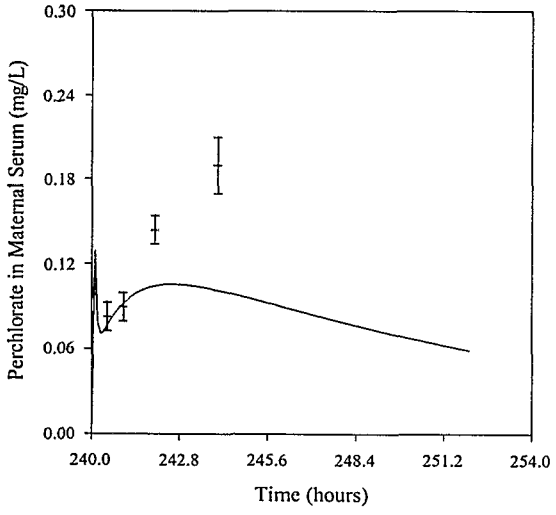

Figure 25. Perchlorate concentration in maternal serum after *iv* dose of $1.0x10^6$ mg/kg ClO_4^- on PND 10

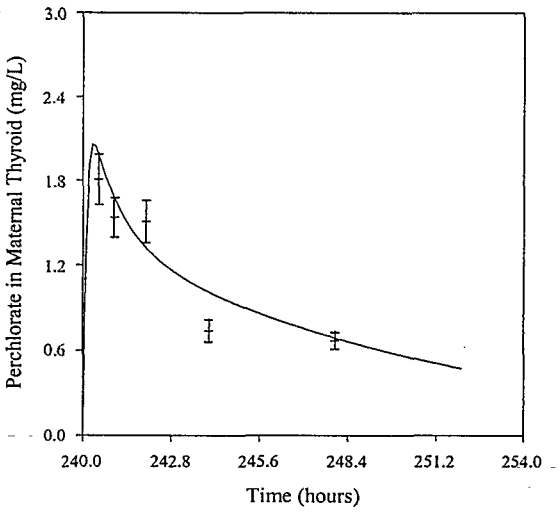

Figure 26. Perchlorate concentration in maternal thyroid after *iv* dose of $1.0x10^6$ mg/kg ClO_4^- on PND 10

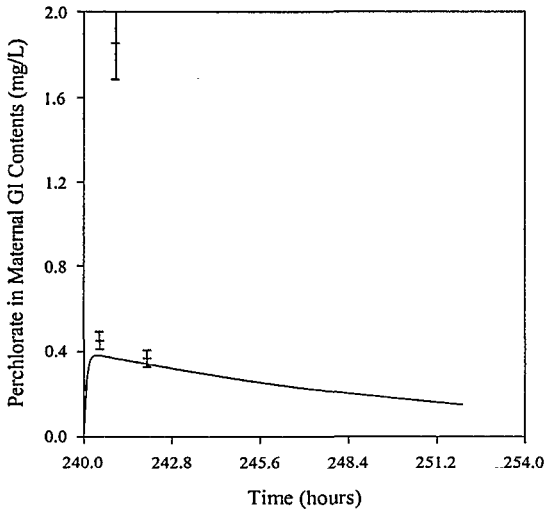

Figure 27. Perchlorate concentration in maternal GI contents after *iv* dose of $1.0x10^6$ mg/kg ClO_4^- on PND 10

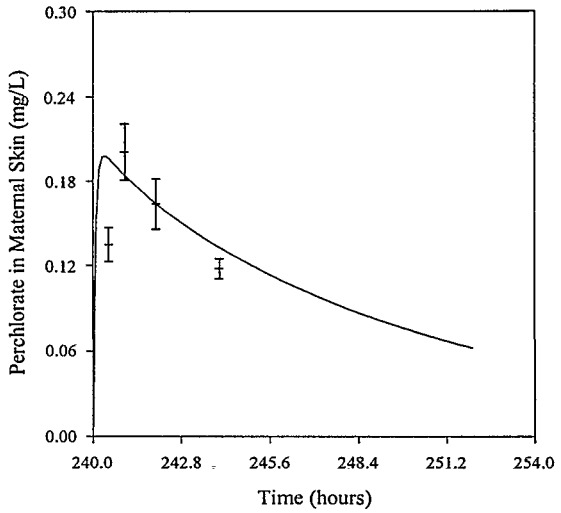

Figure 28. Perchlorate concentration in maternal skin after *iv* dose of $1.0x10^6$ mg/kg ClO_4^- on PND 10

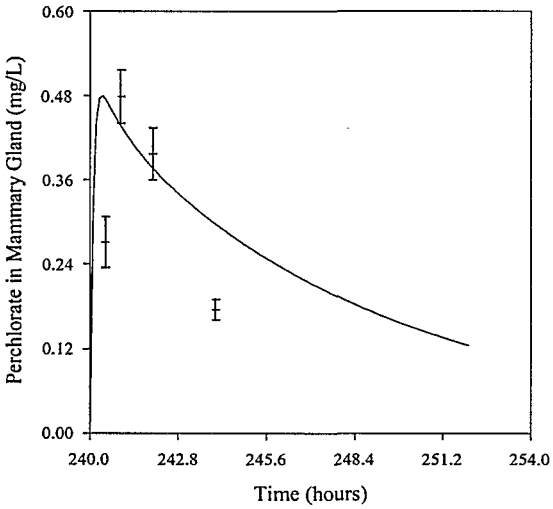

Figure 29. Perchlorate concentration in mammary gland after *iv* dose of $1.0x10^6$ mg/kg ClO_4^- on PND 10

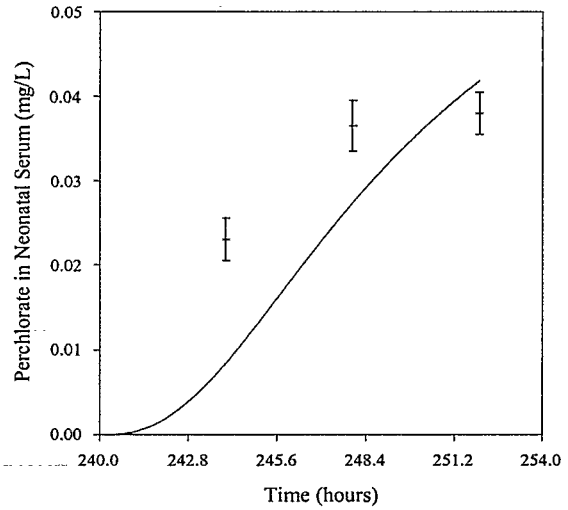

Figure 30. Perchlorate concentration in neonatal serum after *iv* dose of $1.0x10^6$ mg/kg ClO_4^- on PND 10

The acute perchlorate kinetics were simulated with the same parameters determined from the drinking water data. However, it was necessary to increase the transfer of perchlorate through the milk in the acute studies. Therefore, the value for the Vmax into the mammary tissue was increased in order to allow more perchlorate into the mammary compartment; the PA into the milk was decreased in order to minimize the back flow of perchlorate into the mammary from the milk. This essentially forces the perchlorate in the milk to be passed to the neonate rather than returning into the mammary tissue of the mother. The Vmax for the binding in the neonate was decreased slightly from the value used in the drinking water simulations. This may have

been due to increased transfer of iodide in the acute simulations. When the same parameters were used in the mammary compartment that were determined with the drinking water studies, the amount in the mammary tissue was low and the clearance of the mammary was too slow. As a result, acute neonatal serum levels were under-predicted. Through adjusting the Vmax, the model was able to achieve reasonable fits to the available data in the maternal and neonatal tissues. This suggests that different fractions of the dose are transferred through the milk during an acute *iv* exposure versus a drinking water scenario. This phenomenon is unexplained as of yet and, without the use of the model, may have gone unnoticed.

Cross Fostering Study. The cross-fostering study was designed specifically to help in the determination of the importance of gestational versus lactational exposure. To that end, hormones were measured in the neonates from the true exposed, true control and the two groups of pups that were crossed at birth. The comparison of the hormone changes is discussed in detail in another report (Mahle, 2001). Perchlorate measurements were also taken in all four of these groups. It was found that the true control and the neonates that were exposed to perchlorate only during gestation did not have perchlorate in their serum, GI contents or skin at PND 10. This is not surprising, since perchlorate is quickly eliminated in the urine. However, both of the groups that were exposed during lactation (true exposed and the group that was exposed only through lactation) contained similar levels of perchlorate in the tissues. The model was run against these data in order to test the ability of the model against a second drinking water data set and also to examine the behavior of the model when neonates were born with a perchlorate burden and when they began exposure at birth.

As in the original drinking water study, the actual daily perchlorate dose was programmed into the model from the measured daily consumption and body weight measurements. The following plots (Figures 31 through 34) depict the maternal serum and thyroid perchlorate concentrations in the true-exposed (exposed during gestation and lactation) and exposed (only exposed during lactation) groups.

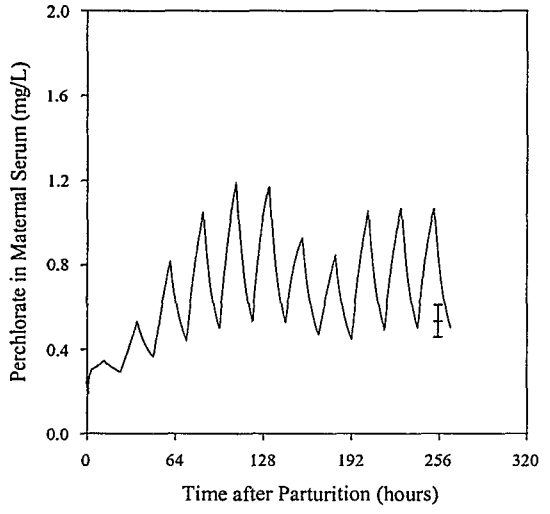

Figure 31. Perchlorate concentration in serum of dams exposed to $1.0x10^6$ mg/kg-day ClO_4^- during gestation and lactation on PND 10

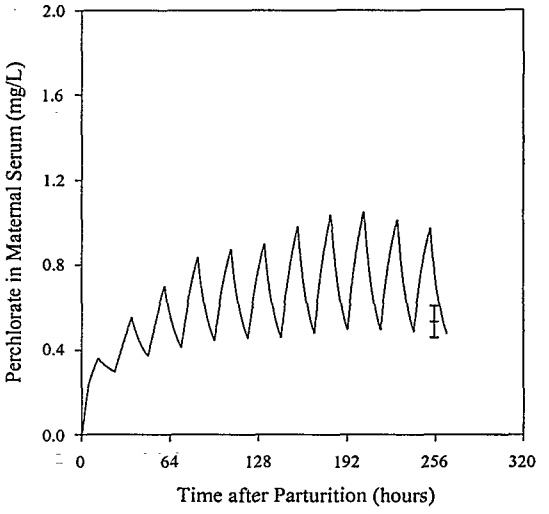

Figure 32. Perchlorate concentration in serum of dams exposed to $1.0x10^6$ mg/kg-day ClO_4^- during lactation only on PND 10

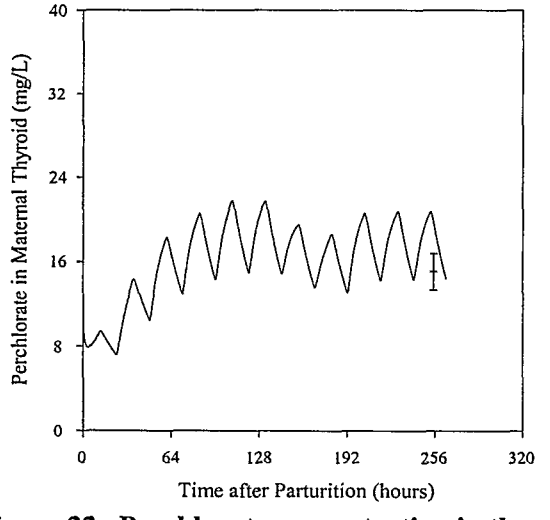

Figure 33. Perchlorate concentration in thyroid of dams exposed to $1.0x10^6$ mg/kg-day ClO_4^- during gestation and lactation on PND 10

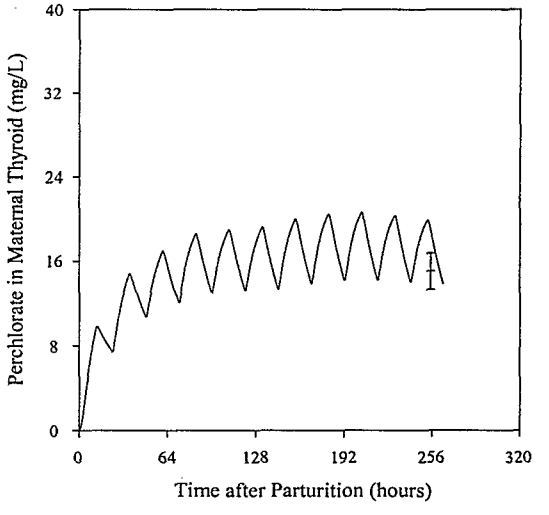

Figure 34. Perchlorate concentration in thyroid of dams exposed to $1.0x10^6$ mg/kg-day ClO_4^- during lactation only on PND 10

The serum of the neonate was also examined with the model. Since the data were taken on PND 10, no significant sex difference was seen between the male and female neonates. As a result, the model simulation for the neonatal plasma was compared to the average of all pups, rather than by sex as in the drinking water study. Figures 35 and 36 illustrate the difference between the true-exposed and exposed neonates.

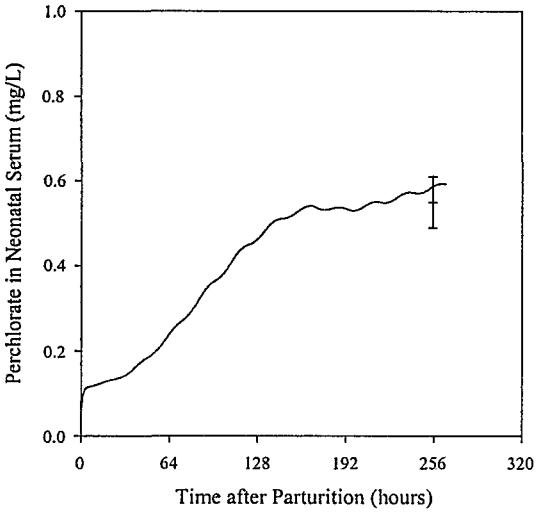

Figure 35. Perchlorate concentration in serum of neonate exposed to $1.0x10^6$ mg/kg-day ClO_4^- during gestation and lactation on PND 10

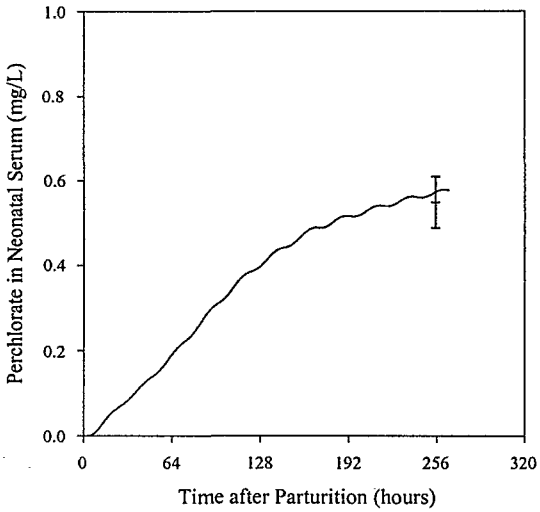

Figure 36. Perchlorate concentration in serum of neonate exposed to $1.0x10^6$ mg/kg-day ClO_4^- during lactation only on PND 10

The model is able to predict the data from the cross-fostering study very well. It is apparent from the data and from the model prediction of the cross-fostering data that the gestational exposure to perchlorate does not affect the perchlorate concentrations of the maternal serum and thyroid, or the neonatal serum. This is in agreement with other studies that indicate the rapid clearance of perchlorate in the urine (Yu *et al.*, 2000). From the model, even though the neonatal urinary excretion is much lower than that of the dam (0.005 vs. 0.07 L/hr-kg), the prenatal exposure does not affect the serum levels of the neonate past PND 2.

Perchlorate Induced Iodide Inhibition. The inhibition of iodide uptake into the thyroid was simulated against the data collected during the in-house inhibition kinetics study on PND 10. The model simulation was compared to available kinetic data in the thyroid, while keeping all iodide parameters as they were described previously during parameterization of the model. The perchlorate parameters determined from the drinking water were used, except in the thyroid and mammary. The partitioning for perchlorate in the thyroid was calculated from Chow and Woodbury (1970) and the perchlorate kinetic study as described above. Figure 37 illustrates the model prediction of thyroidal iodide uptake with and without perchlorate inhibition, utilizing pre-set parameters.

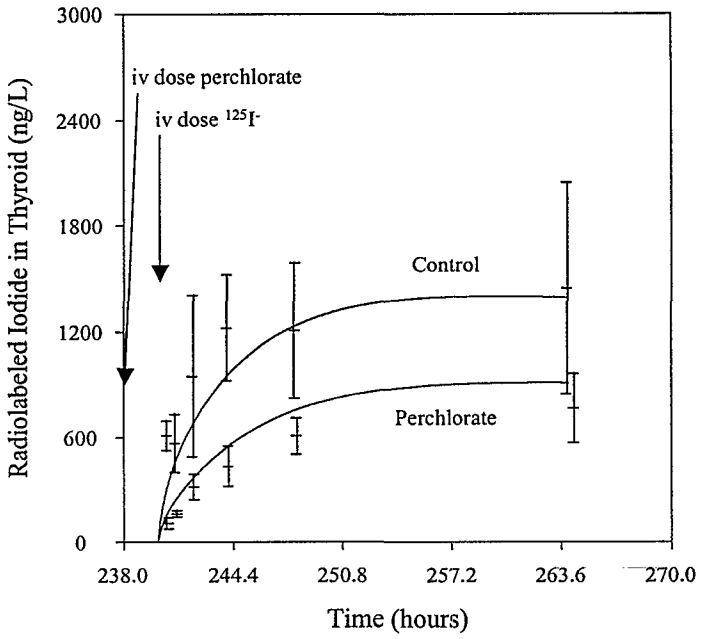

Figure 37. Iodide concentration in maternal thyroid with and without 1.0 mg/kg ClO_4^- *iv* dose 2 hours prior to an *iv* dose of 2.10 ng/kg $^{125}I^-$ to the dam on PND 10. The top simulation (solid line) indicates the control thyroid. The lower simulation and data indicate the inhibited thyroid.

As can be seen in the above figure, the inhibition of iodide in the thyroid gland at 0.5, 1., 2, 4, 8, 12 and 24 hours after dosing with perchlorate was described by the model. The validity of the chosen parameters is supported by the inhibition of iodide, since inhibition is highly dependent on the description of both perchlorate and iodide.

Data of Potter *et al.* (1959). A simulation of data presented by Potter *et al.* (1959) after an injection of 500 μCi carrier free $^{131}I^-$ was performed with the model in order to test the model predictions of diverse data sets collected under different conditions than the data used in parameterization. Since the paper does not specify which animals were dosed on PND 17, 18 or 19, an average value of 18 was used in the model simulation. Previous data sets used in model development were only available for PND 5 and 10. This data set provided an additional time point for the iodide model validation (PND 18). Potter and coauthors were able to measure the amount of iodide in the milk. The milk iodide content was not available in any previous data sets. This study also provides data at time points that were not available in the data used for parameterization (3 and 6 hours post-dosing). Figures 38 through 40 depict the model simulation compared to the experimental data in the maternal serum, thyroid and milk.

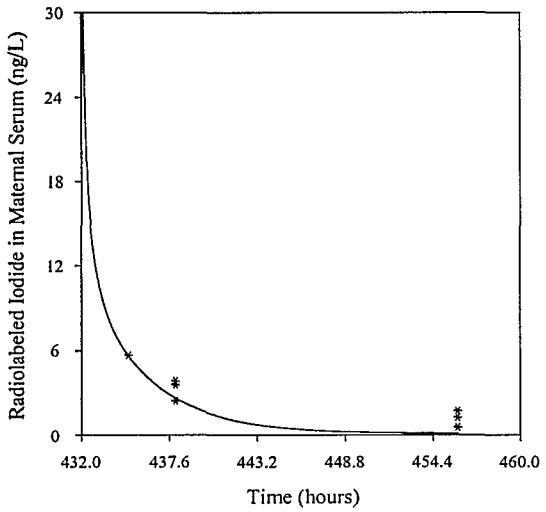

Figure 38. $^{131}I^-$ concentration in maternal serum. The model simulation is shown versus the data from individual dams at 3, 6 and 24 hours post-dosing on PND 18 (Potter *et al.*, 1959).

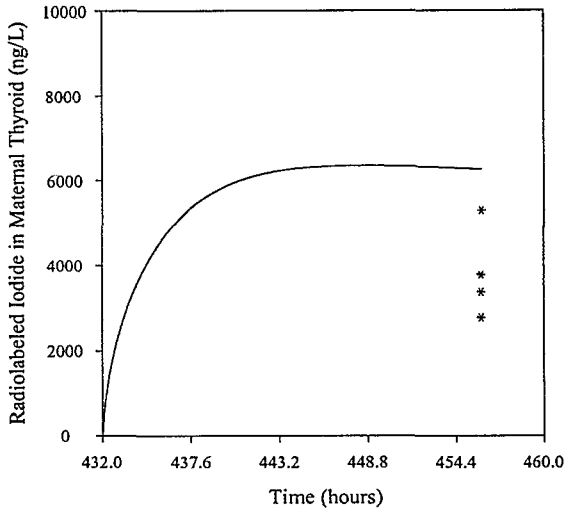

Figure 39. $^{131}I^-$ concentration in maternal thyroid. The model simulation is shown versus the data from individual dams at 24 hours post-dosing on PND 18 (Potter *et al.*, 1959).

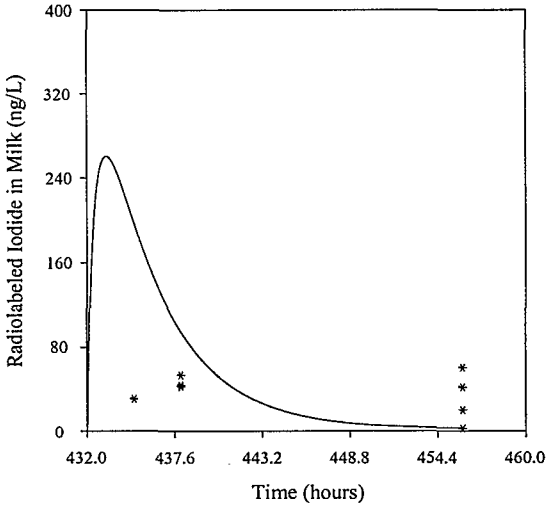

Figure 40. $^{131}I^-$ concentration in milk. The model simulation is shown versus data from individual dams at 3, 6 and 24 hours post-dosing on PND 18 (Potter *et al.*, 1959).

The model was able to produce reasonable simulations of the data of Potter *et al.* (1959) in Long-Evans rats on PND 18. The maternal serum is described very well, using the existing model structure and previously ascribed parameters. The maternal thyroid and milk were slightly over-predicted by the model. The model prediction of the three hour time point in the milk is nearly four times greater than the experimental value. However, the model was within a factor of two from all other data. These fits were achieved without changing any of the parameters. The

ability of the model to simulate data from rats one week later in lactation than the data used in model parameterization is quite remarkable. Additionally, the three and six hour time points were not available in the data used for model parameterization. Thus, the model was able to predict data adequately not only in a different strain of rat, but also later in lactation and at kinetic time points not previously tested during model development.

Data of Sztanyik and Turai, 1988. The data collected by Sztanyik and Turai (1988) allowed the predictive capability of the model to be tested over several days. The authors exposed 3 dams to a dose of either 0.81 or 1.61 ng $^{131}I^-$ by intraperitoneal injection, 24 hours after delivering the neonates. Litter sizes varied with each dam. The total body burden of the neonates were then measured with a whole body counter at 5 hours and 1, 2, 5, 7, 9 and 14 days post-dosing. This data set allowed the model not only to be tested at PND 1, which was a different day from data available previously, but also tested the model description of the neonate by following the body burden of the pup for two weeks after a single dose. The following plots (Figures 41 and 42) show the fit of the model to this data.

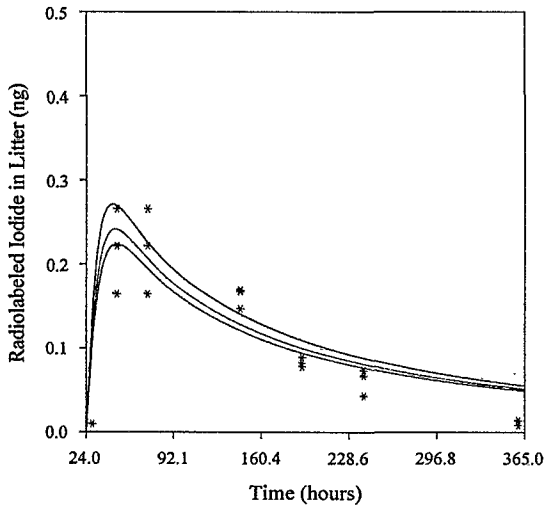

Figure 41. Amount of iodide in total litter at 29 hours and PNDs 2 through 14 after single *iv* dose of 0.81 ng $^{131}I^-$ to dam at 24 hours (Sztanyik & Turai, 1988). Asterisk (*) indicates data point from individual litter. Simulation is shown with litter sizes of 7, 8 and 10 neonates.

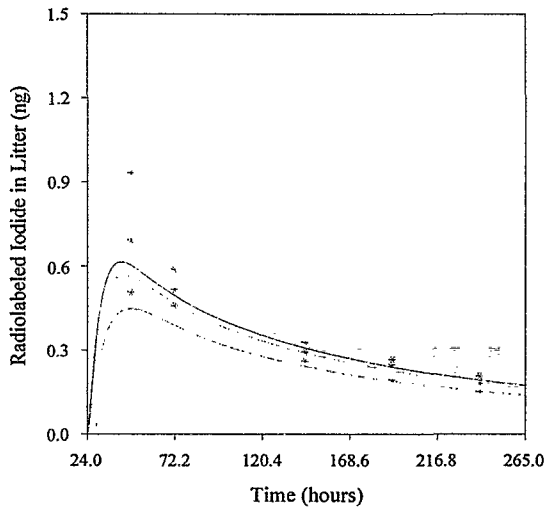

Figure 42. Amount of iodide in total litter at 29 hours and PNDs 2 through 14 after single *iv* dose of 1.61 ng $^{131}I^-$ to dam at 24 hours (Sztanyik & Turai, 1988). Asterisk (*) indicates data point from individual litter. Simulation is shown with litter sizes of 7, 11 and 13 neonates.

The model predicts the data of Sztanyik and Turai (1988) remarkably well out to 14 days post-exposure. The ability of the model to simulate data taken two weeks after a single dose during lactation shows the capability of the model in describing the kinetics of lactation and also illustrates the usefulness of the model when applied to new data sets. Figures 41 and 42 also demonstrate the ability of the model to account for the different kinetic behavior resulting from differing litter sizes. The data reveal that the amount transferred in milk increases with litter

size. The model also responds to the changing number of neonates and reproduces the trend seen in the data.

Drinking Water Inhibition Data. Iodide inhibition and the corresponding behavior in several other maternal and neonatal tissues were measured by AFRL/HEST on PND 5, after maternal exposure to perchlorate in drinking water at doses of 0.0, 0.01, 0.1, 1.0 and 10.0 mg/kg-day for 25 days. The control data from this study were used to test the ability of the model to simulate exposure levels that were more than four orders of magnitude greater than the dose used in model parameterization (33000 ng/kg versus 2.10 ng/kg). Additionally, these data allow the model to be tested at PND 5, a different day in lactation than was used for setting model parameters (PND 10). Figures 41 through 51 illustrate the model prediction of various tissues in the dam and neonate on PND 5. The model was able to produce reasonable fits of the data in the various tissues at the 33000 ng/kg dose on PND 5.

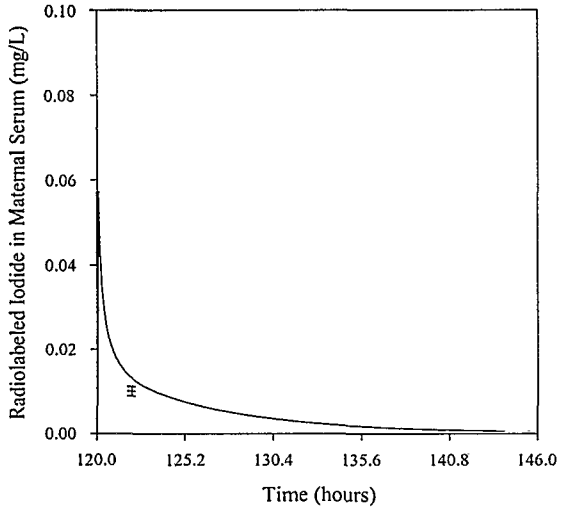

Figure 41. Iodide concentration in maternal serum 2 hours after *iv* dose of 33000 ng/kg $^{125}I^-$ with carrier on PND 5

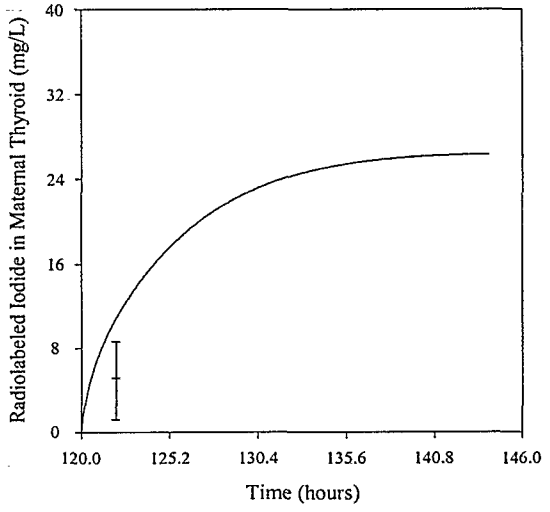

Figure 42. Iodide concentration in maternal thyroid 2 hours after *iv* dose of 33000 ng/kg $^{125}I^-$ with carrier on PND 5

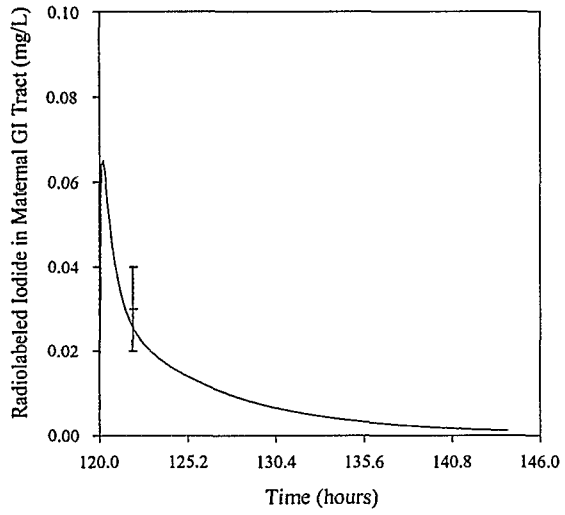

Figure 43. Iodide concentration in maternal GI tract 2 hours after *iv* dose of 33000 ng/kg $^{125}I^-$ with carrier on PND 5

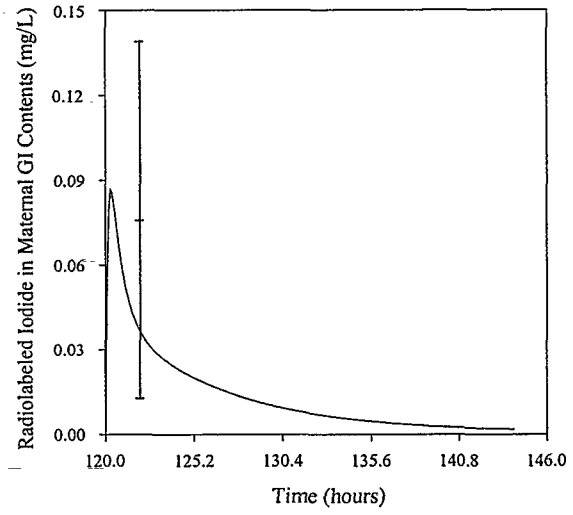

Figure 44. Iodide concentration in maternal GI contents 2 hours after *iv* dose of 33000 ng/kg $^{125}I^-$ with carrier on PND 5

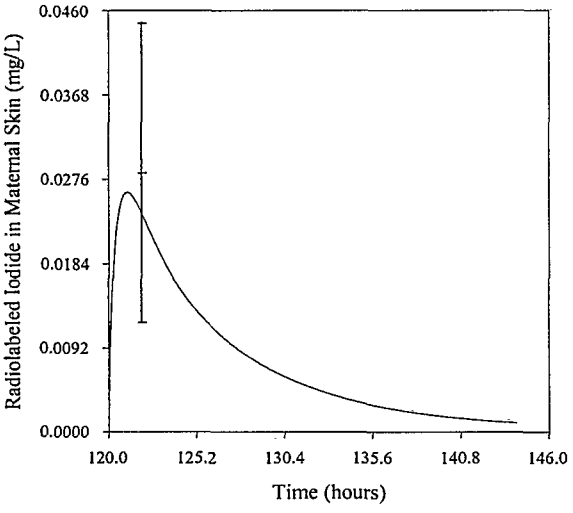

Figure 45. Iodide concentration in maternal skin 2 hours after *iv* dose of 33000 ng/kg $^{125}I^-$ with carrier on PND 5

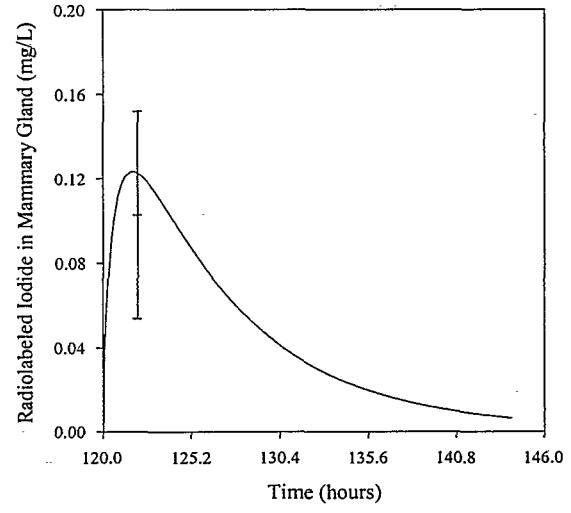

Figure 46. Iodide concentration in mammary gland 2 hours after *iv* dose of 33000 ng/kg $^{125}I^-$ with carrier on PND 5

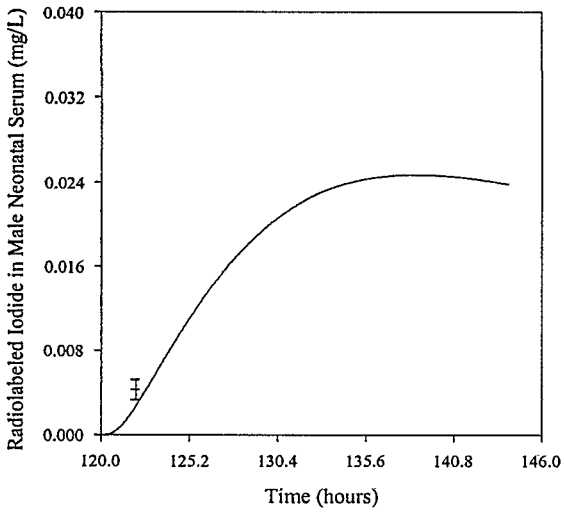

Figure 47. Iodide concentration in male neonatal serum 2 hours after *iv* dose to dam of 33000 ng/kg $^{125}I^-$ with carrier on PND 5

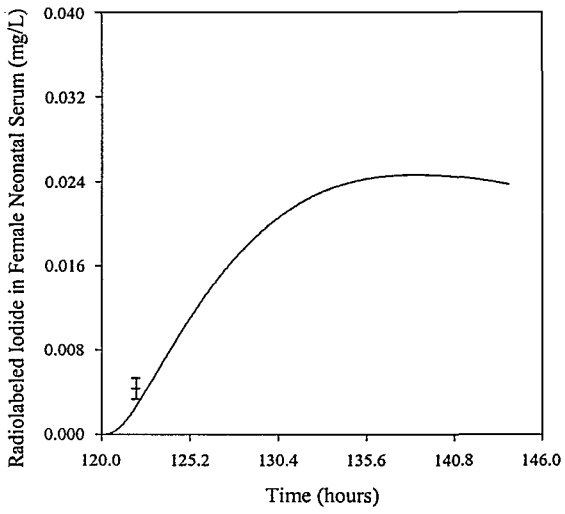

Figure 48. Iodide concentration in female neonatal serum 2 hours after *iv* dose to dam of 33000 ng/kg $^{125}I^-$ with carrier on PND 5

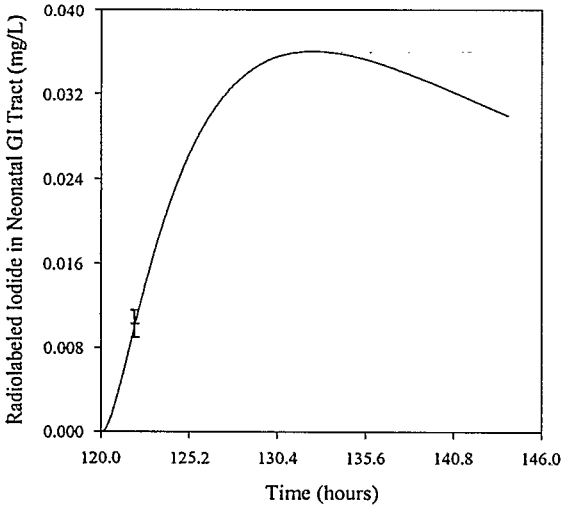

Figure 49. Iodide concentration in neonatal GI tract 2 hours after *iv* dose to dam of 33000 ng/kg $^{125}I^-$ with carrier on PND 5

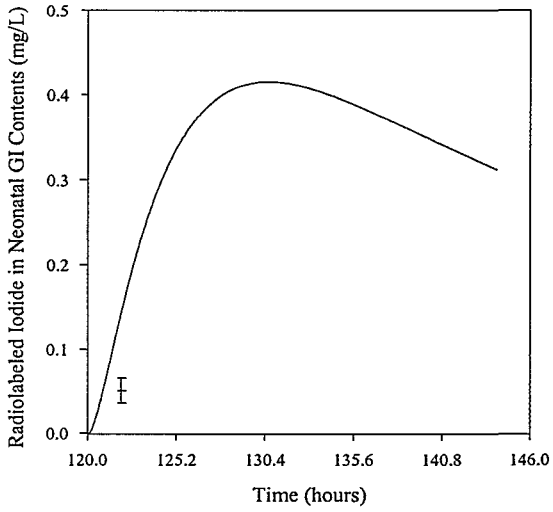

Figure 50. Iodide concentration in neonatal GI contents 2 hours after *iv* dose to dam of 33000 ng/kg $^{125}I^-$ with carrier on PND 5

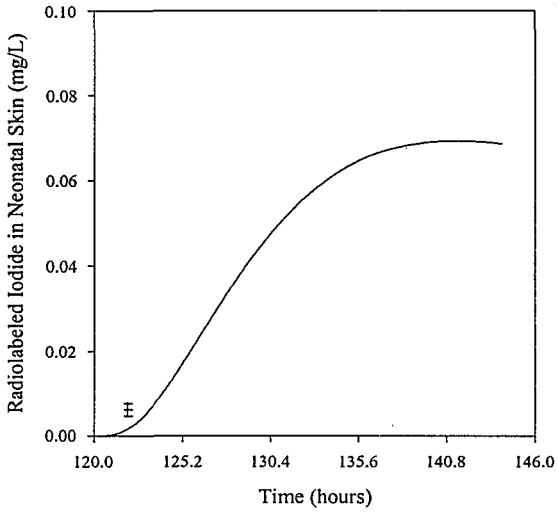

Figure 51. Iodide concentration in neonatal skin 2 hours after *iv* dose to dam of 33000 ng/kg $^{125}I^-$ with carrier on PND 5

The inhibition data collected after maternal exposure to perchlorate contaminated drinking water presented interesting changes in the kinetics of iodide. As is expected, the introduction of perchlorate into the drinking water caused an initial inhibition of the thyroidal iodide uptake, which then resulted in a systemic response resulting in up-regulation of the thyroid. Although data were not collected to verify the initial iodide inhibition, it is evidenced by the subsequent changes in hormones measured in the PND 5 drinking water study (Yu, 2000). The following tables summarize the hormone changes seen in the PND 5 dam (Table 4) and neonate (Table 5) after 23 days of exposure to 0.1, 1.0 and 10.0 mg/kg day ClO_4^- doses, expressed as change from control.

TABLE 4. PERCENT CHANGE IN THYROID HORMONES OF LACTATING RAT AFTER 23 DAYS OF PERCHLORATE EXPOSURE

Perchlorate Dose (mg/kg-day)	**Total T_4** (% change)	**Free T_4** (% change)	**Total T_3** (% change)	**TSH** (%change)
0.01	-5	28***	-8	48***
0.1	-16***	31***	-8	60***
1.0	-21***	32***	-11*	69***
10.0	-37***	36***	-17**	96***

* $0.01<p\leq0.05$
** $0.001<p\leq0.01$
*** $p\leq0.001$

TABLE 5. PERCENT CHANGE IN THYROID HORMONES OF NEONATE AFTER PERCHLORATE EXPOSURE

Perchlorate Dose (mg/kg-day)	Total T_4 (% change)	Free T_4 (% change)	Total T_3 (% change)	TSH (%change)
Male Neonate				
0.01	-2	5	-1	13***
0.1	-3	6	-8	29***
1.0	-6	4	-6	31***
10.0	-6	11	-15*	31***
Female Neonate				
0.01	-9	2	-5	10
0.1	-10	18*	-12	10
1.0	-9	20*	-14*	12*
10.0	-9	29***	-20**	13*

* $0.01<p\leq0.05$
** $0.001<p\leq0.01$
*** $p\leq0.001$

From the results shown in the tables above, it is apparent that even at the lowest dose, the hormonal system has experienced a perturbation and is attempting to compensate for the interruption caused by the perchlorate exposure. Maternal T_4 is shown to decrease in a dose-dependent manner, while TSH increases dose-dependently. Free T_4 is significantly increased at all doses and total T_3 is significantly decreased at the 1.0 and 10.0 mg/kg-day doses. The neonate appears to follow the same trends as those seen in the dam. However, a sex difference is apparent in the response of the neonatal hormone system to perchlorate exposure. In the male neonates, no significant change is seen in the total or free T_4 serum concentrations; only the 10.0 mg/kg-day dose group shows decreased T_3 concentrations. However, all doses show elevated TSH levels. In the female neonates, no significant change is seen in the total T_4 levels, but the 0.1, 1.0 and 10.0 mg/kg-day dose groups show elevated free T_4 concentrations in the serum. The female neonates also show significant decreases in T_3 and increases in TSH at the 1.0 and 10.0 mg/kg-day dose groups only. Hormone changes are discussed in detail elsewhere (Yu, 2000). The statistical analysis of the hormone data is attached (Attachment 3).

From the perspective of iodide kinetics, these hormone changes are important indicators of thyroid up-regulation. When TSH is increased, the thyroid is stimulated to increase iodide uptake. It is evident, then, that after exposure to perchlorate in drinking water for 23 days, the thyroid of the lactating dam has experienced both inhibition and up-regulation and has successfully compensated for the competition of perchlorate for binding sites of NIS. Therefore, it is not surprising that no inhibition was reported in the maternal thyroid on PND5. It is not that the inhibition is not taking place, but rather that the system has compensated for the effect of perchlorate. The thyroid of the dam was able to increase iodide uptake to restore thyroidal iodide uptake to normal levels. Table 6 shows the iodide levels measured in the tissues from the PND 5 drinking water study. The protocol for this study is discussed further in Yu (2000).

TABLE 6. MEAN RADIOLABELED IODIDE UPTAKE IN TISSUES AFTER 23 DAYS OF PERCHLORATE EXPOSURE

Maternal Tissues	Control	0.01 ClO_4^-	0.1 ClO_4^-	1.0 ClO_4^-	10.0 ClO_4^-
Serum (mg/L)	0.018	0.02	0.02	0.04	0.04
Thyroid (mg/L)	8.65	9.14	13.52	16.11	10.49
GI Content (mg/L)	0.08	0.06	0.10	0.12	0.11
GI Tract (mg/L)	0.03	0.05	0.03	0.04	0.04
Skin (mg/L)	0.03	0.03	0.02	0.03	0.03
Mammary (mg/L)	0.10	0.13	0.14	0.09	0.06
Neonatal Tissues					
Male Serum (mg/L)	0.004	0.005	0.006	0.004	0.002
Female Serum (mg/L)	0.004	0.006	0.007	0.005	0.003
Ave. GI Tract (mg/L)	0.007	0.010	0.010	0.005	0.003
Ave. GI Contents (mg/L)	0.052	0.078	0.061	0.027	0.015
Ave. Skin (mg/L)	0.005	0.006	0.005	0.004	0.002

It is evident from the data presented in Table 6 that the uptake of iodide into the mammary tissue is still inhibited after 23 days of perchlorate exposure at the 10.0 mg/kg-day dose group. The fact that the other dose groups do not show this decreased iodide concentration indicates that some sort of mechanism is in place to compensate for the competition of perchlorate for NIS uptake into the mammary tissue. However, only the high dose group shows inhibition after drinking water exposure to perchlorate. There are a couple of possible explanations for this. It is likely that the feedback mechanism, which controls the up-regulation of the mammary tissue, is less efficient than that of the thyroid. Thus, it would take longer for the mammary to compensate for the interference supplied by the perchlorate anion. This would explain why other authors, such as Brown-Grant (1961), did not see up-regulation in any extra-thyroidal tissues. It is possible that the less efficient mechanism in the mammary gland did not have time to up-regulate the symporter within the time frame of the earlier studies. The second possibility is similar to the explanation discussed previously for the diminished perchlorate uptake during long-term exposure. The high anion concentrations in the mammary tissue and milk may overload the second symporter in the mammary gland (the anion exchange transport mechanism), thereby reducing the ability of the gland to transfer the iodide anion as efficiently in the milk.

Whatever the reason for the inability of the gland to compensate for the competitive interference of perchlorate, the lower levels of iodide in the mammary gland evidently result in diminished iodide concentrations in the neonatal serum and tissues. This iodide deficiency is critical in determining the risk to the developing rat. The trend seen in the iodide: over-compensation in the 0.01 and 0.1 mg/kg-day dose groups, compensation in the 1.0 mg/kg-day dose group and the lack of compensation in the 10.0 mg/kg-day dose group, indicates that lower dose groups saw at least transient decreases in transfer of iodide through the milk. Although the mammary tissue has apparently compensated for the competition of the ions before the fifth day of lactation, the short-term deficiency is still critical if any transient change in iodide levels can cause negative developmental effects, as discussed earlier.

The model is not equipped with the capability to account for up-regulation of the thyroid. Therefore, when a simulation of the inhibition is performed with the model, the concentration of iodide is under-predicted in a (ClO_4^-) dose-dependent manner. Figure 52 shows the model prediction of iodide in the thyroid of the dam at drinking water doses of 0.0, 0.1, 1.0 and 10.0 mg/kg-day. The model's prediction of thyroid perchlorate levels from this same study can be seen in Figure 52.

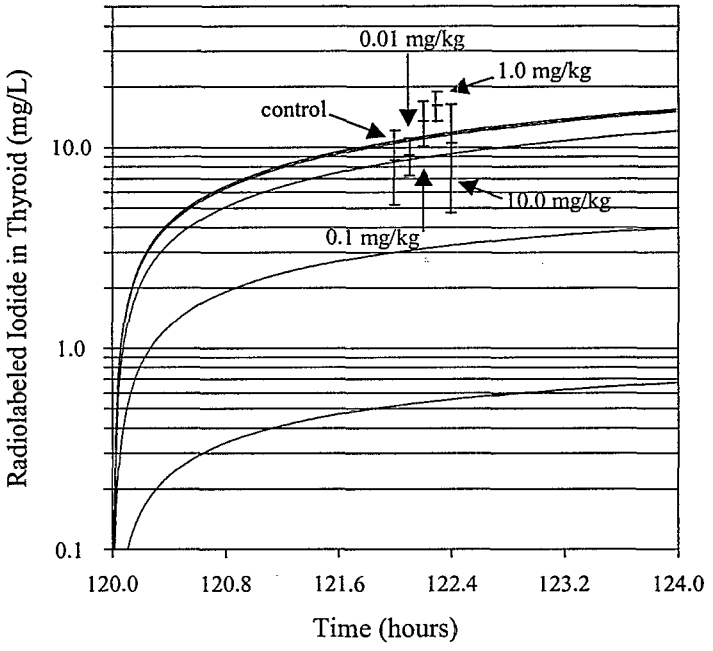

Figure 52. Iodide in thyroid on PND 5 after 23 days of 0.0, 0.1, 1.0 and 10.0 mg/kg-day ClO_4^- in drinking water. All experimental data were taken two hours post-dosing. Data points were separated slightly by time on the plot to make them more visible.

CONCLUSION

Throughout the process of model development, it was evident that several differences exist between the pregnant and lactating females and the male rat. The differences seen between this model and the male rat model that was developed concurrently by Merrill. (2001a) emphasized the need for a lactation model to describe the highly dynamic system. Beyond the more obvious physiological changes occurring during lactation, significant differences exist that affect the kinetics of both perchlorate and iodide. The loss of iodide and perchlorate in the milk result in much faster clearance rates of the anions from the dam. The thyroidal maximum capacities are lower in the lactating and pregnant dam than in the male rat. Model parameterization in the male rat indicated the need for Vmax values for uptake into the follicle of the thyroid of 2.2×10^3 L/hr-kg for perchlorate and 5.5×10^4 L/hr-kg for iodide, while the gestation model required values of 1.5×10^3 L/hr-kg and 4.0×10^4 L/hr-kg for the same parameters. This difference is supported in the literature. Versloot *et al.* (1997) suggest that the pregnant rat may have a

lowered reserve of iodide in the thyroid toward the end of pregnancy, causing increased activity in the thyroid. This is quite possibly true in the lactating rat also. Additionally, studies suggest that the loss of iodide to the mammary gland and milk results in less available iodide for the maternal thyroid (Brown-Grant, 1961; Yu, 2000; Yu *et al.*, 2000). The skin of the lactating dam also required a smaller value for Vmax than the male rat. This is supported by the work of Brown-Grant and Pethes (1959), who reported higher levels of iodide in the skin of male rats than in female rats. Skin, therefore, appears to be a more important iodide reserve in the male rat than the female. It is not surprising that the kinetic behavior of perchlorate and iodide would vary somewhat between a male rat and a lactating female rat, or for that matter a nursing neonate. In fact, it is quite remarkable that the model is able to account for the majority of differences in the uptake, distribution and excretion between the adult male, lactating female and neonate by incorporating known differences in physiology.

The described PBPK lactation model is able to predict the distribution of perchlorate in the tissues of active uptake and serum of the lactating dam and neonate on PND 5 and 10 after exposure to perchlorate in drinking water. Perchlorate distribution in this dynamic system is well described utilizing a pharmacokinetic approach to the modeling and accounting mathematically for physiological changes, such as changing tissue volumes and maternal and neonatal growth. The model predicts the transfer of perchlorate to the neonate and is also able to describe the uptake into tissues of interest in the neonate, such as the GI contents and skin. Most neonate and dam tissues were simulated reasonably against data that range from 0.01 to 10.0 mg/kg-day, or three orders of magnitude.

The clear differences between the perchlorate data from *iv* and drinking water studies draw attention to unresolved issues in the transfer kinetics of perchlorate. Although lactational transfer has long been studied, the transport mechanisms of this ion have yet to be elucidated in the literature. As was previously discussed, a second transporter has been identified in the mammary gland, which actively transports anions against the chemical gradient. However, the relationship of this transporter and the anion concentration resulting from prolonged exposure to the high doses of perchlorate used in these studies is not known. It is possible that the high anion load resulting from the long-term exposure to ClO_4^- may have resulted in decreased transport of the ion. It is feasible that the movement of iodide may be regulated in the mammary tissue, since the ion is vital to the development of the newborn. The data obtained between the acute and drinking water studies suggest that a feedback mechanism is in place, since the model over-predicts the milk transfer in the drinking water data when the acute parameters are used. In-house experiments are currently being conducted that may help resolve these issues.

The kinetic behavior of iodide is well described with the existing model, in spite of the physiological complexity of the described system. The dam and neonate were accurately simulated at a range of doses that spans four orders of magnitude (2.10 to 33,000 ng/kg) between days 1 and 18 of lactation. The active sequestration of iodide in maternal and neonatal tissues and the transfer of iodide between mother and neonate was described kinetically with the model; data have been simulated at a variety of doses and at various time points up to 14 days after exposure. The fact that the model was able to simulate data from other laboratories under a variety of different conditions attests to the validity of the model structure and its applicability to other studies. The purpose of developing a PBPK model is to aid in predicting the effect of

exposure in situations that are not easily or already measured. The usefulness of this model for this purpose is supported by the success the model has already had in reproducing literature studies.

The ability of the model to predict iodide inhibition was also indicative of the usefulness of the model for predictive purposes. It was possible to predict inhibition out to 24 hours, while simulating the serum and thyroid perchlorate and iodide levels with satisfactory accuracy. This provides support for the chosen model structure, as well as validation for the physiological and chemical descriptions used. However, it is important to note that in the majority of the situations of interest, the exposure to perchlorate would very likely be through the ingestion of contaminated drinking water. In this scenario, the endocrine system is given plenty of time to undergo up-regulation. Therefore, the inability of the model to respond to this auto-regulation presents a considerable need for further model development.

Hormone homeostasis is a complex process and is not included in the present model structure. Predicting results from experiments such as the drinking water study would require a model that could account for the hormone levels in tissues and serum and processes such as hormone production, storage and secretion in the thyroid, conversion of T_4 to T_3 in the tissues, deiodination of T_4 and T_3 to less active forms and a feedback mechanism between the hormone levels and thyroid symporter. Our laboratory is currently working toward this goal, viewing the current modeling of iodide kinetics as the first step in the more complex modeling of hormone regulation by the pituitary-iodide axis. Kohn *et al.* (1996) recently developed a PBPK model that attempts to describe the effect of dioxin on thyroid hormones. Although perchlorate and dioxin act on the endocrine system through different modes of action, it is likely that a similar approach to that of Kohn *et al.* could be employed for the hormone feedback system in the case of perchlorate.

The ultimate purpose of PBPK modeling in the evaluation of exposure risk is to predict the dose-response in the human population. This is also the aim of the perchlorate modeling effort. A perchlorate PBPK model for the adult male human has been developed simultaneously with the model described in this report. However, it is evident that large differences exist which would prohibit the use of the current human model from being used in predictions for lactating mothers and nursing infants. The differences seen during the concurrent modeling effort in the male and pregnant and lactating female rats highlight the need for human gestation and lactation models. The next stage, then, would be to modify the present lactation model in order to describe the human. In order to attempt this, the model described in this paper would be equipped with human physiological parameters, such as the growth of human infants and the milk yield of human mothers. The model would then be run with the present kinetic parameters in an effort to predict the behavior of iodide and perchlorate in a lactating human. It is possible that some of the chemical specific parameters would vary from the previously determined rat parameters. For example, Merrill (2001b) found that the thyroidal capacity for iodide in humans is much higher than rats. However, as is evidenced by a comparison of the male rat and human perchlorate models (Merrill 2001a and 2001b), the physiological changes should account for the majority of the differences between the rat and human kinetics within the present model structure. The application of this lactation model to human lactation will be described in future publications.

Ultimately, the lactation model could be a useful tool in determining the dosimetry for specific time points in lactation. These internal dosimetrics could then be compared to periods in which perchlorate exposure and/or iodide deficiency has been linked to developmental effects. It is difficult, however, to determine experimentally the specific times at which the availability of iodide to the neonate is most critical. Although the studies performed to this end are numerous, it is difficult to separate the pre- and postnatal effects of iodide deficiency, due to the fact that many effects are not manifested until later in life (e.g., lowered IQ). It has been suggested that in humans, thyroid hormones are of little importance in early fetal life but are more critical during late fetal life in skeletal development and possibly in brain development, due to the fact that myelination takes place a few weeks before birth. However, since human effects are not easily recognized or measured at birth, it is difficult to say with certainty that this is the case. Developmental effects have been studied extensively in animals, particularly in the rat. However, when using the rat as a species of comparison, the issue is further complicated by the fact that rats are born in a more immature state than human infants. Therefore, much of the development that would take place *in utero* in the human is experienced during the lactation period of the rat (Myant, 1971).

It is conceivable that the PBPK models could be used to help determine the answers to these questions concerning the critical time points and major routes of exposure during development. The models could also be a useful tool to help ferret out whether exposure is more critical during gestation or lactation. A gestation exposure model has also been developed for perchlorate and iodide in the pregnant rat and fetus (Clewell, 2001) utilizing the same approach, general compartmental structure and kinetic parameters as those seen in the lactation model. The physiological differences between lactation and pregnancy are addressed mathematically within the structure of the model. These models, when used together, could provide a complete picture of the perchlorate kinetics during the developmental period. It would be possible to utilize the models to predict dosimetry for specific time points during gestation and lactation, which could then be compared to studies in which developmental effects were studied. Thus the ultimate goal of the lactation and pregnancy models is to compare exposure scenarios between the rat and human at different developmental time points, in order to determine the dose and timing responsible for developmental effects.

ACKNOWLEDGEMENTS

The animals used in in-house studies were handled in accordance with the principles stated in the *Guide for the Care and Use of Laboratory Animals*, National Research Council, 1996, and the Animal Welfare Act of 1966, as amended.

The authors would like to thank Harvey Clewell (ICF Consulting, Ruston, LA) and Mel Andersen (Colorado State University, Fort Collins, CO) for their expert advice. A special thanks is also extended to Latha Narayanan and Gerry Buttler for the sample analyses and Dick Godfrey, Peggy Parish, SSgt Todd Ligman, MSgt Jim McCafferty, Tim Bausman, SSgt Paula Todd, Susan Young and TSgt Rick Black for their work with the lactation studies. The authors would also like to acknowledge Charles Goodyear for performing statistical analyses of the data.

Mr. Goodyear is a statistical consultant for AFRL, Human Effectiveness Directorate, Crew Systems Interface Division (AFRL/HEC), Wright-Patterson Air Force Base, Ohio.

REFERENCES

Ajjan,R.A.; Kamaruddin,N.A.; Crisp,M.; Watson,P.F.; Ludgate,M.; Weetman,A.P. (1998). Regulation and tissue distribution of the human sodium iodide symporter gene. Clin.Endocrinol., 49 (4), p. 517-523.

Altman, P.L., and Dittmer, D.S. (1971). Volume of blood in tissue: Vertebrates: (148):p. 383-387. Respiration and Circulation. Federation of American Societies for Experimental Biology: Bethesda, MD.

Anbar,M., Guttmann,S. and Lewitus,Z. (1959). The mode of action of perchlorate ions on the iodine uptake of the thyroid gland. Int.J.Appl.Radiat.Isot., 7, 87-96.

Bakke, J.L., Lawrence, N.L., Robinson, S., Bennett, J. (1976). Lifelong alterations in endocrine function resulting from brief perinatal hypothyroidism in the rat. J.Lab.Clin.Med., 88 (1), p.3-13.

Brown, R.P., Delp, M.D., Lindstedt, S.L., Rhomberg, L.R., and Beliles, R.P. (1997). Physiological parameter values for physiologically based pharmacokinetic models. Toxicol.Ind.Health, 13, p. 407-484.

Brown-Grant, K. (1957). The iodide concentrating mechanism in the mammary gland. J.Physiol., 135, p. 644-654.

Brown-Grant, K. (1961). Extrathyroidal iodide concentrating mechanisms. Physiol.Rev., 41, p. 189-213.

Brown-Grant,K. and Galton,V.A. (1958). Iodinated compounds in milk after radioiodide administration. Biochim. Biophys. Acta, 27, p. 422-433.

Brown-Grant, K. and Pethes, G. (1959). Concentration of radioiodine in the skin of the rat. J.Physiol., 148, p. 683-693.

Capek, K. and Jelinek, J. (1956) The development of water metabolism. I. The excretion of urine in young rats. Phys.Bohem., 5 (1), p. 91-96.

Carr, C.W. (1952). Studies on the binding of small ions in protein solutions with the use of membrane electrodes. I. The binding of the chloride ion and other inorganic anions in solutions of serum albumin. Arch.Biochem.Biophys., 40, p.286-294.

Chow, S.Y., Chang, L.R. and Yen, M.S. (1969). A comparison between the uptakes of radioactive perchlorate and iodide by rat and guinea pig thyroid glands. J.Endocrinol., 45(1), p. 1-8.

Chow, S.Y. and Woodbury, D.M. (1970). Kinetics of distribution of radioactive perchlorate in rat and guinea-pig thyroid glands. J.Endocrinol., 47(2), p. 207-218.

Clewell, R.A. (2001). Physiologically-Based Pharmacokinetic Model for the Kinetics of Perchlorate-Induced Inhibition of Iodide in the Pregnant Rat and Fetus. AFRL-HE-WP-CL-2001-0006.

Clos, J., Crepel, F., Legrand, C., Legrand, J., Rabie, A., Vigouroux, E. (1974). Thyroid physiology during the postnatal period in the rat: A study of the development of thyroid function and of the morphogenetic effects of thyroxine with special reference to cerebellar maturation. Gen.Comp.Endocrinol., 23, p. 178-192.

Conde, E., Martin-Lacave, I., Godalez-Campora, R., Galera-Davidson, H. (1991) Histometry of normal thyroid glands in neonatal and adult rats. Am.J.Anat., 191, p. 384-390.

Delange, F. (2000). The role of iodine in brain development. Proc.Nutr.Soc., 59, p. 75-79.

Dobbing, J., (1974), in Scientific Foundations of Paediatrics, ed. Daris, J., Dobbing, J., Heineman, J. London, p. 565.

Eguchi, Y., Fukiishi, Y., Hasegawa,Y. (1980). Ontogeny of the pituitary-thyroid system in fetal rats: observations on the fetal thyroid after maternal treatment with goitrogen. Anat.Rec., 198, 4, p. 637-642.

Fisher, J.W., Whittaker, T.A., Taylor, D.H., Clewell, H.J., Anderson, M.E. (1990). Physiologically based pharmacokinetic modeling of the lactating rat and nursing pup: A multiroute exposure model for trichloroethylene and its metabolite, trichloroacetic acid. Toxicol. Appl. Pharmacol., 102, p. 497-513.

Florsheim, W.H., Faircloth, M.A., Corcorran, N.L., and Rudko. (1966). Perinatal Thyroid Function in the Rat. Acta Endocrinol., 32, p. 375-332.

Geloso, J.P., (1961). Date de l'entrée en fonction do la thyroide chez lel foetus de rat. C.R.Soc.Biol. (Paris)., 155, p. 1239-1244.

Gluzman, B.E. and Niepomniszcze, H. (1983). Kinetics of the iodide trapping mechanism in normal and pathological human thyroid slices. Acta Endocrinol., 103, p. 34-39.

Gokmen I.G. and Dagu, G. (1995), Determination of Iodine Content in human Milk, Cow's Milk and Infant Formula and Estimation of Daily Iodine Intake of Infants. Analyst, 120, p. 2005-2008.

Golstein, P., Abramow, M., Dumont, J.E., and Beauwens, R. (1992). The iodide channel of the thyroid: a membrane vesicle study. Am.J.Physiol., 263 (3 pt.1), p. C590-597.

Haddow, J.E., Palomaki, G.E., Allan, W.C., Williams, J.R., Knight, G.J., Gagnon, J., O'Heir, C.E., Mitchell, M.L., Hermos, R.J., Waisbren, S.E., Faix, J.D., Klein, R.Z. (1999). Maternal thyroid deficiency during pregnancy and subsequent neuropsychological development of the child. New Eng.J.Med., 341, (8), p. 549-555.

Halmi,N.S. and Stuelke,R.G. (1959). Comparison of Thyroidal and Gastric Iodide Pumps in Rats. Endocrinology, 64, p.103-109.

Halmi,N.S., Stuelke,R.G. and Schnell,M.D. (1956). Radioiodide in the thyroid and in other organs of rats treated with large doses of perchlorate. Endocrinology, 58, p. 634-650.

Hanwell, A., and Linzell, J.L. (1973) The time course of cardiovascular changes in the rat. J.Physiol., 233, p. 99-109.

Harden,R.G., Alexander,W.D., Shimmins,J., and Robertson,J.W. (1968). A comparison between the inhibitory effect of perchlorate on iodide and pertechnetate concentrations in saliva in man. Q.J.Exp.Physiol.Cogn.Med.Sci., 3 (53), p.227-238.

Hays M.T. and Green, F.A. (1973). In vitro studies of 99mTc-Pertechnetate binding by human serum and tissues. J.Nucl.Med., 14 (3), p.149-158.

Hetzel, B.S. and Dunn, J.T., (1989) Ann.Rev.Nutr., 9, p. 21

Honour,A.J., Myant,N.B., Rowlands,E.N. (1952). Secretion of radioiodine in digestive juices and milk in man. Clin.Sci., 11, p. 447-463.

Iino,S. and Greer,M.A. (1961). Thyroid function in the rat during pregnancy and lactation. Endocrinology, 68, p. 253-262.

Klein, A.H., Meltzer, S., Kenny, F.M., (1972). Improved prognosis in congenital hypothyroidism treated before age three months. J.Pediatr., 81, (5), p. 912-915.

Knight, C.H., Docherty, A.H., and Peaker, M., (1984). Milk yield in the rat in relation to activity and size of the mammary secretory cell population. J.Dairy.Res., 51, p. 29-35.

Kohn MC, Sewall CH, Lucier GW, Portier CJ. (1996). A mechanistic model of effects of dioxin on thyroid hormones in the rat. Toxicol.Appl.Pharmacol. 136(1):29-48.

Kotani,T., Ogata,Y., Yamamoto,I., Aratake,Y., Kawano,J.I., Suganuma,T., Ohtaki,S. (1998). Characterization of gastric Na+/I- symporter of the rat. Clin.Immunol.Immunopathol., 89 (3), p. 271-278.

Lazarus, J.H., Harden, R.M., and Robertson, J.W.K. (1974). Quantitative studies of the inhibitory effect of perchlorate on the concentration of $^{36}ClO_4^-$, $^{125}I^-$, and $^{99m}TcO_4^-$ in salivary glands of male and female mice. Arch.Oral.Biol., 19, p.493-498.

Mahle, D.A. (2001). Hormone and perchlorate data from cross-fostering study. AFRL-HE-WP-CL-2001-0001

Malendowicz, L.K., and Bednarek, J. (1986). Sex dimorphism in the thyroid gland. Acta Anat., 127, p. 115-118.

Mattie, D.R, Jarabek, AM. (1999). Perchlorate Environmental Contamination: Testing Strategy Based on Mode of Action. The Toxicologist. Toxicol.Sci., 48, 113.

Merrill E.A. (2001a). PBPK Model for Perchlorate-Induced Inhibition in the Male Rat. AFRL-HE-WP-CL-2001-0005.

Merrill E.A. (2001b). PBPK model for perchlorate-induced inhibition of radioiodide uptake in humans. AFRL-HE-WP-CL-2001-0008.

Myant, N.B. (1971). The role of thyroid hormone in the fetal and postnatal development of mammals. in Hormones in Development. Appleton-Century-Crofts, NY., p. 465-471.

Naismith, D.J., Richardson, D.P., and Pritchard, A.E. (1982). The utilization of protein and energy during lactation in the rat, with particular regard to the use of fat accumulated during pregnancy. Br.J.Nutr., 48, p.433-441.

Nataf, B. and Sfez, M. (1961). Debut du fonctionement de la thyroide foetale du rat. C.R.Soc.Biol. (Paris), 55, p.1235-1238.

Perlman,I., Chaikoff,I.L. and Morton,M.E. (1941). Radioactive iodine as an indicator of the metabolism of iodine. I. The turnover of iodine in the tissues of the normal animal, with particular reference to the thyroid. J.Biol.Chem., 149, p. 433-447.

Pena,H.G., Kessler,W.V., Christian,J.E., Cline,T.R. and Plumlee,M.P. (1976). A comparative study of iodine and potassium perchlorate metabolism in the laying hen. 2. Uptake, distribution, and excretion of potassium perchlorate. Poult.Sci., 55(1), p. 188-201.

Porterfield, S.P. (1994). Vulnerability of the Developing Brain to Thyroid Abnormalities: Environmental Insults to the Thyroid System. Environ.Health Perspect., 102 (Suppl 2), p. 125-130.

Potter, G.D., Tong, W., Chaikoff, I.L. (1959). The metabolism of I131-labeled iodine, thyroxine, and triiodothyronine in the mammary gland of the lactating rat. J. Biol. Chem., 243 (2), p. 350-354.

Rall,J.E., Power,M.H., Albert,A. (1950). Distribution of radioiodine in erythrocytes and plasma of man. Proc.Soc.Exp.Biol.Med., 74, p. 460-461.

Roti, E., Gnudi, A., Braverman, L.E. (1983). The placental transport, synthesis and metabolism of hormones and drugs which affect thyroid function. Endocrine Rev., 4, p. 131-149.

Sampson,D.A. and Jansen,G.R. (1984). Measurement of milk yield in the lactating rat from pup weight and weight gain. J. Ped. Gastroenterology and Nutr., 3, p. 613-617.

Samuel, M. and Caputa, A. (1965). The role of the mother in I131 metabolism of suckling and weaning rats. Can. J. Physiol. Pharmacol., 43, p. 431-436

Sato,T.; Suzuki,Y. (1979). Presence of triiodothyronine, no detectable thyroxine and reverse triiodothyronine in human milk. Endocrinol. Japan, 26, p. 507-513.

Scatchard, G. and Black, E.S. (1949). The effects of salts on the isoionic and isoelectric points of proteins. J.Phys.Colloid Chem., 53, p. 88-99.

Shennan,D.B. (2001). Iodide transport in lactating rat mammary tissue via a pathway independent from the Na^+/I^- cotransporter: evidence for sulfate/iodide exchange. Biochem. And Biophys. Res. Commun., 280, p. 1359-1363.

Shishiba,Y., Shimizu,T., Yoshimura,S. and Shimizu,K. (1970). [Effect of thiocyanate and perchlorate on free thyroxine fraction]. Nippon.Naibunpi.Gakkai.Zasshi., 46 (1), p. 16-19.

Spitzweg, C., Joba, W., Eisenmenger, W. and Heufelder, A.E. (1998). Analysis of human sodium iodide symporter gene expression in extrathyroidal tissues and cloning of its complementary deoxyribonucleic acids from salivary gland, mammary gland, and gastric mucosa. J.Clin.Endocrinol.Metab., 83, p. 1746-1751.

Sztanyik, L.B. and Turai, I. (1988). Modification of radioiodine incorporation in the fetus and newborn rats by the thyroid blocking agents. Acta Phys.Hungaria., 72, p.343-354.

Tazebay, U.H., Wapnir, I.L., Levy, O., Dohan, O., Zuckier, L.S., Zhao, Q.H., Deng, H.F., Amenta, P.S., Fineberg, S., Pestell., R.G., Carrasco, N. (2000). The mammary gland iodide transporter is expressed during lactation and in breast cancer. Nat.Med., 6(8), p.871-878.

Urbansky, E.T. (1998). Perchlorate chemistry: implications for analysis and remediation. Bioremed.J., 2(2), p. 81-95.

Urbansky, E.T., and Schock, M.R. (1999). Issue in managing risks associated with perchlorate in drinking water. J.Environ.Management, 56, p. 79-95.

Versloot, P.M., Schroder-Van Der Elst, J.P., Van Der Heide, D., and Boogerd, L. (1997). Effects of marginal iodine deficiency during pregnancy: iodide uptake by the maternal and fetal thyroid. Am.J.Physiol., 273 (6 pt. 1), E1121-E1126.

Vigouroux,E.; Rostaqui,N., (1980). Particular aspects of thyroid function development in the postnatal rat with special reference to interrelationships between mother and young. Reprod.Nutr.Develop., 20, p. 209-215.

Vigouroux,E.; Rostaqui,N.; Fenerole,J.M., (1980). Estimation of hormonal and non-hormonal iodine uptake from maternal milk in suckling rats. Acta Endocrinol., 93, 332-338.

Wolff, J. (1998) Perchlorate and the thyroid gland. Pharmacolog.Rev., 50, p. 89-105.

Wolff, J. and Maurey, J.R. (1961) Thyroidal iodide transport: II. Comparison with non-thyroid iodide-concentrating tissues. Biochim.Biophys.Acta, 47, p. 467-474.

Wolff, J. and Maurey, J.R. (1963) Thyroidal iodide transport: IV. The role of ion size. Biochim.Biophys.Acta, 69, p. 48-58.

Yamada, T. (1967). Effects of perchlorate and other anions on thyroxin metabolism in the rat. Endocrinology, 81, p. 1285-1290.

Yu, K.O. (2000). Tissue distribution and inhibition of iodide uptake in the thyroid by perchlorate with corresponding hormonal changes in pregnant and lactating rats (drinking water study). AFRL-HE-WP-CL-0038.

Yu, K.O., Narayanan, L., Godfrey, R.J., Todd, P.N., Goodyear, C.D., Sterner, T.R., Bausman, T.A., Young, S.M., Mattie, D.R., Fisher, J.W. (2000). Effects of perchlorate on thyroidal uptake of iodide with corresponding hormonal changes. AFRL-HE-WP-TR-2000-0076.

Zeghal N, Gondran F, Redjem M, Giudicelli MD, Aissouni Y, Vigouroux E. (1992). Iodide and T4 kinetics in plasma, thyroid gland and skin of 10-day-old rats: effects of iodine deficiency. Acta Endocrinol (Copenh), 127 (5), p. 425-34

Zeghal,N., Redjem,M., Gondran,F. and Vigouroux,E. (1995). [Analysis of iodine compounds in young rat skin in the period of suckling and in the adult. Effect of perchlorate]. Arch.Physiol.Biochem., 103 (4), p. 502-511.

PND 10 Drinking Water Consumption Statistical Summary

Charles D. Goodyear

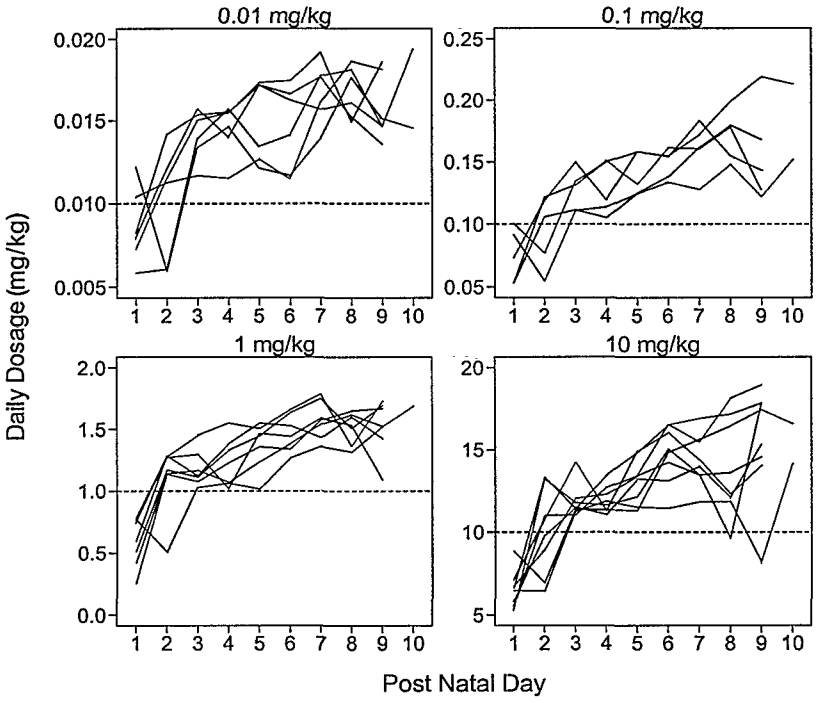

Daily dosage for each dam

Mean and standard deviation of dams for daily dosage (mg/kg)

	0.01 mg/kg		0.1 mg/kg		1 mg/kg		10 mg/kg	
PND	N	Mean ± StD	N	Mean ± StD	N	Mean ± StD	N	Mean ± StD
1	6	0.0087 ± 0.0023	5	0.074 ± 0.022	7	0.58 ± 0.20	8	6.6 ± 1.1
2	6	0.0102 ± 0.0034	5	0.096 ± 0.029	7	1.11 ± 0.27	8	10.1 ± 2.6
3	6	0.0142 ± 0.0015	5	0.127 ± 0.017	7	1.18 ± 0.15	8	11.8 ± 1.0
4	6	0.0145 ± 0.0016	5	0.128 ± 0.021	7	1.24 ± 0.20	8	12.0 ± 0.8
5	6	0.0150 ± 0.0025	5	0.139 ± 0.017	7	1.37 ± 0.19	8	13.1 ± 1.4
6	6	0.0146 ± 0.0026	5	0.148 ± 0.012	7	1.47 ± 0.15	8	14.7 ± 1.8
7	6	0.0167 ± 0.0018	5	0.161 ± 0.021	7	1.58 ± 0.15	8	14.4 ± 1.6
8	6	0.0168 ± 0.0016	5	0.172 ± 0.021	7	1.51 ± 0.13	8	13.9 ± 3.0
9	6	0.0158 ± 0.0021	5	0.156 ± 0.040	7	1.52 ± 0.22	8	15.5 ± 3.4

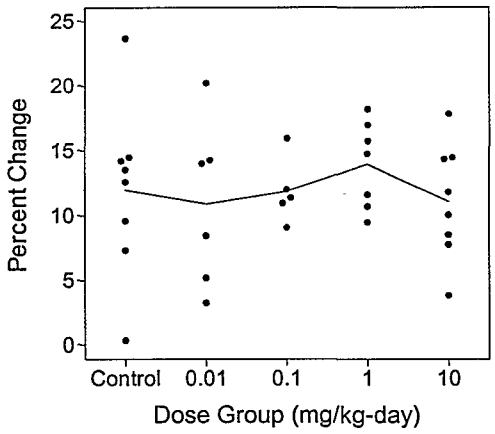

Percent change in maternal body weight from PND1 to PND10 for each dam. Line segments connect means from each dose group. There was not a significant difference among the dose groups {F(4,29) = 0.39, p = 0.8154}.

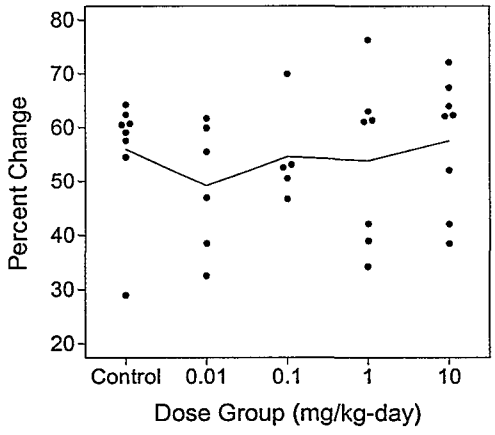

Percent change in maternal body weight from GD3 to PND10 for each dam. Line segments connect means from each dose group. There was not a significant difference among the dose groups {F(4,29) = 0.44, p = 0.7804}.

Mean and standard deviation of dams for maternal body weight (grams). The StD for the overall mean was a pooled StD across dose groups.

	Control		0.01 mg/kg		0.1 mg/kg		1 mg/kg		10 mg/kg		Overall
PND	N	Mean ± StD	N	Mean ± StD	N	Mean ± StD	N	Mean ± StD	N	Mean ± StD	Mean ± StD
1	8	273.1 ± 15.4	6	285.3 ± 26.0	5	277.9 ± 18.1	7	271.2 ± 13.8	8	277.4 ± 15.2	277.0 ± 17.7
2	8	278.8 ± 15.1	6	283.5 ± 20.6	5	276.6 ± 12.6	7	279.7 ± 17.2	8	277.2 ± 11.4	279.2 ± 15.6
3	8	277.0 ± 18.1	6	288.4 ± 18.6	5	279.7 ± 13.5	7	281.5 ± 14.5	8	281.8 ± 12.6	281.7 ± 15.7
4	8	282.0 ± 22.5	6	293.8 ± 19.7	5	285.1 ± 10.9	7	286.5 ± 16.6	8	284.7 ± 10.4	286.4 ± 17.0
5	8	282.9 ± 18.4	6	298.1 ± 17.2	5	288.9 ± 13.2	7	289.3 ± 15.1	8	287.0 ± 6.8	289.2 ± 14.7
6	8	290.2 ± 16.4	6	301.2 ± 15.0	5	294.9 ± 14.8	7	296.4 ± 15.8	8	292.8 ± 8.0	295.1 ± 14.2
7	8	296.0 ± 19.8	6	306.7 ± 14.2	5	296.6 ± 12.2	7	301.7 ± 17.2	8	298.0 ± 7.9	299.8 ± 15.1
8	8	299.8 ± 19.7	6	309.8 ± 20.5	5	309.9 ± 14.6	7	301.3 ± 14.7	8	298.4 ± 10.6	303.8 ± 16.4
9	8	304.4 ± 17.0	6	315.9 ± 11.4	5	311.6 ± 20.3	7	308.4 ± 18.4	8	308.5 ± 10.2	309.7 ± 15.6

Serum Hormone (TSH, T_3, T_4) Statistical Report (Postnatal Day 5)

Charles D. Goodyear

Serum thyroid hormone levels were determined from 40 dams and some of their pups (male and female) in each of 5 dose groups (control, 0.01, 0.1, 1, and 10 mg/kg/day). Since all 40 dams could not be handled at the same time, 10 dams were brought in at 4 different times. Two dams from each time group were assigned to each of the 5 dose groups. At most, pooled serum of male and female pups from each dam was used.

T_3, T_4, Free T_4, and TSH were used as dependent variables in a one-factor (dose group) analysis of variance, performed separately for the dams, male pups, and female pups. In preliminary analyses, time group was included as a factor (for dams only). Since there were no significant main effects of time group or interactions between time group and dose group ($0.1776<p$), time group was removed as a factor. Results of the one-factor analyses are shown in table 1. Paired comparisons among the dose groups used 2-tailed t-tests with pooled error. Results are shown in tables 2-5.

Figures 1a&1c, 2a&2c, 3a&3c, and 4a&4c show the hormone levels for each dam and pup (male and female) respectively, along with the mean for each dose group. Figures 1b&1d, 2b&2d, 3b&3d, and 4b&4d show the mean % change from control for each dose group.

Table 1. Analysis of variance results. The dependent variable was hormone level.

Hormone	Rat	Source	SS	DF	SSE	DFE	F	P
T_3	Dam	Dose	7.39E+02	4	1.27E+03	31	4.52	0.0054
	Male Pup	Dose	8.01E+01	4	1.55E+02	20	2.58	0.0688
	Female Pup	Dose	4.82E+01	4	3.35E+01	11	3.96	0.0315
T_4	Dam	Dose	1.25E+00	4	4.70E-01	33	21.88	0.0001
	Male Pup	Dose	1.26E-02	4	8.79E-02	18	0.64	0.6381
	Female Pup	Dose	5.87E-03	4	1.33E-02	11	1.22	0.3588
Free T_4	Dam	Dose	4.54E-01	4	4.34E-01	32	8.37	0.0001
	Male Pup	Dose	7.11E-04	4	4.23E-03	22	0.92	0.4678
	Female Pup	Dose	4.88E-03	4	3.72E-03	18	5.90	0.0032
TSH	Dam	Dose	1.86E+02	4	3.82E+01	30	36.45	0.0001
	Male Pup	Dose	2.26E+01	4	1.78E+01	27	8.59	0.0001
	Female Pup	Dose	2.05E+00	4	6.32E+00	21	1.70	0.1869

Table 2. Paired comparisons of dose group for T_3. Values listed under each dose column are p-values (2-tailed t-test with pooled error) for comparing row dose and column dose.

Rat	Dose Group mg/kg/day	N	Mean T_3 (ng/dL)	Std Dev T_3 (ng/dL)	Dose Group mg/kg/day			
					0.01	0.1	1	10
Dam	Control	7	82.0	3.8	0.0793	0.0658	0.0118	0.0002
	0.01	6	75.5	6.9		0.9858	0.4916	0.0415
	0.1	7	75.5	6.8			0.4849	0.0354
	1	8	73.1	6.9				0.1323
	10	8	68.2	6.8				
Male Pup	Control	4	32.3	1.7	0.9003	0.2043	0.2916	0.0126
	0.01	4	32.0	3.2		0.2524	0.3562	0.0170
	0.1	5	29.8	2.5			0.7682	0.1572
	1	6	30.3	2.8				0.0784
	10	6	27.3	3.2				
Female Pup	Control	2	24.9	1.7	0.4654	0.1043	0.0422	0.0046
	0.01	2	23.5	2.6		0.3323	0.1822	0.0239
	0.1	2	21.8	1.4			0.8049	0.1960
	1	4	21.4	0.6				0.1886
	10	6	19.8	2.1				

Table 3. Paired comparisons of dose group for T_4. V alues listed under each dose column are p-values (2-tailed t-test with pooled error) for comparing row dose and column dose.

Rat	Dose Group mg/kg/day	N	Mean T_4 (ug/dL)	Std Dev T_4 (ug/dL)	Dose Group mg/kg/day			
					0.01	0.1	1	10
Dam	Control	8	1.38	0.15	0.3231	0.0010	0.0001	0.0001
	0.01	7	1.31	0.13		0.0172	0.0008	0.0001
	0.1	7	1.15	0.12			0.2701	0.0001
	1	8	1.09	0.10				0.0011
	10	8	0.87	0.08				
Male Pup	Control	3	1.03	0.04	0.6997	0.5734	0.1939	0.2403
	0.01	2	1.01	0.01		0.9540	0.4745	0.5472
	0.1	6	1.00	0.07			0.3545	0.4426
	1	6	0.96	0.07				0.8706
	10	6	0.97	0.09				
Female Pup	Control	3	0.52	0.01	0.0814	0.1316		0.0814
	0.01	5	0.47	0.03		0.9197		1.0000
	0.1	2	0.47	0.02				0.9197
	1	1	0.47					
	10	5	0.47	0.04				

Table 4. Paired comparisons of dose group for free T_4. Values listed under each dose column are p-values (2-tailed t-test with pooled error) for comparing row dose and column dose.

Rat	Dose Group mg/kg/day	N	Mean Free T_4 (ng/dL)	Std Dev Free T_4 (ng/dL)	Dose Group mg/kg/day			
					0.01	0.1	1	10
Dam	Control	7	0.863	0.086	0.0005	0.0001	0.0001	0.0001
	0.01	7	1.104	0.117		0.6333	0.5997	0.2336
	0.1	7	1.134	0.108			0.9742	0.4788
	1	8	1.136	0.130				0.4840
	10	8	1.177	0.131				
Male Pup	Control	4	0.150	0.008	0.3990	0.3619	0.4643	0.0760
	0.01	5	0.158	0.013		0.9687	0.8753	0.3132
	0.1	6	0.158	0.016			0.8370	0.3092
	1	6	0.157	0.010				0.2248
	10	6	0.167	0.018				
Female Pup	Control	4	0.140	0.018	0.8086	0.0106	0.0145	0.0010
	0.01	4	0.143	0.010		0.0190	0.0243	0.0017
	0.1	7	0.166	0.013			0.8452	0.1303
	1	4	0.168	0.013				0.2347
	10	4	0.180	0.018				

Table 5. Paired comparisons of dose group for TSH. Values listed under each dose column are p-values (2-tailed t-test with pooled error) for comparing row dose and column dose.

Rat	Dose Group mg/kg/day	N	Mean TSH (ng/mL)	Std Dev TSH (ng/mL)	Dose Group mg/kg/day			
					0.01	0.1	1	10
Dam	Control	7	7.24	0.49	0.0001	0.0001	0.0001	0.0001
	0.01	7	10.71	1.04		0.1711	0.0121	0.0001
	0.1	6	11.59	1.13			0.2731	0.0002
	1	8	12.27	1.34				0.0022
	10	7	14.23	1.37				
Male Pup	Control	7	6.79	0.69	0.0841	0.0003	0.0001	0.0001
	0.01	6	7.63	0.85		0.0229	0.0092	0.0086
	0.1	6	8.76	0.84			0.7636	0.7446
	1	7	8.90	0.99				0.9792
	10	7	8.91	0.64				
Female Pup	Control	4	6.69	0.44	0.0739	0.0866	0.0304	0.0304
	0.01	5	7.38	0.61		0.9893	0.7824	0.6455
	0.1	4	7.39	0.22			0.8084	0.6741
	1	8	7.47	0.64				0.8141
	10	5	7.54	0.55				

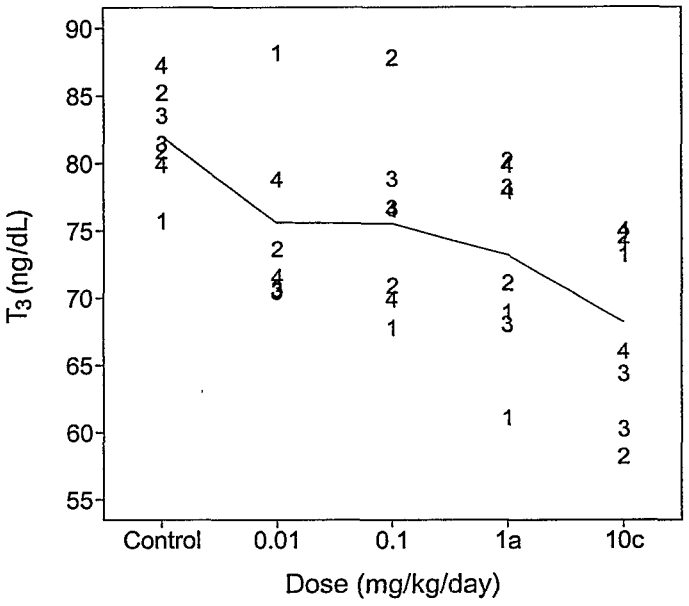

Figure 1a. T_3 for each dam. Line segments connect means from each dose group. Legend is value of # for each PND5-# group. Comparisons with control (a: $0.01<p\leq0.05$, b: $0.001<p\leq0.01$, c: $p\leq0.001$) used 2-tailed t-tests with pooled error.

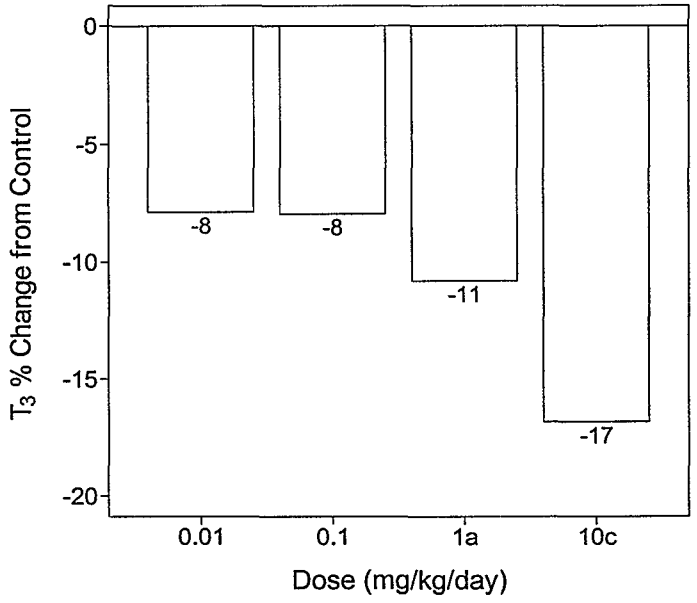

Figure 1b. Dams mean percent change from control for T_3. Comparisons with control (a: $0.01<p\leq0.05$, b: $0.001<p\leq0.01$, c: $p\leq0.001$) used 2-tailed t-tests with pooled error.

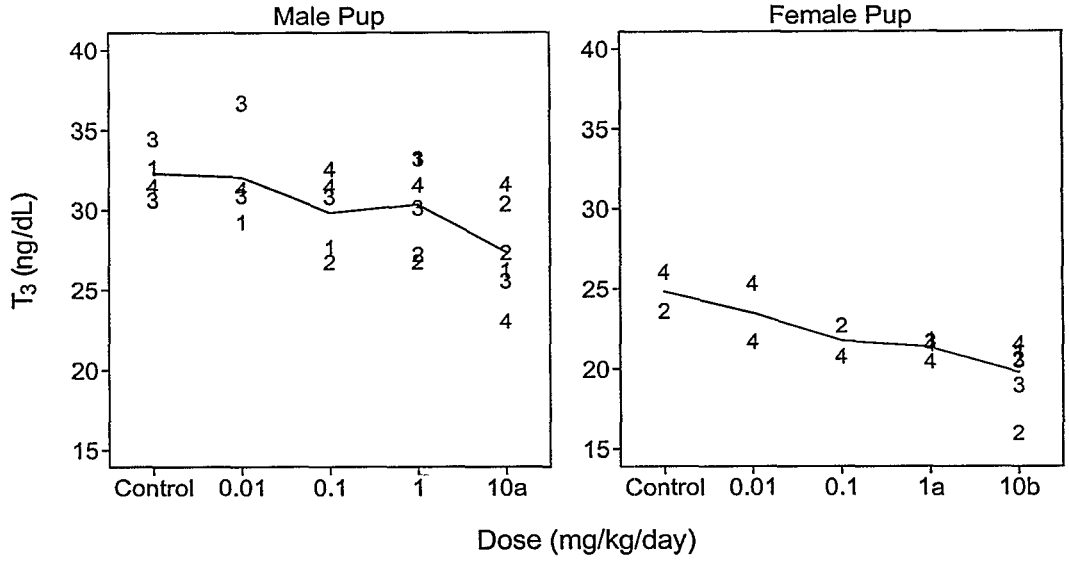

Figure 1c. T_3 for each male and female pup. Line segments connect means from each dose group. Legend is value of # for each PND5-# group. Comparisons with control (a: $0.01<p\leq0.05$, b: $0.001<p\leq0.01$, c: $p\leq0.001$) used 2-tailed t-tests with pooled error.

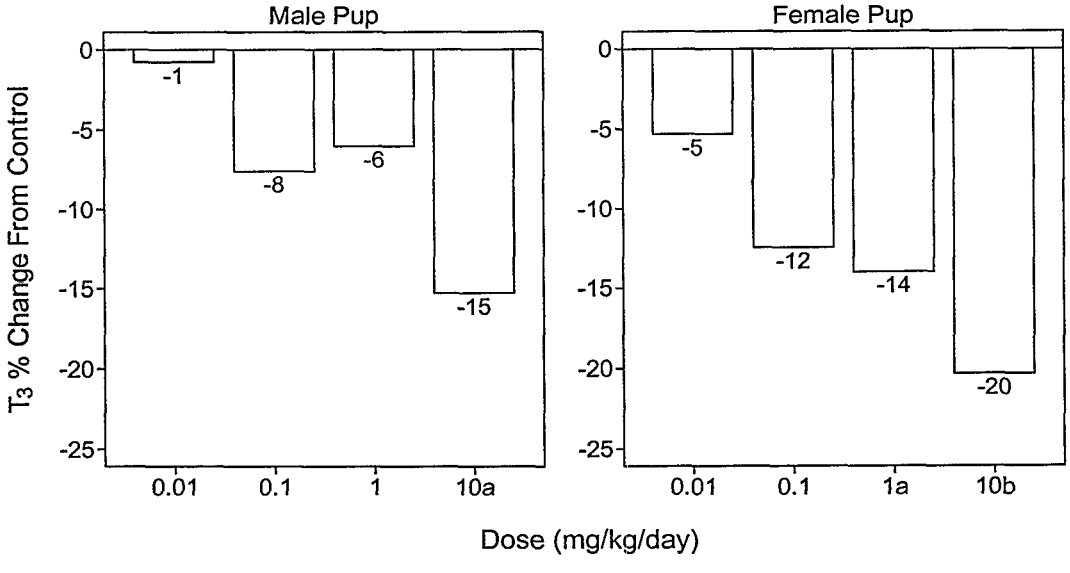

Figure 1d. Mean percent change from control for T_3. Comparisons with control (a: $0.01<p\leq0.05$, b: $0.001<p\leq0.01$, c: $p\leq0.001$) used 2-tailed t-tests with pooled error.

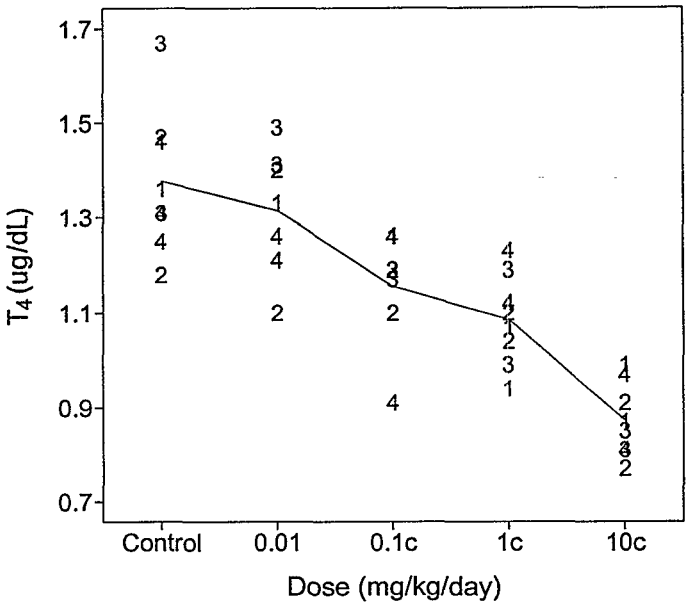

Figure 2a. T_4 for each dam. Line segments connect means from each dose group. Legend is value of # for each PND5-# group. Comparisons with control (a: $0.01<p\leq0.05$, b: $0.001<p\leq0.01$, c: $p\leq0.001$) used 2-tailed t-tests with pooled error.

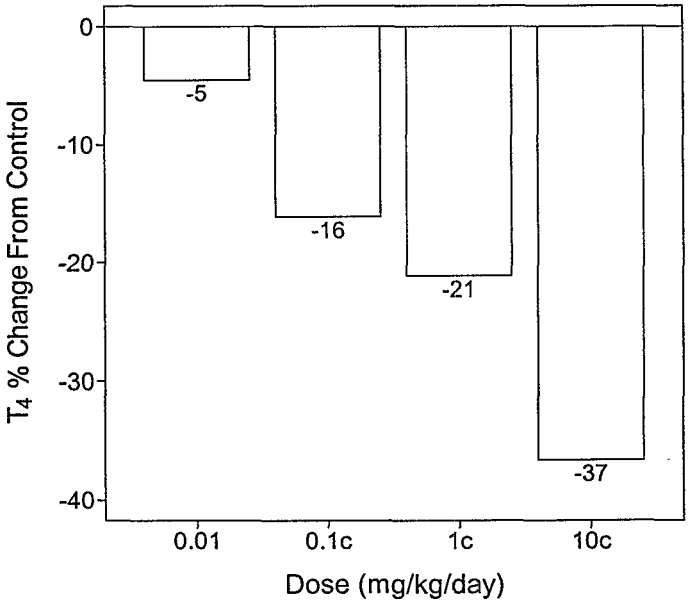

Figure 2b. Dams mean percent change from control for T_4. Comparisons with control (a: $0.01<p\leq0.05$, b: $0.001<p\leq0.01$, c: $p\leq0.001$) used 2-tailed t-tests with pooled error.

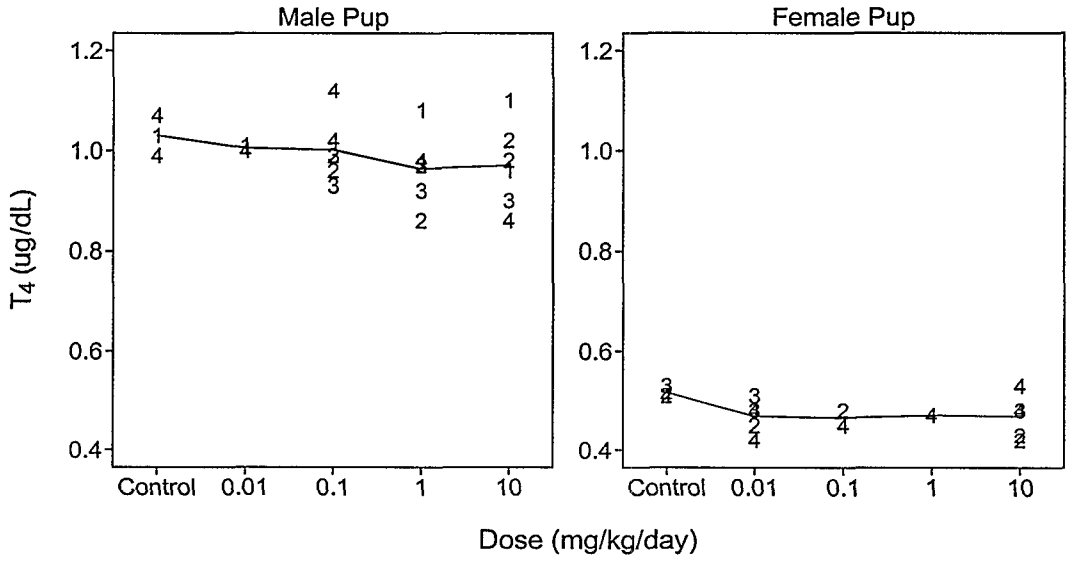

Figure 2c. T_4 for each male and female pup. Line segments connect means from each dose group. Legend is value of # for each PND5-# group. Comparisons with control (a: 0.01<p≤0.05, b: 0.001<p≤0.01, c: p≤0.001) used 2-tailed t-tests with pooled error.

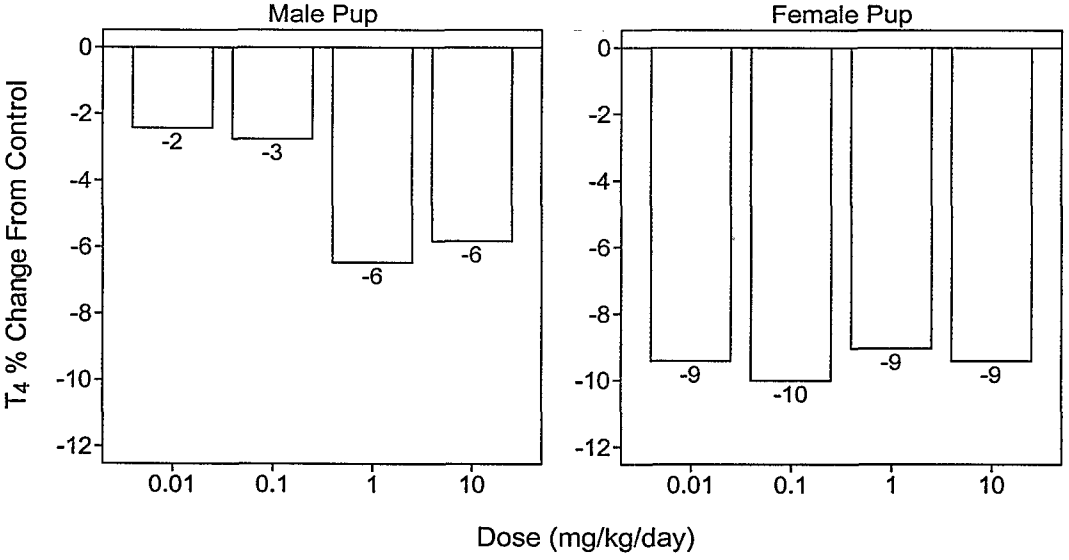

Figure 2d. Mean percent change from control for T_4. Comparisons with control (a: 0.01<p≤0.05, b: 0.001<p≤0.01, c: p≤0.001) used 2-tailed t-tests with pooled error.

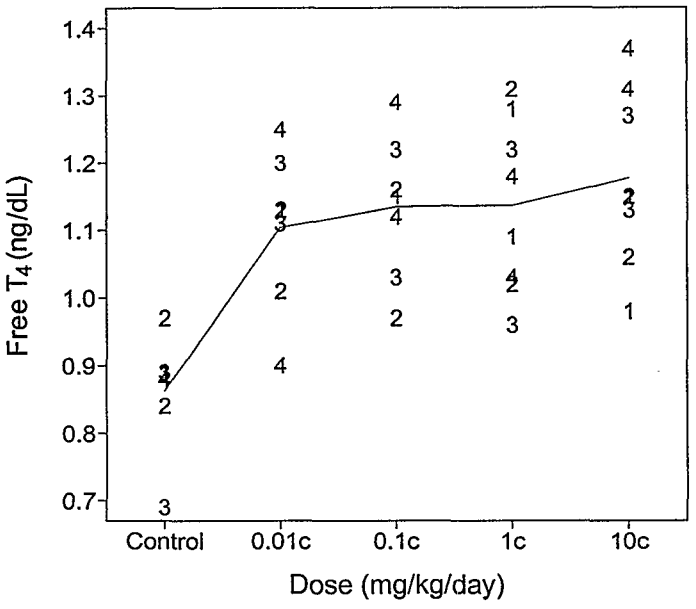

Figure 3a. Free T_4 for each dam. Line segments connect means from each dose group. Legend is value of # for each PND5-# group. Comparisons with control (a: $0.01<p\leq0.05$, b: $0.001<p\leq0.01$, c: $p\leq0.001$) used 2-tailed t-tests with pooled error.

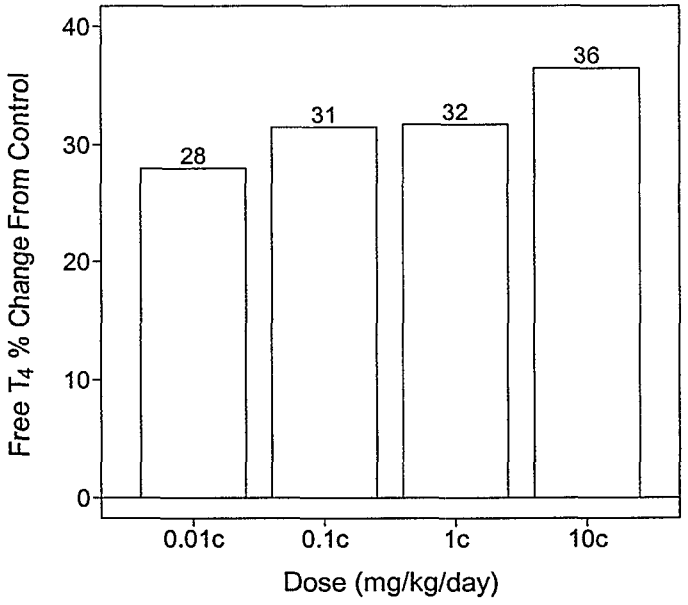

Figure 3b. Dams mean percent change from control for Free T_4. Comparisons with control (a: $0.01<p\leq0.05$, b: $0.001<p\leq0.01$, c: $p\leq0.001$) used 2-tailed t-tests with pooled error.

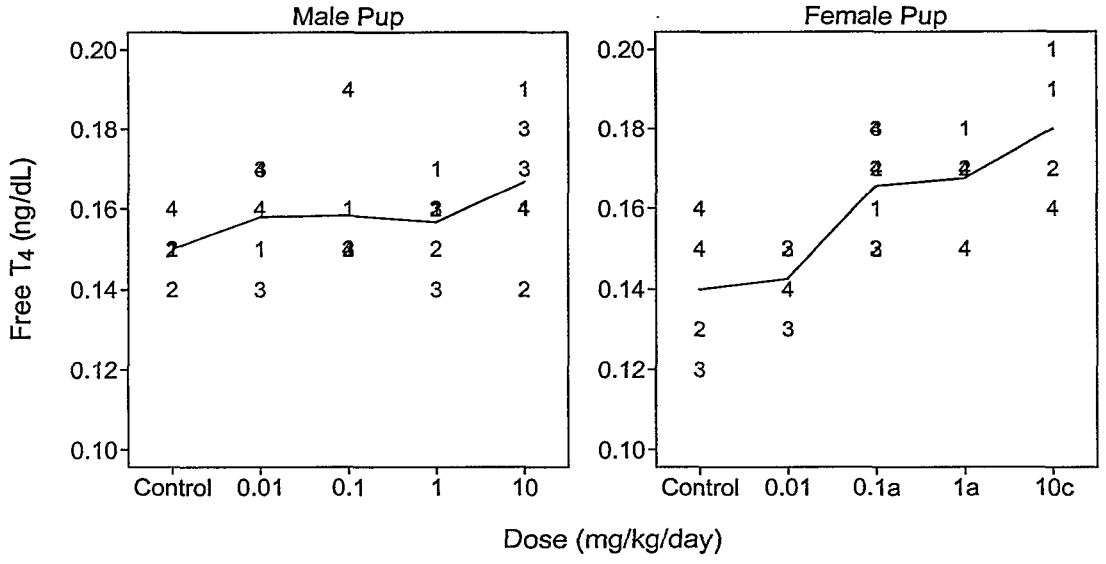

Figure 3c. Free T_4 for each male and female pup. Line segments connect means from each dose group. Legend is value of # for each PND5-# group. Comparisons with control (a: $0.01<p\leq0.05$, b: $0.001<p\leq0.01$, c: $p\leq0.001$) used 2-tailed t-tests with pooled error.

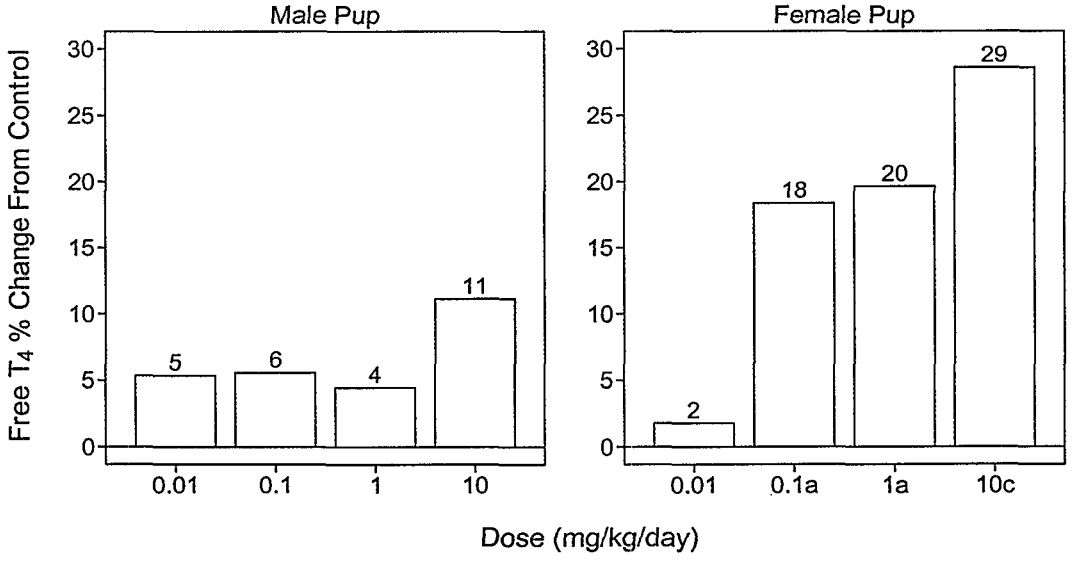

Figure 3d. Mean percent change from control for Free T_4. Comparisons with control (a: $0.01<p\leq0.05$, b: $0.001<p\leq0.01$, c: $p\leq0.001$) used 2-tailed t-tests with pooled error.

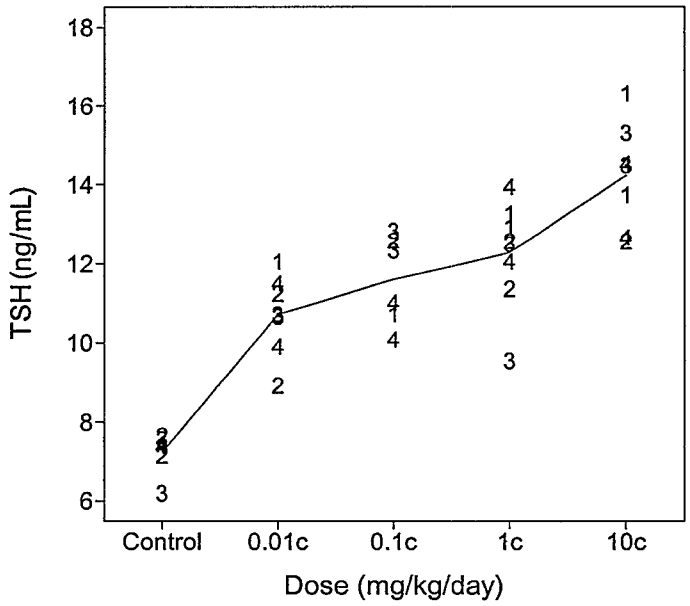

Figure 4a. TSH for each dam. Line segments connect means from each dose group. Legend is value of # for each PND5-# group. Comparisons with control (a: 0.01<p≤0.05, b: 0.001<p≤0.01, c: p≤0.001) used 2-tailed t-tests with pooled error.

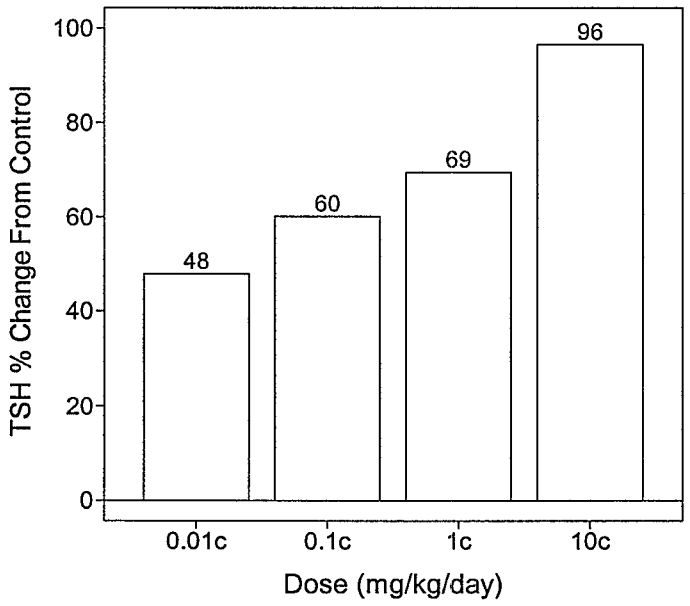

Figure 4b. Dams mean percent change from control for TSH. Comparisons with control (a: 0.01<p≤0.05, b: 0.001<p≤0.01, c: p≤0.001) used 2-tailed t-tests with pooled error.

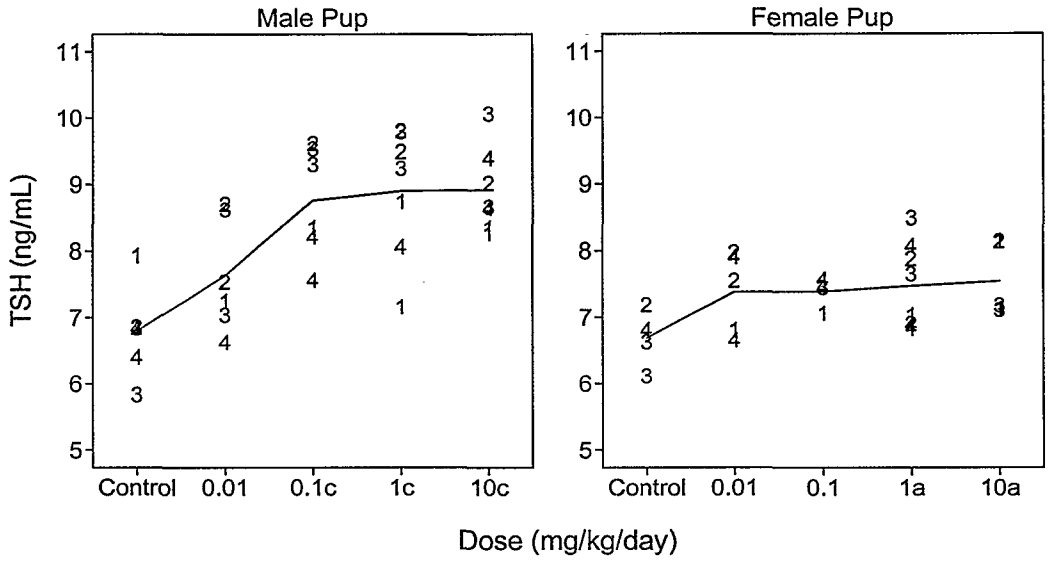

Figure 4c. TSH for each male and female pup. Line segments connect means from each dose group. Legend is value of # for each PND5-# group. Comparisons with control (a: 0.01<p≤0.05, b: 0.001<p≤0.01, c: p≤0.001) used 2-tailed t-tests with pooled error.

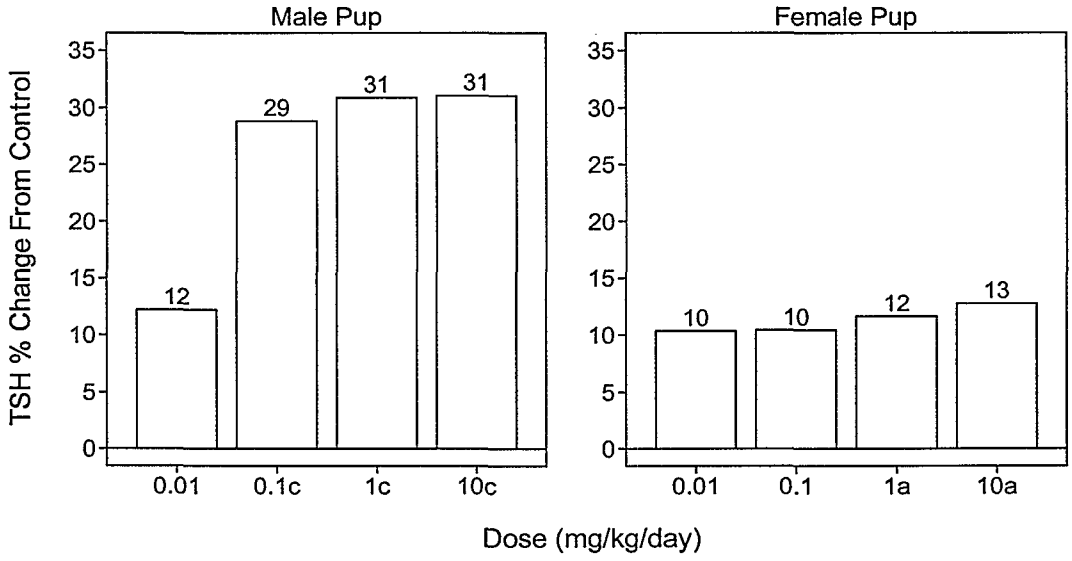

Figure 4d. Mean percent change from control for TSH. Comparisons with control (a: 0.01<p≤0.05, b: 0.001<p≤0.01, c: p≤0.001) used 2-tailed t-tests with pooled error.